ELSEVIER

Driven quantum transport on the nanoscale

Sigmund Kohler*, Jörg Lehmann[1], Peter Hänggi

Institut für Physik, Universität Augsburg, Universitätsstraße 1, D-86135 Augsburg, Germany

Abstract

We explore the prospects to control by use of time-dependent fields quantum transport phenomena in nanoscale systems. In particular, we study for driven conductors the electron current and its noise properties. We review recent corresponding theoretical descriptions which are based on Floquet theory. Alternative approaches, as well as various limiting approximation schemes are investigated and compared. The general theory is subsequently applied to different representative nanoscale devices, like non-adiabatic pumps, gates, quantum ratchets, and transistors. Potential applications range from molecular wires under the influence of strong laser fields to microwave-irradiated quantum dots.
© 2004 Elsevier B.V. All rights reserved.

PACS: 05.60.Gg; 85.65.+h; 05.40. − a; 72.40.+w

Keywords: Quantum transport; Driven systems; Noise

Contents

* Corresponding author.
 E-mail address: sigmund.kohler@physik.uni-augsburg.de (S. Kohler).

[1] Present address: Departement für Physik und Astronomie, Universität Basel, Klingelbergstrasse 82, CH-4056 Basel, Switzerland.

1. Introduction

As anticipated by Richard Feynman in his visionary lecture "There's plenty of room at the bottom" [1], we witness an ongoing progress in the study of physical phenomena on ever smaller scales. Partly, this has been made possible by the continuous technical achievements in fabrication and miniaturization of electronic devices. However, it was the invention of scanning probe microscopes [2], which brought about the realization of Feynman's dream, namely the selective manipulation of matter on the nanoscale. Since then, much progress has been made in nanosciences. In particular, the field of molecular electronics has emerged, which deals with the realization of electronic devices based on the properties of a single or a few molecules. The theoretical proposal of a molecular rectifier by Aviram and Ratner [3] has been trend-setting for investigating the distinct features of electrical transport on the nanoscale. On the experimental side, an ancestor of molecular electronics was the pioneering work by Mann and Kuhn [4] on transport through hybrid acid–salt surface adlayers. The ongoing advance in contacting single molecules by nanoelectrodes allows one to perform transport measurements [5–9]. In these experiments, the quantum nature of the electrons and the quantum coherence across the wire, which is connected to adjacent macroscopic lead electrodes, influence various physical properties such as the conductance and the corresponding current noise statistics. The rapid evolution of molecular conduction is documented by recent monographs and article collections [10–13].

For the corresponding theoretical investigations, two lines of research are presently pursued. A first one starts out from the ab initio computation of the orbitals relevant for the motion of excess charges through the molecular wire [14–18]. At present, however, the results of such computations generally differ by more than one order of magnitude from experimental data, possibly due to the equilibrium treatment of exchange correlations [19]. The second line employs corresponding phenomenological models in order to gain a qualitative understanding of the transport mechanisms involved [20–25]. Two particular problems addressed within model calculations are the conduction mechanism in the presence of electron–phonon coupling [21–23,26–34] and the length dependence of the current–voltage characteristics [20,24]. The present work also employs rather universal models: we describe the molecules by a linear arrangement of tight-binding levels with the terminating sites attached to leads. Still it is possible to suitably parametrize such tight-binding models in order to obtain qualitative results for real systems [35–37]. Furthermore, these models also capture the physics of the so-called artificial molecules, i.e., coupled quantum dots and quantum dot arrays [38,39].

One particular question that arises in this context is the influence of excitations by electromagnetic fields and gate voltages on the electron transport. Such excitations bear intriguing phenomena like photon-assisted tunneling [39–42] and the adiabatic [43–45] and non-adiabatic pumping [46,47] of electrons. From a fundamental point of view, these effects are of interest because the external fields enable selective electron excitations and allow one to study their interplay with the underlying transport mechanism. In practical applications, time-dependent effects can be used to control and steer currents in coherent

conductors. However, such control schemes can be valuable only if they operate at tolerable noise levels. Thus, the corresponding current noise is of equal interest.

An intuitive description of the coherent electron transport through time-independent mesoscopic systems is provided by the Landauer scattering formula [48] and its various generalizations. Both the average current [49–53] and the transport noise characteristics [54] can be expressed in terms of the quantum transmission coefficients for the respective scattering channels. By contrast, the theory for driven quantum transport is less developed. Scattering of a single particle by arbitrary time-dependent potentials has been considered [55–57] without relating the resulting transmission probabilities to a current between electron reservoirs. Such a relation is indeed non-trivial since the driving opens inelastic transport channels and, therefore, in contrast to the static case, an ad hoc inclusion of the Pauli principle is no longer unique. This gave rise to a discussion about "Pauli blocking factors" [58–60]. In order to resolve such conflicts, one should start out from a many-particle description. In this spirit, within a Green function approach, a formal solution for the current through a time-dependent conductor has been presented [61,62] without taking advantage of the full Floquet theory for the wire and without obtaining a "scattering form" for the current in the general driven case. The spectral density of the current fluctuations has been derived for the low-frequency ac conductance [63,64] and the scattering by a slowly time-dependent potential [65]. For arbitrary driving frequencies, the noise can be characterized by its zero-frequency component. A remarkable feature of the current noise in the presence of time-dependent fields is its dependence on the phase of the transmission *amplitudes* [65–67]. By clear contrast, both the noise in the static case [54] and the current in the driven case [66] depend solely on transmission *probabilities*.

In Section 3, we derive within a *Floquet approach* explicit expressions for both the current and the noise properties of the electron transport through a driven nanoscale conductor under the influence of time-dependent forces [66,67]. This approach is applicable to arbitrary periodically driven tight-binding systems and, in particular, is valid for arbitrary driving strength and extends beyond the adiabatic regime. The dynamics of the electrons is solved by integrating the Heisenberg equations of motion for the electron creation and annihilation operators in terms of the single-particle propagator. For this propagator, in turn, we provide a solution within a generalized Floquet approach. Such a treatment is valid only for effectively non-interacting electrons, i.e., in the absence of strong correlations. Moreover, this *Floquet scattering approach* cannot be generalized straightforwardly to the case with additional electron–vibrational coupling. Better suited for this situation is a quantum kinetic equation formalism which, however, is perturbative in both the wire–lead coupling and the electron–vibrational coupling [68,69].

An experimental starting point for the investigation of the influence of electromagnetic fields on molecular conduction is the excitation of electrons to higher orbitals of the contacted molecule. In molecular physics, specific excitations are usually performed with laser fields. The resulting changes of the current through a contacted molecule due to the influence of a laser field are studied in Section 5. In particular, we focus on the modification of the length dependence of the conductivity [70,71].

An intriguing phenomenon in strongly driven systems is the so-termed ratchet or Brownian motor effect [72–77], originally discovered for overdamped classical Brownian motion in asymmetric non-equilibrium systems. Counter-intuitively to the second law of thermodynamics, one then observes a directed transport although none of the acting forces possesses any net bias. This effect has been established also within the regime of dissipative, incoherent quantum Brownian motion [77–79]. A mesoscopic device related to ratchets is an electron pump [43–47,80,81] which indeed might be regarded as a localized ratchet. Such systems have already been realized in the quantum domain, but almost exclusively operating in the

regime of incoherent tunneling [82–86]. In Section 6, we study the possibilities for molecular wires to act as coherent quantum ratchets and explore the crossover from electron pumps to quantum ratchets. This requires to investigate thoroughly such quantum ratchet systems in the coherent tunneling regime [68,87].

The tunneling dynamics of a particle in a bistable potential can be altered significantly by ac fields. In particular, it is possible to bring tunneling to a standstill by the purely coherent influence of a time-periodic driving [88,89]. This so-called coherent destruction of tunneling has also been found in other systems [90–92]. In Section 7, we address the question whether a related effect exists also for the electron transport through a driven conductor between two leads. Moreover, we study the noise properties of the resulting transport process [66,67,93,94].

1.1. Experimental motivation

1.1.1. Coupled quantum dots

The experimental achievement of the coherent coupling of quantum dots [38] enabled the measurement of intriguing phenomena in mesoscopic transport [39]. A remarkable feature of coupled quantum dots—the so-called artificial molecules with the single dots representing the atoms—is that the energy levels of each "atom" can be controlled by an appropriate gate voltage. In particular, the highest occupied levels of neighboring dots can be tuned into resonance. At such resonances, the conductance as a function of the gate voltage exhibits a peak. This behavior is modified by the influence of microwave radiation: with increasing microwave intensity, the resonance peaks become smaller and side-peaks emerge. The distance between the central peak and the side-peaks is determined by the frequency of the radiation field which provides evidence for photon-assisted tunneling [39–42]. Photon-assisted tunneling through quantum dots is, in comparison to its counterpart in superconductor–insulator–superconductor junctions [95], a potentially richer phenomenon. The reason for this is that quantum dots form a multi-barrier structure which permits real occupation and resonant tunneling. Therefore, a theoretical description requires to also take into account the influence of the field on the dynamics of the electrons localized in the central region between the barriers. The quantum dot setup used for the observation of photon-assisted tunneling can also be employed as an implementation [96] of the theoretically suggested non-adiabatic pump [62,97,98]. Alternatively, mesoscopic conductors can also be driven by coherent phonon pulses [99–101].

Related experiments have been performed also with single quantum dots exposed to laser pulses which resonantly couple the highest occupied orbital and the lowest unoccupied orbital of the quantum dot [102]. Such a pulse can create an electron–hole pair which in turn is transformed by a transport voltage into a current pulse. Depending on their duration, pulses may not only excite an electron but also coherently de-excite the electron and thereby reduce the resulting current [103]. In the ideal case, the electron–hole pair is excited with probability one and finally yields a dc current consisting of exactly one electron per pulse. This effect might be employed for the realization of a current standard. At present, however, the deviations from the ideal value of the current are still of the order of a few percent.

1.1.2. Molecular wires

During the last years, it became possible to chemisorb organic molecules via thiol groups to a metallic gold surface. Thereby a stable contact between the molecule and the gold is established. This enables reproducible measurements of the current not only through artificial but also through real molecules. Single molecule conductance can be achieved in essentially two ways: one possible setup is an open

break junction bridged by a molecule [5,7,104]. This setup can be kept stable for several hours. More-over, it provides evidence for *single* molecule conductance because asymmetries in the current–voltage characteristics reflect asymmetries of the molecule [7,105]. Alternatively, one can use a gold substrate as a contact and grow a self-assembled monolayer of molecules on it. The other contact is provided by a gold cluster on top of a scanning tunneling microscope tip which contacts one or a few molecules on the substrate [6,106]. Yet another interesting device is based on the setup of a single-molecule chemical field effect transistor in which the current through a hybrid-molecular diode is controlled by nanometer-sized charge transfer complex which is covalently linked to a molecule in a scanning tunneling microscope junction [107]. Therein, the effect is due to an interface dipole which shifts the substrate work function. Naturally, the experimental effort with such molecular wires is accompanied by vivid theoretical interest [8,10,24].

Typical energy scales of molecules lie in the infrared regime where most of today's lasers work. Hence, lasers represent a natural possibility to excite the electrons of the molecular wire and, thus, to study the corresponding changes of the conduction properties. At present, such experiments are attempted, but still no clear-cut effect has been reported. The molecule–lead contacts seem stable even against relatively intense laser fields, but a main problem is the exclusion of side effects like, e.g., heating of the break junction which might distort the molecule–tip setup and, thus, be responsible for the observed enhancement of the conductance [108].

In a recent experiment, Yasutomi et al. measured the photocurrent induced in a self-assembled mono-layer of asymmetric molecules [86]. They have found that even the current direction depends on the wavelength of the irradiating light. Albeit not a single-molecule experiment, this measurement represents a first experimental demonstration of a ratchet-like effect in molecular wires.

2. Basic concepts

Before going in medias res and addressing specific quantum transport situations, we introduce the reader to our archetypal working model and the main theoretical methods and tools.

2.1. Model for driven conductor coupled to leads

The entire setup of our nanoscale system is described by the time-dependent Hamiltonian

$$H(t) = H_{\text{wire}}(t) + H_{\text{leads}} + H_{\text{contacts}} , \tag{1}$$

where the different terms correspond to the wire, the leads, and the wire–lead couplings, respectively. We focus on the regime of coherent quantum transport where the main physics at work occurs on the wire itself. In doing so, we neglect other possible influences originating from driving-induced hot electrons in the leads, dissipation on the wire and, as well, electron–electron interaction effects. Then, the wire Hamiltonian reads in a tight-binding approximation with N orbitals $|n\rangle$

$$H_{\text{wire}}(t) = \sum_{n,n'} H_{nn'}(t) c_n^\dagger c_{n'} . \tag{2}$$

For a molecular wire, this constitutes the so-called Hückel description where each site corresponds to one atom. The fermion operators c_n, $c_n^\dagger$ annihilate and create, respectively, an electron in the orbital
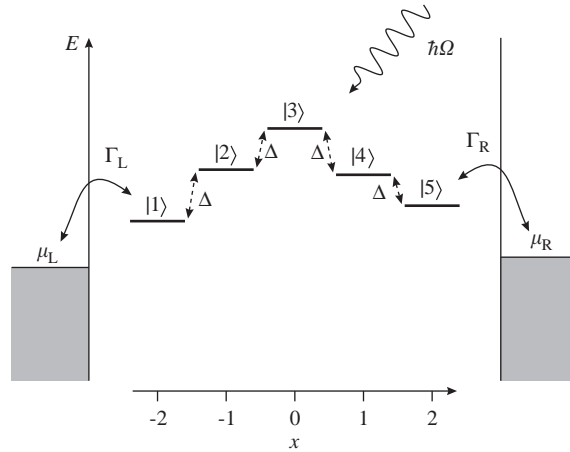
Fig. 1. Level structure of a nanoconductor with $N = 5$ orbitals. The end sites are coupled to two leads with chemical potentials μ_L and $\mu_R = \mu_L + eV$.

$|n\rangle$. Note that in the absence of driving a diagonalization of the system Hamiltonian would yield the stationary eigenvalues of the wire levels. The influence of an externally applied ac field with frequency $\Omega = 2\pi/\mathcal{T}$ results in a periodic time-dependence of the wire Hamiltonian: $H_{nn'}(t + \mathcal{T}) = H_{nn'}(t)$. In an experiment, the driving is switched on at a specific time and, thus, the Hamiltonian is, strictly speaking, not time-periodic. This can be modeled by a slowly time-dependent driving amplitude that assumes its ultimate value after a transient stage [89,109]. The switch-on of the driving field, however, depends on the specific experimental setup and will not be considered herein.

The leads are modeled by ideal electron gases,

$$H_{\text{leads}} = \sum_q \epsilon_q (c^\dagger_{Lq} c_{Lq} + c^\dagger_{Rq} c_{Rq}) \ , \tag{3}$$

where $c^\dagger_{Lq}$ ($c^\dagger_{Rq}$) creates an electron in the state $|Lq\rangle$ ($|Rq\rangle$) in the left (right) lead. The tunneling Hamiltonian

$$H_{\text{contacts}} = \sum_q (V_{Lq} c^\dagger_{Lq} c_1 + V_{Rq} c^\dagger_{Rq} c_N) + \text{h.c.} \tag{4}$$

establishes the contact between the sites $|1\rangle$, $|N\rangle$ and the respective lead, as depicted with Fig. 1. This tunneling coupling is described by the spectral density

$$\Gamma_\ell(\epsilon) = 2\pi \sum_q |V_{\ell q}|^2 \delta(\epsilon - \epsilon_q) \tag{5}$$

of lead $\ell = \text{L, R}$ which becomes a smooth function if the lead modes are dense. If the leads are modeled by a tight-binding lattice, the $\Gamma_\ell(\epsilon)$ assume a semi-elliptic shape, the so-called Newns–Anderson density of states [110], which is sometimes employed in the context of molecular conduction [20,111,112]. Within the present context, however, we are mainly interested in the influence of the driving field on the conductor

and not in the details of the coupling to the leads. Therefore, we later on often choose for $\Gamma_\ell(\epsilon)$ a rather generic form by assuming that in the relevant regime, it is practically energy-independent,

$$\Gamma_\ell(\epsilon) \longrightarrow \Gamma_\ell \ . \tag{6}$$

This so-called wide-band limit is justified whenever the conduction bandwidth of the leads is much larger than all other relevant energy scales.

To fully specify the dynamics, we choose as an initial condition for the left (right) lead a grand-canonical electron ensemble at temperature T and electro-chemical potential $\mu_{L(R)}$. Thus, the initial density matrix reads

$$\rho_0 \propto e^{-(H_{\text{leads}} - \mu_L N_L - \mu_R N_R)/k_B T} \ , \tag{7}$$

where $N_\ell = \sum_q c_{\ell q}^\dagger c_{\ell q}$ is the number of electrons in lead ℓ and $k_B T$ denotes the Boltzmann constant multiplied by the temperature. An applied voltage V maps to a chemical potential difference $\mu_R - \mu_L = eV$ with $-e$ being the electron charge. Then, at initial time t_0, the only non-trivial expectation values of the lead operators read $\langle c_{\ell' q'}^\dagger c_{\ell q} \rangle = f_\ell(\epsilon_q) \delta_{\ell \ell'} \delta_{qq'}$ where $f_\ell(\epsilon) = (1 + \exp[(\epsilon - \mu_\ell)/k_B T])^{-1}$ denotes the Fermi function.

Below, we specify the wire Hamiltonian as a tight-binding model composed of N sites as sketched in Fig. 1. Each orbital is coupled to its nearest neighbor by a hopping matrix element Δ, thus, the single-particle wire Hamiltonian reads

$$\mathscr{H}_{\text{wire}}(t) = -\Delta \sum_{n=1}^{N-1} (|n\rangle\langle n+1| + |n+1\rangle\langle n|) + \sum_n [E_n + x_n\, a(t)] |n\rangle\langle n| \ , \tag{8}$$

where E_n stands for the on-site energies of the tight-binding levels. Although the theoretical approach derived below is valid for an arbitrary periodically driven wire Hamiltonian, we always assume that the time dependence results from the coupling to an oscillating dipole field that causes the time-dependent level shifts $x_n a(t)$, where $x_n = (N + 1 - 2n)/2$ denotes the scaled position of site $|n\rangle$. The energy $a(t) = a(t + \mathscr{T})$ is determined by the electrical field strength multiplied by the electron charge and the distance between two neighboring sites. For the evaluation of the dc current and the zero-frequency noise, we mainly restrict ourselves to zero temperature. The zero-temperature limit is physically well justified for molecular wires at room temperature and for quantum dots at helium temperature since in both cases, thermal electron excitations do not play a significant role.

In a realistic wire molecule, the hopping matrix element Δ is of the order 0.1 eV. Thus, a typical wire–lead hopping rate $\Gamma = 0.1\Delta$ yields a current $e\Gamma/\hbar = 2.56 \times 10^{-5}$ A and $\Omega \approx 10\Delta/\hbar$ corresponds to a laser frequency in the near infrared, i.e., to wavelengths of the order 1 μm. For a typical distance of 5 Å between two neighboring sites, a harmonic driving $a(t) = A \cos(\Omega t)$ with an amplitude $A = \Delta$ is equivalent to an electrical field strength of 2×10^6 V/cm. It has to be emphasized that the amplitude A is determined by the local electrical field between the contacts. The difference to the incident field can be huge: model calculations demonstrated that the presence of metallic tips enhances the local field by several orders of magnitude [113,114]. This explains the observation that the Raman scattering intensity increases drastically once the molecules are adsorbed to a metallic surface [115,116]. Coupled quantum dots typically [38,39,41] have a distance of less than 1 μm while the coupling matrix element Δ is of the order of 30 μeV which corresponds to a wavelength of roughly 1 cm. The dipole approximation inherent to the time-dependent part of the Hamiltonian (8) neglects the propagation of the electromagnetic field

and, thus, is valid only for wavelengths that are much larger than the size of the sample [117]. This condition is indeed fulfilled for both applications we have in mind.

2.2. AC transport voltage

Within this work, we focus on the models presented in the previous subsection, i.e., models where the driving enters solely by means of time-dependent matrix elements of the wire Hamiltonian while the leads and the wire–lead couplings remain time-independent. However, it is worthwhile to demonstrate that a setup with an oscillating external voltage can be mapped by a gauge transformation to the model introduced above. Consequently, it is possible to apply the formalism derived below also to situations with an oscillating transport voltage.

For the discussion of a time-dependent transport voltage, we restrict ourselves to a situation where the electron energies of only the left lead are modified by an external $\mathscr{T}$-periodic voltage $V_{ac}(t)$ with zero time-average, thus

$$\epsilon_q \rightarrow \epsilon_q - eV_{ac}(t) \ . \tag{9}$$

The generalization to a situation where also the levels in the right lead are $\mathscr{T}$-periodically time-dependent is straightforward. Since an externally applied voltage causes a potential drop along the wire [118–120], we have to assume for consistency that for an ac voltage, the wire Hamiltonian also obeys a time-dependence. Ignoring such a time-dependent potential profile enables a treatment of the transport problem within the approach of Refs. [121,122]. In the general case, however, we have to resort to the approach put forward with this work.

We start out by a gauge transformation of the Hamiltonian (1) with the unitary operator

$$U_{ac}(t) = \exp\left\{ -i\phi(t)\left(c_1^\dagger c_1 + \sum_q c_{Lq}^\dagger c_{Lq} \right) \right\} \ , \tag{10}$$

where

$$\phi(t) = -\frac{e}{\hbar} \int^t dt' V_{ac}(t') \tag{11}$$

describes the phase accumulated from the oscillating voltage. The transformation (10) has been constructed such that the new Hamiltonian $\widetilde{H}(t) = U_{ac}^\dagger H(t) U_{ac} - i\hbar U_{ac}^\dagger \dot{U}_{ac}$ possesses a time-independent tunnel coupling. Since, the operator c_1 transforms as $c_1 \rightarrow c_1 \exp(-i\phi(t))$, the matrix elements $H_{nn'}(t)$ of the wire Hamiltonian acquire an additional time-dependence,

$$H_{nn'}(t) \rightarrow \widetilde{H}_{nn'}(t) = H_{nn'}(t)e^{-i\phi(t)(\delta_{n'1}-\delta_{n1})} + eV_{ac}(t)\delta_{n1}\delta_{n'1} \ . \tag{12}$$

The second term in the Hamiltonian (12) stems from $-i\hbar U_{ac}^\dagger \dot{U}_{ac}$. Owing to the zero time-average of the voltage $V_{ac}(t)$, the phase $\phi(t)$ is $\mathscr{T}$-periodic. Therefore, the transformed wire Hamiltonian is also $\mathscr{T}$-periodic while the contact and the lead contributions are time-independent, thus, $\widetilde{H}(t)$ is of the same form as the original Hamiltonian (1).

2.3. Tien–Gordon theory

In order to explain the steps in the current–voltage characteristics of microwave-irradiated super-conductor–insulator–superconductor junctions [95], Tien and Gordon [123] proposed a heuristical theoretical treatment which is of appealing simplicity but nevertheless captures some essential features of driven transport. The central idea of this approach is to model the influence of the driving fields by a periodic shift of the energies in the, e.g., left lead according to $\tilde{\epsilon}_{Lq}(t) = \epsilon_{Lq} + A \cos(\Omega t)$, cf. Eq. (9). Then the corresponding lead eigenstates evolve as

$$|Lq\rangle_t = \exp\left(-\frac{i}{\hbar}\epsilon_{Lq}t - i\frac{A}{\hbar\Omega}\sin(\Omega t)\right)|Lq\rangle \tag{13}$$

$$= \sum_{k=-\infty}^{\infty} J_k(A/\hbar\Omega)\exp\left(-\frac{i}{\hbar}(\epsilon_{Lq} + k\hbar\Omega)t\right)|Lq\rangle , \tag{14}$$

where J_k denotes the kth-order Bessel function of the first kind. The interpretation of the Fourier decomposition (14) is that each state consists of sidebands whose energies are shifted by multiples of $\hbar\Omega$. For the evaluation of the dc current, this is equivalent to replacing the Fermi function of the left lead by

$$f_L(E) \longrightarrow \sum_k J_k^2(A/\hbar\Omega)f_L(E + k\hbar\Omega) \tag{15}$$

and formally treating the system as time-independent [123]. While this effective static treatment indeed captures the photon-assisted dc current, it naturally fails to describe any time-dependent response.

For time-dependent wire–lead models where the driving shifts all wire levels simultaneously, it is possible to map the driving field by a gauge transformation to oscillating chemical potentials. Then, the average current can be evaluated from an effective electron distribution like the one in Eq. (15) [124–126]. However, generally the time-dependent field also influences the dynamics of the electrons on the wire. In particular, this is the case for the dipole driving (8). Then, a treatment beyond Tien–Gordon theory becomes necessary. Deriving an approach which is valid in the general case is the objective of Section 3.

2.4. Scattering approach for static conductors

In the absence of a driving field, the computation of the coherent transport through mesoscopic structures has become a standard procedure [50–53]. The crucial idea goes back to Landauer who postulated already in 1957 [48] that in the absence of both inelastic effects and electron–electron interaction, conduction can be described as a coherent scattering process of independent electrons. Then, an infinitesimal voltage V causes the current $I = GV$ with the (linear) conductance

$$G = \frac{e^2}{h} T , \tag{16}$$

of a one-dimensional conductor, where T is the total transmission of an electron at the Fermi surface. Since conductors may have non-vanishing reflection probability $1 - T$, the transmission probability does not necessarily assume an integer value. The prefactor $e^2/h = (25.8 \text{ k}\Omega)^{-1}$ is the so-called conductance quantum.

Originally [48], the conductance (16) has been proposed with T replaced by $T/(1-T)$. In the beginning of the 1980s, there has been a theoretical debate [127–129] whether or not, the reflection coefficient $1-T$ has to be included. The controversy was resolved by considering four-terminal devices where two terminals act as voltage probes and are considered as a part of the mesoscopic conductor [49,130]. Then, V represents the probed voltage and the factor $1/(1-T)$ indeed is justified. In a two-terminal device, however, V denotes the externally applied voltage and the conductance includes a contact resistance and is given by Eq. (16).

With the same ideas, Landauer theory can be generalized to the case of a finite voltage for which the current reads

$$I = \frac{e}{h} \int dE [f_R(E) - f_L(E)] T(E) \tag{17}$$

with $T(E)$ being the electron transmission probability at energy E. The electron distribution in the left (right) lead is given by the Fermi function $f_{L(R)}$ with the chemical potential $\mu_{L(R)}$ whose difference $\mu_R - \mu_L = eV$ is determined by the applied voltage. The linearization for small voltages yields the conductance (16). The current formula (17) and the conductance (16) have been derived from Kubo formula [128–132] and by means of non-equilibrium Green function methods [131,133–136] for various microscopic models. In doing so, one usually starts by defining a current operator, e.g., as the change of the electron charge eN_L in the left lead, i.e., $I = ie[H, N_L]/\hbar$. Finally, one obtains the expected expression for the current together with the relation

$$T(E) = \text{tr}[G^\dagger(E)\Sigma_R(E)G(E)\Sigma_L(E)] \tag{18}$$

between the transmission probability $T(E)$ and the Green function of the electrons. The trace sums over all single-particle states of the wire and $\Sigma_\ell = |n_\ell\rangle \frac{\Gamma_\ell}{2} \langle n_\ell|$ denotes the imaginary part of the self-energy of the terminating wire sites which results from the coupling to the respective leads.

In order to obtain an expression for the related current noise, one considers the symmetrized correlation function

$$S(t, t') = \frac{1}{2} \langle [\Delta I(t), \Delta I(t')]_+ \rangle \tag{19}$$

of the current fluctuation operator $\Delta I(t) = I(t) - \langle I(t) \rangle$, where the anticommutator $[A, B]_+ = AB + BA$ ensures hermiticity. For a stationary process, the correlation function $S(t, t') = S(t - t')$ is a function of only the time difference. Then, the noise strength can be characterized by the zero-frequency component

$$S = \int_{-\infty}^{\infty} d\tau S(\tau) , \tag{20}$$

which obeys $S \geqslant 0$ according to the Wiener–Khinchine theorem. In terms of the transmission function $T(E)$, the noise strength reads [54]

$$S = \frac{e^2}{h} \int dE \{T(E)[f_L(E)[1 - f_L(E)] + f_R(E)[1 - f_R(E)]]$$
$$+ T(E)[1 - T(E)][f_R(E) - f_L(E)]^2\} . \tag{21}$$

A dimensionless measure for the *relative* noise strength, is the so-called Fano factor [137]

$$F = \frac{S}{e|I|} \; . \tag{22}$$

Note that in a two-terminal device, both the absolute value of the average current and the noise strength are independent of the contact ℓ. Historically, the zero-frequency noise (20) contains a factor 2, i.e., one considers $S' = 2S$, resulting from a different definition of the Fourier transform. Then, the Fano factor is defined as $F = S'/2e|I|$. The definition (22) is such that a Poisson process corresponds to $F = 1$.

The generalization of the noise expression (21) to driven systems must also account for absorption and emission. Owing to this energy non-conserving processes, the zero-frequency noise is no longer given solely in terms of transmission *probabilities* but also depends on the phases of the transmission *amplitudes* [65–67]; cf. Eq. (50), below.

2.5. Master equation

A different strategy for the computation of stationary currents relies on the derivation of a master equation for the dynamics of the wire electrons. There, the central idea is to consider the contact Hamiltonian (4) as a perturbation, while the dynamics of the leads and the wire, including the external driving, is treated exactly. From the Liouville–von Neumann equation $i\hbar\dot{\varrho}(t) = [H(t), \varrho(t)]$ for the total density operator $\varrho(t)$ one obtains by standard techniques [138,139] the approximate equation of motion

$$\dot{\varrho}(t) = -\frac{i}{\hbar}[H_{\text{wire}}(t) + H_{\text{leads}}, \varrho(t)]$$
$$-\frac{1}{\hbar^2}\int_0^\infty \mathrm{d}\tau[H_{\text{contacts}}, [\widetilde{H}_{\text{contacts}}(t - \tau, t), \varrho(t)]] \; . \tag{23}$$

The tilde denotes operators in the interaction picture with respect to the molecule and the lead Hamiltonian without the molecule–lead coupling, $\widetilde{X}(t, t') = U_0^\dagger(t, t')XU_0(t, t')$, where U_0 is the propagator without the coupling. For the evaluation of Eq. (23) it is essential to use an exact expression for the zeroth-order time evolution operator $U_0(t, t')$. The use of any approximation bears the danger of generating artifacts, which, for instance, may lead to a violation of fundamental equilibrium properties [140,141].

In order to make practical use of Eq. (23), one has to trace over the lead degrees of freedom and thereby obtains a master equation for the reduced density operator of the wire electrons. Subsequently, the reduced density operator is decomposed into the eigenstates of the wire Hamiltonian H_{wire}—or the corresponding Floquet states if the system is driven. As a further simplification, one might neglect off-diagonal matrix elements and, thus, obtain a master equation of the Pauli type, i.e., a closed equation for the occupation *probabilities* of the eigenstates [98,142,143]. For driven systems close to degeneracies of the quasienergies, however, such a Pauli master equation is not reliable as has been exemplified in Ref. [69].

3. Floquet approach to the driven transport problem

In the following, we present the Floquet approach for our working model of Section 2.1. This derivation is rigorous and exact: it is equivalent to an exact treatment in terms of a Keldysh Green

function calculation [61]. However, the chosen Floquet derivation is here more direct and technically rather transparent.

We start out from the Heisenberg equations of motion for the annihilation operators in lead ℓ, i.e.,

$$\dot{c}_{\ell q} = -\frac{\mathrm{i}}{\hbar}\,\epsilon_q c_{\ell q} - \frac{\mathrm{i}}{\hbar}\,V_{\ell q} c_{n_\ell} \ , \tag{24}$$

where n_ℓ denotes the conductor site attached to lead ℓ, i.e., $n_{\mathrm{L}} = 1$ and $n_{\mathrm{R}} = N$. These equations are straightforwardly integrated to read

$$c_{\ell q}(t) = c_{\ell q}(t_0)\mathrm{e}^{-\mathrm{i}\epsilon_q(t-t_0)/\hbar} - \frac{\mathrm{i}}{\hbar}\,V_{\ell q}\int_0^{t-t_0}\mathrm{d}\tau\,\mathrm{e}^{-\mathrm{i}\epsilon_q\tau/\hbar}c_{n_\ell}(t-\tau) \ . \tag{25}$$

Inserting (25) into the Heisenberg equations for the wire operators yields in the asymptotic limit $t_0 \to -\infty$

$$\dot{c}_{n_\ell}(t) = -\frac{\mathrm{i}}{\hbar}\sum_{n'}H_{n_\ell,n'}(t)\,c_{n'}(t) - \frac{1}{\hbar}\int_0^\infty\mathrm{d}\tau\,\Gamma_\ell(\tau)c_{n_\ell}(t-\tau) + \xi_\ell(t) \ , \tag{26}$$

$$\dot{c}_n(t) = -\frac{\mathrm{i}}{\hbar}\sum_{n'}H_{nn'}(t)\,c_{n'}(t), \quad n = 2,\dots,N-1 \ , \tag{27}$$

where the lead response function $\Gamma_\ell(t)$ results from the Fourier transformation of the spectral density (5),

$$\Gamma_\ell(t) = \int\frac{\mathrm{d}\epsilon}{2\pi\hbar}\,\mathrm{e}^{-\mathrm{i}\epsilon t/\hbar}\Gamma_\ell(\epsilon) \ . \tag{28}$$

In the wide-band limit (6), one obtains $\Gamma_\ell(t) = \Gamma_\ell\,\delta(t)$ and, thus, the equations of motion for the wire operators are memory-free. The influence of the operator-valued Gaussian noise

$$\xi_\ell(t) = -\frac{\mathrm{i}}{\hbar}\sum_q V_{\ell q}^*\,\mathrm{e}^{-\mathrm{i}\epsilon_q(t-t_0)/\hbar}\,c_{\ell q}(t_0) \tag{29}$$

is fully specified by the expectation values

$$\langle\xi_\ell(t)\rangle = 0 \ , \tag{30}$$

$$\langle\xi_{\ell'}^\dagger(t')\xi_\ell(t)\rangle = \delta_{\ell\ell'}\int\frac{\mathrm{d}\epsilon}{2\pi\hbar^2}\,\mathrm{e}^{-\mathrm{i}\epsilon(t-t')/\hbar}\,\Gamma_\ell(\epsilon)f_\ell(\epsilon) \ , \tag{31}$$

which for the uncorrelated initial state (7) follow from the definition (29). It is convenient to define the Fourier representation of the noise operator, $\xi_\ell(\epsilon) = \int\mathrm{d}t\,\exp(\mathrm{i}\epsilon t/\hbar)\xi_\ell(t)$ whose correlation function

$$\langle\xi_\ell^\dagger(\epsilon)\xi_{\ell'}(\epsilon')\rangle = 2\pi\Gamma_\ell(\epsilon)f_\ell(\epsilon)\delta(\epsilon-\epsilon')\,\delta_{\ell\ell'} \tag{32}$$

is obtained directly from Eq. (31). All higher-order correlation functions follow from the Gaussian property of the noise (29) which is a direct consequence of the initial thermal-equilibrium preparation (7).

3.1. Retarded Green function

The equations of motion (26) and (27) represent a set of linear inhomogeneous equations and, thus, can be solved with the help of the retarded Green function $G(t, t') = -(\mathrm{i}/\hbar)U(t, t')\Theta(t - t')$ which obeys

$$\left(\mathrm{i}\hbar \frac{\mathrm{d}}{\mathrm{d}t} - \mathscr{H}(t)\right) G(t, t') + \mathrm{i} \int_0^\infty \mathrm{d}\tau\, \Gamma(\tau) G(t - \tau, t') = \delta(t - t') \,, \tag{33}$$

where $\Gamma(t) = |1\rangle\Gamma_{\mathrm{L}}(t)\langle 1| + |N\rangle\Gamma_{\mathrm{R}}(t)\langle N|$. At this stage, it is important to note that in the asymptotic limit $t_0 \to -\infty$, the l.h.s. of this equation is periodic in t. As demonstrated in Appendix A, this has the consequence that the propagator of the homogeneous equations obeys $U(t, t') = U(t + \mathscr{T}, t' + \mathscr{T})$ and, accordingly, the retarded Green function

$$G(t, \epsilon) = -\frac{\mathrm{i}}{\hbar} \int_0^\infty \mathrm{d}\tau\, \mathrm{e}^{\mathrm{i}\epsilon\tau/\hbar} U(t, t - \tau) = G(t + \mathscr{T}, \epsilon) \tag{34}$$

is also $\mathscr{T}$-periodic in the time argument. Thus, we can employ the Fourier decomposition $G(t, \epsilon) = \sum_k \mathrm{e}^{-\mathrm{i}k\Omega t} G^{(k)}(\epsilon)$, with the coefficients

$$G^{(k)}(\epsilon) = \frac{1}{\mathscr{T}} \int_0^{\mathscr{T}} \mathrm{d}t\, \mathrm{e}^{\mathrm{i}k\Omega t} G(t, \epsilon) \,. \tag{35}$$

Physically, $G^{(k)}(\epsilon)$ describes the propagation of an electron with initial energy ϵ under the absorption (emission) of $|k|$ photons for $k > 0$ ($k < 0$). In the limiting case of a time-independent situation, $G(t, \epsilon)$ becomes independent of t and, consequently, identical to $G^{(0)}(\epsilon)$ while all sideband contributions with $k \neq 0$ vanish.

From the definition of the Green function, it can be shown that the solution of the Heisenberg equations (26), (27) reads

$$c_n(t) = \mathrm{i}\hbar \sum_\ell \int_0^\infty \mathrm{d}\tau\, G_{n,n_\ell}(t, t - \tau)\, \xi_\ell(t - \tau) \,. \tag{36}$$

Inserting for $G_{n,n_\ell}(t, t') = \langle n|G(t, t')|n_\ell\rangle$ the Fourier representation (34), one obtains the form

$$c_n(t) = \frac{\mathrm{i}}{2\pi} \sum_\ell \int \mathrm{d}\epsilon\, \mathrm{e}^{-\mathrm{i}\epsilon t/\hbar} G_{n,n_\ell}(t, \epsilon)\, \xi_\ell(\epsilon) \,, \tag{37}$$

which proves more convenient.

Below, we need for the elimination of back-scattering terms the relation

$$\begin{aligned}
G^\dagger(t, \epsilon') - G(t, \epsilon) &= \left(\mathrm{i}\hbar \frac{\mathrm{d}}{\mathrm{d}t} - \epsilon' + \epsilon\right) G^\dagger(t, \epsilon')G(t, \epsilon) \\
&\quad + \mathrm{i} \int_0^\infty \mathrm{d}\tau\, \mathrm{e}^{\mathrm{i}\epsilon\tau/\hbar} G^\dagger(t, \epsilon')\Gamma(\tau)G(t - \tau, \epsilon) \\
&\quad + \mathrm{i} \int_0^\infty \mathrm{d}\tau\, \mathrm{e}^{-\mathrm{i}\epsilon'\tau/\hbar} G^\dagger(t - \tau, \epsilon')\Gamma^\dagger(\tau)G(t, \epsilon) \,.
\end{aligned} \tag{38}$$

A proof of this relation starts from the definition of the Green function, Eq. (33). By Fourier transformation with respect to t', we obtain

$$\left(i\hbar \frac{d}{dt} + \epsilon - \mathscr{H}(t)\right) G(t, \epsilon) + i \int_0^\infty d\tau\, e^{i\epsilon\tau/\hbar} \Gamma(\tau) G(t - \tau, \epsilon) = \mathbf{1} \tag{39}$$

which we multiply by $G^\dagger(t, \epsilon')$ from the left. The difference between the resulting expression and its hermitian adjoint with ϵ and ϵ' interchanged is relation (38).

3.2. Current through the driven nanosystem

The (net) current flowing across the contact of lead ℓ into the conductor is determined by the negative change of the electron number in lead ℓ multiplied by the electron charge $-e$. Thus, the current operator reads $I_\ell = ie[H(t), N_\ell]/\hbar$, where $N_\ell = \sum_q c_{\ell q}^\dagger c_{\ell q}$ denotes the corresponding electron number. By using Eqs. (25) and (29), we obtain

$$\begin{aligned}
I_\ell(t) = &\frac{e}{\hbar} \int_0^\infty d\tau \{\Gamma_\ell(\tau) c_1^\dagger(t) c_1(t - \tau) + \Gamma_\ell^*(\tau) c_1^\dagger(t - \tau) c_1(t)\} \\
&- e\{c_1^\dagger(t)\xi_\ell(t) + \xi_\ell^\dagger(t)c_1(t)\} \ .
\end{aligned} \tag{40}$$

This operator-valued expression for the time-dependent current is a convenient starting point for the evaluation of expectation values like dc current, ac current, and current noise.

3.2.1. Average current

In order to evaluate the current $\langle I_L(t)\rangle$, we insert the solution (37) of the Heisenberg equation into the current operator (40) and use the expectation values (32). The resulting expression

$$\begin{aligned}
\langle I_L(t)\rangle = &\frac{e}{h} \sum_\ell \int d\epsilon \int_0^\infty d\tau \{e^{i\epsilon\tau/\hbar} G_{1\ell}^*(t, \epsilon) \Gamma_L(\tau) G_{1\ell}(t - \tau, \epsilon) \Gamma_\ell(\epsilon) f_\ell(\epsilon) \\
&+ e^{-i\epsilon\tau/\hbar} G_{1\ell}^*(t - \tau, \epsilon) \Gamma_L^*(\tau) G_{1\ell}(t, \epsilon) \Gamma_\ell(\epsilon) f_\ell(\epsilon)\} \\
&+ ie \int d\epsilon (G_{11}^*(t, \epsilon) - G_{11}(t, \epsilon)) \Gamma_L(\epsilon) f_L(\epsilon)
\end{aligned} \tag{41}$$

still contains back-scattering terms G_{11} and, thus, is not of a "scattering form". Indeed, bringing (41) into a form that resembles the static current formula (17) requires some tedious algebra. Such a derivation has been presented for the linear conductance of time-independent systems [131], for finite voltage in the static case for tunneling barriers [133] and mesoscopic conductors [134], a wire consisting of levels that couple equally to both leads [61], and for weak wire–lead coupling [59]. For the general time-dependent case in the absence of electron–electron interactions, such an expression has been *derived* only recently [66,67].

Inserting the matrix element $\langle 1|\ldots|1\rangle$ of Eq. (38), eliminates the back-scattering terms and we obtain for the time-dependent current the expression

$$\langle I_L(t)\rangle = \frac{e}{h} \int d\epsilon \{T_{LR}(t, \epsilon) f_R(\epsilon) - T_{RL}(t, \epsilon) f_L(\epsilon)\} - \frac{d}{dt} q_L(t) \ , \tag{42}$$

where

$$q_{\mathrm{L}}(t) = \frac{e}{2\pi} \int \mathrm{d}\epsilon \, \Gamma_{\mathrm{L}}(\epsilon) \sum_n |G_{n1}(t, \epsilon)|^2 f_{\mathrm{L}}(\epsilon) \tag{43}$$

denotes the charge oscillating between the left lead and the wire. Obviously, since $q_{\mathrm{L}}(t)$ is time-periodic and bounded, its time derivative cannot contribute to the average current. The corresponding charge arising from the right lead, $q_{\mathrm{R}}(t)$, is a priori unrelated to $q_{\mathrm{L}}(t)$; the actual charge on the wire reads $q_{\mathrm{L}}(t) + q_{\mathrm{R}}(t)$. The time-dependent current is determined by the time-dependent transmission

$$T_{\mathrm{LR}}(t, \epsilon) = 2 \, \mathrm{Re} \int_0^\infty \mathrm{d}\tau \, \mathrm{e}^{\mathrm{i}\epsilon\tau/\hbar} \Gamma_{\mathrm{L}}(\tau) G_{1N}^*(t, \epsilon) G_{1N}(t - \tau, \epsilon) \Gamma_{\mathrm{R}}(\epsilon) \; . \tag{44}$$

The corresponding expression for $T_{\mathrm{RL}}(t, \epsilon)$ follows from the replacement $(\mathrm{L}, 1) \leftrightarrow (\mathrm{R}, N)$. We emphasize that (42) obeys the form of the current formula obtained for a *static* conductor within a scattering formalism. The time-dependent transmission (44) denotes the probability that an electron coming from the right lead with the initial energy ϵ is situated at the final time t in the left lead. Moreover, consistent with Refs. [51,58,59], no "Pauli blocking factors" $(1 - f_\ell)$ appear in our derivation. In contrast to a static situation, this is in the present context relevant since for a driven system generally

$$T_{\mathrm{RL}}(t, \epsilon) \neq T_{\mathrm{LR}}(t, \epsilon) \tag{45}$$

such that a contribution proportional to $f_{\mathrm{L}}(\epsilon_{q'}) f_{\mathrm{R}}(\epsilon_q)$ would not cancel [59,60].

In order to obtain an expression for the dc current, we insert for the Green function the Fourier representation (35) followed by performing the average over time t. Then, the average current becomes

$$\bar{I} = \frac{e}{h} \sum_{k=-\infty}^\infty \int \mathrm{d}\epsilon \left\{ T_{\mathrm{LR}}^{(k)}(\epsilon) f_{\mathrm{R}}(\epsilon) - T_{\mathrm{RL}}^{(k)}(\epsilon) f_{\mathrm{L}}(\epsilon) \right\} \; , \tag{46}$$

where

$$T_{\mathrm{LR}}^{(k)}(\epsilon) = \Gamma_{\mathrm{L}}(\epsilon + k\hbar\Omega) \Gamma_{\mathrm{R}}(\epsilon) |G_{1N}^{(k)}(\epsilon)|^2 \; , \tag{47}$$

$$T_{\mathrm{RL}}^{(k)}(\epsilon) = \Gamma_{\mathrm{R}}(\epsilon + k\hbar\Omega) \Gamma_{\mathrm{L}}(\epsilon) |G_{N1}^{(k)}(\epsilon)|^2 \; , \tag{48}$$

denote the transmission probabilities for electrons from the right lead, respectively, from the left lead, with initial energy ϵ and final energy $\epsilon + k\hbar\Omega$, i.e., the probability for an scattering event under the absorption (emission) of $|k|$ photons if $k > 0$ ($k < 0$).

For a static situation, the transmission probabilities $T_{\mathrm{LR}}^{(k)}(\epsilon)$ and $T_{\mathrm{RL}}^{(k)}(\epsilon)$ are identical and contributions with $k \neq 0$ vanish. Thus, it is possible to write the current (46) in the form (17) as a product of a *single* transmission probability $T(\epsilon)$, which is independent of the direction, and the difference of the Fermi functions, $f_{\mathrm{R}}(\epsilon) - f_{\mathrm{L}}(\epsilon)$. We emphasize that in the driven case this is no longer true.

We close this section by noting that for a wire Hamiltonian that includes electron–electron interaction, the current formula (41) is still valid, but generally can no longer be expressed in terms of a scattering formula that resembles Eq. (42).

3.2.2. Noise power

Like in the static case, we characterize the noise power by the zero-frequency component of the current–current correlation function (19). However, in the driven case, $S_\ell(t, t') = S_\ell(t + \mathcal{T}, t' + \mathcal{T})$ is still time-dependent. Since it shares the time-periodicity of the driving, it is possible to characterize the noise level by the zero-frequency component of $S_\ell(t, t - \tau)$ averaged over the driving period,

$$\bar{S}_\ell = \frac{1}{\mathcal{T}} \int_0^{\mathcal{T}} dt \int_{-\infty}^{+\infty} d\tau \, S_\ell(t, t - \tau) \; . \tag{49}$$

It can be shown [67] that for driven two-terminal devices, $\bar{S}_\ell$ is independent of the contact ℓ, i.e., $\bar{S}_L = \bar{S}_R \equiv \bar{S}$.

We start by writing $S_L(t, t - \tau)$ with the current operator (40) and insert the solution (37) of the Heisenberg equations. We again employ relation (38) and finally obtain

$$\bar{S} = \frac{e^2}{h} \sum_k \int d\epsilon \left\{ \Gamma_R(\epsilon^{(k)}) \Gamma_R(\epsilon) \left| \sum_{k'} \Gamma_L(\epsilon^{(k')}) G_{1N}^{(k'-k)}(\epsilon^{(k)}) [G_{1N}^{(k')}(\epsilon)]^* \right|^2 f_R(\epsilon) \bar{f}_R(\epsilon^{(k)}) \right.$$

$$\left. + \Gamma_R(\epsilon^{(k)}) \Gamma_L(\epsilon) \left| \sum_{k'} \Gamma_L(\epsilon^{(k')}) G_{1N}^{(k'-k)}(\epsilon^{(k)}) [G_{11}^{(k')}(\epsilon)]^* - i G_{1N}^{(-k)}(\epsilon^{(k)}) \right|^2 f_L(\epsilon) \bar{f}_R(\epsilon^{(k)}) \right\}$$

$$+ \text{ same terms with the replacement } (L, 1) \leftrightarrow (R, N) \; . \tag{50}$$

We have defined $\epsilon^{(k)} = \epsilon + k\hbar\Omega$ and $\bar{f}_\ell = 1 - f_\ell$. It can be shown (cf. Section 3.5.1) that in the undriven limit, the noise power (50) depends solely on the transmission *probabilities* and is given by Eq. (21). In the time-dependent case, however, the noise expression (50) cannot be brought into such a convenient form and, thus, generally depends on the phase of the transmission amplitude.

3.2.3. Floquet decomposition

For energy-independent wire–lead coupling, i.e., in the so-called wide-band limit $\Gamma_\ell(\epsilon) = \Gamma_\ell$ the lead response function (28) reads $\Gamma_\ell(t) = \Gamma_\ell \delta(t)$. Consequently, the integro-differential equation (33) for the Green function becomes a pure differential equation. Then, determining the Green function is equivalent to computing a complete set of solutions for the equation

$$i\hbar \frac{d}{dt} |\psi(t)\rangle = (\mathcal{H}_{\text{wire}}(t) - i\Sigma) |\psi(t)\rangle \; , \tag{51}$$

where the self-energy

$$\Sigma = |1\rangle \frac{\Gamma_L}{2} \langle 1| + |N\rangle \frac{\Gamma_R}{2} \langle N| \tag{52}$$

results from the coupling to the leads. Eq. (51) is linear and possesses time-dependent, $\mathcal{T}$-periodic coefficients. Thus, following the reasoning of Appendix A, it is possible to construct a complete solution

with the Floquet ansatz

$$|\psi_\alpha(t)\rangle = \exp[(-i\epsilon_\alpha/\hbar - \gamma_\alpha)t]|u_\alpha(t)\rangle \ , \tag{53}$$

$$|u_\alpha(t)\rangle = \sum_k |u_{\alpha,k}\rangle \exp(-ik\Omega t) \ . \tag{54}$$

The so-called Floquet states $|u_\alpha(t)\rangle$ obey the time-periodicity of $\mathscr{H}_{\text{wire}}(t)$ and have been decomposed into a Fourier series. In a Hilbert space that is extended by a periodic time coordinate, the so-called Sambe space [144], they obey the Floquet eigenvalue equation [145,146]

$$\left(\mathscr{H}_{\text{wire}}(t) - i\Sigma - i\hbar \frac{d}{dt}\right)|u_\alpha(t)\rangle = (\epsilon_\alpha - i\hbar\gamma_\alpha)|u_\alpha(t)\rangle \ . \tag{55}$$

Due to the Brillouin zone structure of the Floquet spectrum [144–147], it is sufficient to compute all eigenvalues of the first Brillouin zone, $-\hbar\Omega/2 < \epsilon_\alpha \leqslant \hbar\Omega/2$. Since the operator on the l.h.s. of Eq. (55) is non-Hermitian, the eigenvalues $\epsilon_\alpha - i\hbar\gamma_\alpha$ are generally complex valued and the (right) eigenvectors are not mutually orthogonal. Thus, to determine the propagator, we also need to solve the adjoint Floquet equation $(\mathscr{H}_{\text{wire}}(t) + i\Sigma - i\hbar d/dt)|u_\alpha^+(t)\rangle = (\epsilon_\alpha + i\hbar\gamma_\alpha)|u_\alpha^+(t)\rangle$ yielding the complex conjugate eigenvalues and the adjoint eigenvectors $|u_\alpha^+(t)\rangle$. It can be shown that the Floquet states $|u_\alpha(t)\rangle$ together with the adjoint states $|u_\alpha^+(t)\rangle$ form at equal times a complete bi-orthogonal basis: $\langle u_\alpha^+(t)|u_\beta(t)\rangle = \delta_{\alpha\beta}$ and $\sum_\alpha |u_\alpha(t)\rangle\langle u_\alpha^+(t)| = 1$. A proof requires to account for the time-periodicity of the Floquet states since the eigenvalue equation (55) holds in a Hilbert space extended by a periodic time coordinate [145,148]. For details, see Appendix A.

For the special case [62] of a wire with $N = 2$ sites which couple equally strong to both leads, i.e., $\Gamma_L = \Gamma_R$, the self-energy is proportional to the unity matrix. Consequently, the Floquet states $|u_\alpha^+(t)\rangle$ become independent of the self-energy which manifests itself solely by a broadening of the quasienergies.

Using the Floquet equation (55), it is straightforward to show that with the help of the Floquet states $|u_\alpha(t)\rangle$ the propagator can be written as

$$U(t, t') = \sum_\alpha e^{-i(\epsilon_\alpha/\hbar - i\gamma_\alpha)(t-t')}|u_\alpha(t)\rangle\langle u_\alpha^+(t')| \ , \tag{56}$$

where the sum runs over all Floquet states within one Brillouin zone. Consequently, the Fourier coefficients of the Green function read

$$G^{(k)}(\epsilon) = -\frac{i}{\hbar} \int_0^{\mathscr{T}} \frac{dt}{\mathscr{T}} e^{ik\Omega t} \int_0^\infty d\tau \, e^{i\epsilon\tau/\hbar} U(t, t - \tau) \tag{57}$$

$$= \sum_{\alpha,k'} \frac{|u_{\alpha,k'+k}\rangle\langle u_{\alpha,k'}^+|}{\epsilon - (\epsilon_\alpha + k'\hbar\Omega - i\hbar\gamma_\alpha)} \ . \tag{58}$$

For the exact computation of current and noise, we solve numerically the Floquet equation (55). With the resulting Floquet states and quasienergies, we obtain the Green function (35). In the zero temperature limit, the Fermi functions in the expressions for the average current (46) and the zero-frequency noise (50) become step functions. Then, the remaining energy integrals can be performed analytically since the integrands are rational functions.

3.3. Symmetries

A system obeys a discrete symmetry if its Hamiltonian is invariant under a symmetry operation $\mathscr{S} = (\mathscr{S}^+)^{-1}$, i.e., if $\mathscr{S}^+ H(t)\mathscr{S} = H(t)$. Then the transformed propagator $\widetilde{U}(t, t') = \mathscr{S}^+ U(t, t')\mathscr{S}$ obeys the equation of motion $\pm i\hbar \, d\widetilde{U}(t, t')/dt = H(t)\widetilde{U}(t, t')$, where the minus sign applies if the symmetry operation $\mathscr{S}$ includes time-inversion. Integrating this equation formally and comparing it to the corresponding expression for $U(t, t')$, yields for the transition amplitude in position representation the relation

$$\langle x|\widetilde{U}(t, t')|x'\rangle = \langle x|\mathscr{S}^+ U(t, t')\mathscr{S}|x'\rangle = \langle x|U(t, t')|x'\rangle^{(*)} \ . \tag{59}$$

This implies that the corresponding transmission *probabilities* are identical. The complex conjugation in Eq. (59) holds in the case in which the equation of motion contains a minus sign, i.e., it reflects time inversion [149]; in that case, the r.h.s. becomes $\langle x'|U(t', t)|x\rangle$. If $\mathscr{S}|x'\rangle \neq |x\rangle$, relation (59) states that two *different* scattering processes occur with the same probability. Correspondingly, in a time-dependent transport problem as defined by the Hamiltonian (1), the presence of a symmetry implies that two different transport channels have equal transmission probability.

Here, we identify the channel which is related to $T_{\mathrm{LR}}^{(k)}(\epsilon)$ given a certain symmetry is present. In particular, we consider systems that are invariant under the transformations studied in the Appendix A.3, which are combinations of the transformations

$$\mathscr{S}_{\mathrm{P}} : x \to -x \ , \tag{60}$$

$$\mathscr{S}_{\mathrm{T}} : t \to -t \ , \tag{61}$$

$$\mathscr{S}_{\mathrm{G}} : t \to t + \mathscr{T}/2 \ . \tag{62}$$

For the tight-binding model sketched in Fig. 1, the parity operation (60) maps the lead states and the wire sites according to

$$\mathscr{S}_{\mathrm{P}} : (\mathrm{L}q, n) \leftrightarrow (\mathrm{R}q, N + 1 - n) \ , \tag{63}$$

where $n = 1, \ldots, N$ labels the wire sites and $\mathrm{L}q$ ($\mathrm{R}q$) the states in the left (right) lead. Both the parity $\mathscr{S}_{\mathrm{P}}$ and the time inversion $\mathscr{S}_{\mathrm{T}}$ can be generalized by an additional shift of position and time, respectively. Alternatively, one can place the origin of the corresponding axis properly. For convenience, we choose the latter option.

It should be mentioned that for the periodic driving considered in this work, the system contains a further symmetry, namely the time-translation by a full driving period. This has already been taken into account when deriving a Floquet transport theory and cannot be exploited further.

3.3.1. Time-reversal symmetry

If the Hamiltonian obeys time-reversal symmetry $\mathscr{S}_{\mathrm{T}}$, i.e., if $H(t) = H(-t)$, Eq. (59) yields $\langle 1|U(t, t')|N\rangle = \langle N|U(-t', -t)|1\rangle$. Inserting into the definition of the Green function $G^{(k)}(\epsilon)$, Eqs. (34) and (35), results in the relation $G_{1N}^{(k)}(\epsilon) = G_{N1}^{(-k)}(\epsilon + k\hbar\Omega)$, where we have shifted the limits of
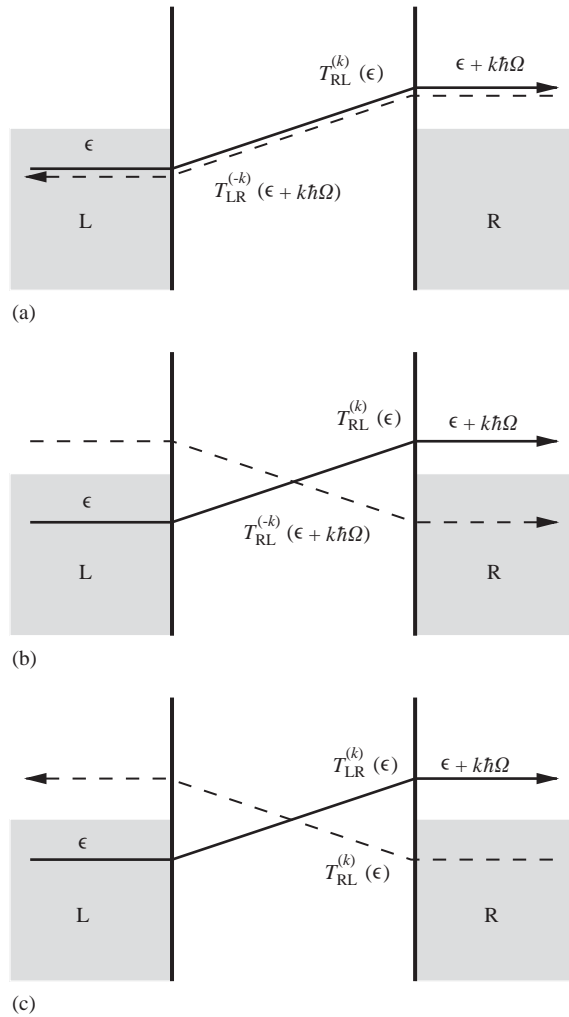
Fig. 2. Transmission of an electron with energy ϵ under the absorption of k photons (solid line) and its symmetry related process (dashed) for (a) time-reversal symmetry, (b) time-reversal parity, and (c) generalized parity. The sketched processes occur with equal probability.

the t-integration using the relation $G(t, \epsilon) = G(t + \mathcal{T}, \epsilon)$. Thus, the transmission probabilities obey

$$T_{RL}^{(k)}(\epsilon) = T_{LR}^{(-k)}(\epsilon + k\hbar\Omega) \ , \tag{64}$$

i.e., the scattering processes sketched in Fig. 2a occur with equal probability.

A time-independent system in the absence of magnetic fields represents a particular case of time-reversal symmetry since all transmissions probabilities with $k \neq 0$ vanish and, thus, $T_{RL}^{(0)}(\epsilon) = T_{LR}^{(0)}(\epsilon) = T(\epsilon)$.

3.3.2. Time-reversal parity

Systems driven by a dipole force with purely harmonic time-dependence obey the so-called time-reversal parity $\mathscr{S}_{TP} = \mathscr{S}_T\mathscr{S}_P : (x,t) \to (-x,-t)$, i.e., a combination of time-reversal symmetry and parity. This of course implies that the static part of the Hamiltonian has to obey spatial parity which requires identical wire–lead couplings, $\Gamma_L(\epsilon) = \Gamma_R(\epsilon)$. The consequences for the Floquet states are discussed in the Appendix A.3 while here, we derive the consequences for the transmission probabilities.

By the same reasoning as in the case of time-reversal symmetry discussed above, but with additionally interchanging left and right, we find $G_{1N}^{(k)}(\epsilon) = G_{1N}^{(-k)}(\epsilon + k\hbar\Omega)$ which yields equal transmission probabilities for the scattering events sketched in Fig. 2b, i.e.,

$$T_{RL}^{(k)}(\epsilon) = T_{RL}^{(-k)}(\epsilon + k\hbar\Omega) \ . \tag{65}$$

Interestingly, time-reversal parity relates two scattering events that both go into the same direction. Therefore, relation (65) has no obvious consequence for the dc current. Still time-reversal parity entails an intriguing and more hidden consequence for non-adiabatic electron pumping by harmonic mixing as a function of the wire–lead coupling [68]. We discuss this effect in the context of non-adiabatic electron pumping in Section 6.3.

3.3.3. Generalized parity

A further spatio-temporal symmetry that has an impact on the transmission properties is the so-called generalized parity $\mathscr{S}_{GP} = \mathscr{S}_G\mathscr{S}_P : (x,t) \to (-x, t+\mathscr{T}/2)$, i.e., a parity operation combined with a time shift by half a driving period. This symmetry also explains qualitatively the quasienergy spectra found in the context of driven quantum tunneling [88,89,150,151].

If the wire–lead Hamiltonian is invariant under $\mathscr{S}_{GP}$, the time evolution operator obeys $\langle 1|U(t,t')|N\rangle = \langle N|U(t+\mathscr{T}/2, t'+\mathscr{T}/2)|1\rangle$. Inserting into Eq. (34) results in $G_{1N}^{(k)}(\epsilon) = G_{N1}^{(k)}(\epsilon)$ and, thus, the scattering events sketched in Fig. 2c obey

$$T_{RL}^{(k)}(\epsilon) = T_{LR}^{(k)}(\epsilon) \ . \tag{66}$$

Again, we have shifted the integration limits by using the time-periodicity of the Green function $G(t,\epsilon)$.

3.4. Approximations

In Section 3.2, expressions for the current and the noise power have been derived for a periodic but otherwise arbitrary driving. Within the wide-band limit, both quantities can be expressed in terms of the solutions of the Floquet equation (55), i.e., the solution of a non-Hermitian eigenvalue problem in an extended Hilbert space. Thus, for large systems, the numerical computation of the Floquet states can be rather costly. Moreover, for finite temperatures, the energy integration in the expressions (46) and (50) have to be performed numerically. Therefore, approximation schemes which allow a more efficient computation are of much practical use.

3.4.1. Weak-coupling limit

In the limit of a weak wire–lead coupling, i.e., for coupling constants Γ_ℓ which are far lower than all other energy scales of the wire Hamiltonian, it is possible to derive within a master equation approach a closed expression for the dc current [68]; cf. Section 4. The corresponding approximation within the

present Floquet approach is based on treating the self-energy contribution $-i\Sigma$ in the non-Hermitian Floquet equation (55) as a perturbation. Then, the zeroth order of the Floquet equation

$$\left(\mathscr{H}_{\text{wire}}(t) - i\hbar \frac{d}{dt} \right) |\phi_\alpha(t)\rangle = \epsilon_\alpha^0 |\phi_\alpha(t)\rangle \tag{67}$$

describes the driven wire in the absence of the leads, where $|\phi_\alpha(t)\rangle = \sum_k \exp(-ik\Omega t)|\phi_{\alpha,k}\rangle$ are the "usual" Floquet states with quasienergies ϵ_α^0. In the absence of degeneracies the first-order correction to the quasienergies is $-i\hbar\gamma_\alpha^1$ where

$$\gamma_\alpha^1 = \frac{1}{\hbar} \int_0^{\mathscr{T}} \frac{dt}{\mathscr{T}} \langle\phi_\alpha(t)|\Sigma|\phi_\alpha(t)\rangle \tag{68}$$

$$= \frac{\Gamma_L}{2\hbar} \sum_k |\langle 1|\phi_{\alpha,k}\rangle|^2 + \frac{\Gamma_R}{2\hbar} \sum_k |\langle N|\phi_{\alpha,k}\rangle|^2 . \tag{69}$$

Within the first-order approximation for the current and the noise, it is consistent to consider only the corrections of the quasienergies and to neglect the first-order correction of the Floquet states. Thus, the unperturbed Floquet states $|u_\alpha(t)\rangle = |u_\alpha^+(t)\rangle = |\phi_\alpha(t)\rangle$ are already sufficient for the present purpose. Consequently, the transmission probability (47) assumes the form [67]

$$T_{\text{LR}}^{(k)}(\epsilon) = \Gamma_L \Gamma_R \sum_{\alpha,\beta,k',k''} \frac{\langle N|\phi_{\alpha,k'}\rangle\langle\phi_{\alpha,k'+k}|1\rangle\langle 1|\phi_{\beta,k''+k}\rangle\langle\phi_{\beta,k''}|N\rangle}{[\epsilon - (\epsilon_\alpha^0 + k'\hbar\Omega + i\hbar\gamma_\alpha^1)][\epsilon - (\epsilon_\beta^0 + k''\hbar\Omega - i\hbar\gamma_\beta^1)]} \tag{70}$$

and $T_{\text{RL}}^{(k)}(\epsilon)$ accordingly. The transmission probability (70) exhibits for small values of Γ_ℓ sharp peaks at energies $\epsilon_\alpha^0 + k'\hbar\Omega$ and $\epsilon_\beta^0 + k''\hbar\Omega$ with widths $\hbar\gamma_\alpha^1$ and $\hbar\gamma_\beta^1$. Therefore, the relevant contributions to the sum come from terms for which the peaks of both factors coincide and, in the absence of degeneracies in the quasienergy spectrum, we keep only terms with

$$\alpha = \beta, \quad k' = k'' . \tag{71}$$

Then provided that γ_α^1 is small, the fraction in (70) is a Lorentzian and can be approximated by $\pi\delta(\epsilon - \epsilon_\alpha^0 - k'\hbar\Omega)/\hbar\gamma_\alpha^1$ yielding the transmission probability

$$T_{\text{LR}}^{(k)}(\epsilon) = \Gamma_L\Gamma_R \sum_{\alpha,k'} \frac{\pi}{\hbar\gamma_\alpha^1} |\langle 1|\phi_{\alpha,k'+k}\rangle\langle\phi_{\alpha,k'}|N\rangle|^2 \delta(\epsilon - \epsilon_\alpha^0 + k'\hbar\Omega) \tag{72}$$

$$= T_{\text{RL}}^{(-k)}(\epsilon + k\hbar\Omega) . \tag{73}$$

The last line follows by substituting $k' \to k' - k$. Note that Eq. (73) is identical to Eq. (64). This means that within the weak-coupling limit, even in the absence of any symmetry, the transmission behaves as if the system was time-reversal symmetric.

The energy integration in (46) can now be performed even for finite temperature and we obtain for the dc current the expression

$$\bar{I} = \frac{e}{\hbar} \sum_{\alpha,k,k'} \frac{\Gamma_{L\alpha k}\Gamma_{R\alpha k'}}{\Gamma_{L\alpha} + \Gamma_{R\alpha}} [f_R(\epsilon_\alpha^0 + k'\hbar\Omega) - f_L(\epsilon_\alpha^0 + k\hbar\Omega)] . \tag{74}$$

The coefficients

$$\Gamma_{\text{L}\alpha k} = \Gamma_{\text{L}} |\langle 1 | \phi_{\alpha,k} \rangle|^2, \quad \Gamma_{\text{L}\alpha} = \sum_k \Gamma_{\text{L}\alpha k} \ , \tag{75}$$

$$\Gamma_{\text{R}\alpha k} = \Gamma_{\text{R}} |\langle N | \phi_{\alpha,k} \rangle|^2, \quad \Gamma_{\text{R}\alpha} = \sum_k \Gamma_{\text{R}\alpha k} \ , \tag{76}$$

denote the overlap of the kth sideband $|\phi_{\alpha,k}\rangle$ of the Floquet state $|\phi_\alpha(t)\rangle$ with the first site and the last site of the wire, respectively. We have used $2\hbar\gamma_\alpha^1 = \Gamma_{\text{L}\alpha} + \Gamma_{\text{R}\alpha}$ which follows from (69). Expression (74) can been derived also within a rotating-wave approximation of a Floquet master equation approach [68]; cf. Section 4.3.

Within the same approximation, we expand the zero-frequency noise (50) to lowest-order in Γ_ℓ: after inserting the spectral representation (58) of the Green function, we again keep only terms with identical Floquet index α and identical sideband index k to obtain

$$\begin{aligned}
\bar{S} = \frac{e^2}{\hbar} \sum_{\alpha,k,k'} \frac{\Gamma_{\text{R}\alpha k'} \bar{f}_{\text{R}}(\epsilon_\alpha^0 + k'\hbar\Omega)}{(\Gamma_{\text{L}\alpha} + \Gamma_{\text{R}\alpha})^3} & \left\{ 2\Gamma_{\text{L}\alpha}^2 \Gamma_{\text{R}\alpha k} f_{\text{R}}(\epsilon_\alpha^0 + k\hbar\Omega) \right. \\
& \left. + (\Gamma_{\text{L}\alpha}^2 + \Gamma_{\text{R}\alpha}^2) \Gamma_{\text{L}\alpha k} f_{\text{L}}(\epsilon_\alpha^0 + k\hbar\Omega) \right\} \\
& + \text{same terms with the replacement } \text{L} \leftrightarrow \text{R} \ .
\end{aligned} \tag{77}$$

Of particular interest for the comparison to the static situation is the limit of a large applied voltage such that practically $f_{\text{R}} = 1$ and $f_{\text{L}} = 0$. Then, in Eqs. (74) and (77), the sums over the sideband indices k can be carried out such that

$$\bar{I}_\infty = \frac{e}{\hbar} \sum_\alpha \frac{\Gamma_{\text{L}\alpha} \Gamma_{\text{R}\alpha}}{\Gamma_{\text{L}\alpha} + \Gamma_{\text{R}\alpha}} \ , \tag{78}$$

$$\bar{S}_\infty = \frac{e^2}{\hbar} \sum_\alpha \frac{\Gamma_{\text{L}\alpha} \Gamma_{\text{R}\alpha} (\Gamma_{\text{L}\alpha}^2 + \Gamma_{\text{R}\alpha}^2)}{(\Gamma_{\text{L}\alpha} + \Gamma_{\text{R}\alpha})^3} \ . \tag{79}$$

These expressions resemble the corresponding expressions for the transport across a *static* double barrier [54]. If now $\Gamma_{\text{L}\alpha} = \Gamma_{\text{R}\alpha}$ for all Floquet states $|\phi_\alpha(t)\rangle$, we find $F = \frac{1}{2}$. This is in particular the case for systems obeying reflection symmetry. In the presence of such symmetries, however, the existence of exact crossings, i.e., degeneracies, limits the applicability of the weak-coupling approximation and a master equation approach (cf. Section 4) is more appropriate.

3.4.2. High-frequency limit

Many effects occurring in driven quantum systems, such as coherent destruction of tunneling [88] or current and noise control [66,93], are most pronounced for a large excitation frequency Ω. Thus, it is particularly interesting to derive for the present Floquet approach an expansion in terms of $1/\Omega$. Thereby, the driven system will be approximated by a static system with renormalized parameters. Such a perturbation scheme has been developed for two-level systems in Ref. [147] and applied to driven tunneling in bistable systems [89] and superlattices [151]. For open quantum system, the coupling to the external degrees of freedom (e.g., the leads or a heat bath) bears additional complications that have been solved heuristically in Ref. [94] by replacing the Fermi functions by effective electron distributions.

In the following, we present a rigorous derivation of this approach based on a perturbation theory for the Floquet equation (55).

We assume a driving that leaves all off-diagonal matrix elements of the wire Hamiltonian time-independent while the tight-binding levels undergo a position-dependent, time-periodic driving $f_n(t) = f_n(t + \mathcal{T})$ with zero time-average. Then, the wire Hamiltonian is of the form

$$\mathscr{H}_{\mathrm{wire}}(t) = \mathscr{H}_0 + \sum_n f_n(t)|n\rangle\langle n| \; . \tag{80}$$

If $\hbar\Omega$ represents the largest energy scale of the problem, we can in the Floquet equation (55) treat the *static* part of the Hamiltonian as a perturbation. Correspondingly, the eigenfunctions of the operator $\sum_n f_n(t)|n\rangle\langle n| - \mathrm{i}\hbar\, \mathrm{d}/\mathrm{d}t$ determine the zeroth-order Floquet states

$$\mathrm{e}^{-\mathrm{i}F_n(t)}|n\rangle \; . \tag{81}$$

We have defined the accumulated phase

$$F_n(t) = \frac{1}{\hbar}\int_0^t \mathrm{d}t'\, f_n(t') = F_n(t + \mathcal{T}) \; , \tag{82}$$

which is $\mathcal{T}$-periodic due to the zero time-average of $f_n(t)$. As a consequence of this periodicity, to zeroth order the quasienergies are zero (mod $\hbar\Omega$) and the Floquet spectrum is given by multiples of the photon energy, $k\hbar\Omega$. Each $k = 0, \pm 1, \pm 2, \ldots$ defines a degenerate subspace of the extended Hilbert space. If now $\hbar\Omega$ is larger than all other energy scales, the first-order correction to the Floquet states and the quasienergies can be calculated by diagonalizing the perturbation in the subspace defined by $k = 0$. Thus, we have to solve the time-independent eigenvalue equation

$$(\mathscr{H}_{\mathrm{eff}} - \mathrm{i}\Sigma)|\alpha\rangle = (\epsilon_\alpha^1 - \mathrm{i}\hbar\gamma_\alpha^1)|\alpha\rangle \; . \tag{83}$$

The static effective Hamiltonian $\mathscr{H}_{\mathrm{eff}}$ is defined by the matrix elements of the original static Hamiltonian $\mathscr{H}_0$ with the zeroth-order Floquet states (81),

$$(\mathscr{H}_{\mathrm{eff}})_{nn'} = \int_0^{\mathcal{T}} \frac{\mathrm{d}t}{\mathcal{T}}\, \mathrm{e}^{\mathrm{i}F_n(t)}(\mathscr{H}_0)_{nn'}\mathrm{e}^{-\mathrm{i}F_{n'}(t)} \; . \tag{84}$$

The t-integration constitutes the inner product in the Hilbert space extended by a periodic time coordinate [144] (for details, see Appendix A.2). To first order in $1/\Omega$, the quasienergies $\epsilon_\alpha^1 - \mathrm{i}\hbar\gamma_\alpha^1$ are given by the eigenvalues of the static equation (83) and, consequently, the corresponding Floquet states read

$$|u_\alpha(t)\rangle = \sum_n \mathrm{e}^{-\mathrm{i}F_n(t)}|n\rangle\langle n|\alpha\rangle \; . \tag{85}$$

The fact that all $F_n(t)$ are $\mathcal{T}$-periodic, allows one to write in (85) the time-dependent phase factor as a Fourier series,

$$\mathrm{e}^{-\mathrm{i}F_n(t)} = \sum_k a_{n,k}\mathrm{e}^{-\mathrm{i}k\Omega t} \; . \tag{86}$$

Thus, $\langle n|u_{\alpha,k}\rangle = a_{n,k}\langle n|\alpha\rangle$ and the Green function for the high-frequency driving reads

$$G_{nn'}^{(k)}(\epsilon) = \sum_{k'} a_{n,k'+k}a_{n',k'}^* G_{nn'}^{\mathrm{eff}}(\epsilon - k'\hbar\Omega) \; , \tag{87}$$

where $G^{\text{eff}}(\epsilon)$ denotes the Green function corresponding to the static Hamiltonian $\mathscr{H}_{\text{eff}}$ with the self-energy Σ. Finally, substituting $\epsilon \to \epsilon + k'\hbar\Omega$ and using the sum rule $\sum_{k'} a_{n,k+k'} a_{n,k'}^* = \delta_{k,0}$, we obtain

$$\bar{I} = \frac{e}{h} \int d\epsilon \, T_{\text{eff}}(\epsilon) \{ f_{\text{R,eff}}(\epsilon) - f_{\text{L,eff}}(\epsilon) \} \; . \tag{88}$$

The effective transmission probability $T_{\text{eff}}(\epsilon) = \Gamma_{\text{L}} \Gamma_{\text{R}} |G_{1N}^{\text{eff}}(\epsilon)|^2$ is computed from the effective Hamiltonian (84); the electron distribution is given by

$$f_{\text{L,eff}}(\epsilon) = \sum_k |a_{1,k}|^2 f_{\text{L}}(\epsilon + k\hbar\Omega) \tag{89}$$

and $f_{\text{R,eff}}$ follows from the replacement $(1, \text{L}) \to (N, \text{R})$. Note that for a purely harmonic driving, $a(t) \propto \cos(\Omega t)$, the coefficients $a_{n,k}$ are given by Bessel functions of the first kind; cf. the specific example in Section 7.2.

In order to derive a high-frequency approximation for the zero-frequency noise $\bar{S}$, we insert (87) into (50) and neglect products of the type $G^{\text{eff}}(\epsilon - k\hbar\Omega) G^{\text{eff}}(\epsilon - k'\hbar\Omega)$ for $k \neq k'$. Employing the above sum rule for the Fourier coefficients $a_{n,k}$, we obtain for the noise the static expression (21), but with the transmission probability $T(\epsilon)$ and the Fermi functions $f_{\text{R,L}}(\epsilon)$ replaced by the effective transmission probability $T_{\text{eff}}(\epsilon)$ and the effective distribution function (89), respectively.

Note that in general, $a_{1,k} \neq a_{N,k}$ such that $f_{\text{R,eff}} \neq f_{\text{L,eff}}$. This means that the driving can create an effective bias and thereby create a non-adiabatic pump current. Moreover, if all F_n are identical, the phase factors in (84) cancel each other and the effective Hamiltonian $\mathscr{H}_{\text{eff}}$ equals the original static Hamiltonian.

3.4.3. Linear-response limit

For small driving amplitudes, it is often sufficient to treat the driving in the linear-response limit [152]. In doing so, we denote by $g(t - t')$ the undriven limit of the Green function $G(t, t')$ and by $\mathscr{H}_1(t)$ the time-dependent part of the Hamiltonian which is considered as a perturbation. Then, a formal solution of Eq. (33) is given by the Dyson equation

$$G(t, t - \tau) = g(\tau) + \int_{-\infty}^{+\infty} dt' \, g(t - t') \mathscr{H}_1(t') G(t', t - \tau) \; , \tag{90}$$

as can be shown by inserting (90) into (33). A self-consistent solution of this equation has been presented by Brandes [153]. Here, we restrict ourselves to the lowest order in the driving and, thus, can replace in the integral $G(t', t - \tau)$ by $g(t' - t + \tau)$. Inserting moreover the Fourier representations

$$\mathscr{H}_1(t) = \int \frac{d\omega}{2\pi} e^{-i\omega t} \mathscr{H}_1(\omega) \; , \tag{91}$$

$$g(t) = \int \frac{d\epsilon}{2\pi\hbar} e^{-i\epsilon t/\hbar} g(\epsilon) \tag{92}$$

and Eq. (34), we obtain

$$G(t, \epsilon) = g(\epsilon) + \int \frac{d\omega}{2\pi} \, e^{-i\omega t} g(\epsilon + \hbar\omega) \mathscr{H}_1(\omega) g(\epsilon) \ . \tag{93}$$

For purely harmonic driving, $\mathscr{H}_1(t) = \mathscr{H}_1 \cos(\Omega t)$, one finds for the Fourier coefficients (35) of the Green function the expressions

$$G^{(0)}(\epsilon) = g(\epsilon) \ , \tag{94}$$

$$G^{(\pm 1)}(\epsilon) = \tfrac{1}{2} g(\epsilon \pm \hbar\Omega) \mathscr{H}_1 g(\epsilon) \ , \tag{95}$$

while all Fourier components $G^{(k)}$ with $|k| > 1$ vanish to linear order. Consequently, the elastic transmission probability $T^{(0)}(\epsilon)$ is independent of the driving, i.e., it equals the result in the absence of external driving. The transmission probabilities under emission/absorption of a single photon are, however, proportional to the intensity of the driving field, i.e., $\propto |\mathscr{H}_1|^2$, and read

$$T_{\mathrm{LR}}^{(\pm 1)}(\epsilon) = \Gamma_{\mathrm{L}}(\epsilon \pm \hbar\Omega) \Gamma_{\mathrm{R}}(\epsilon) |\langle 1| g(\epsilon \pm \hbar\Omega) \mathscr{H}_1 g(\epsilon)|N\rangle|^2 \ . \tag{96}$$

$T_{\mathrm{RL}}^{(\pm 1)}(\epsilon)$ follows from the replacement $(\mathrm{L}, 1) \leftrightarrow (\mathrm{R}, N)$.

3.5. Special cases

In some special cases, the results of our Floquet approach reduce to simpler expressions. In particular, this is the case for zero driving amplitude, i.e., in the absence of driving, and for a driving that results from a time-dependent gate voltage and, thus, is homogeneous along the wire.

3.5.1. Static conductor and adiabatic limit

For consistency, the expressions (46) and (50) for the dc current and the zero-frequency noise, respectively, must coincide in the undriven limit with the corresponding expressions of the time-independent scattering theory, Eqs. (17) and (21), respectively. This is indeed the case because the static situation is characterized by two relations: first, in the absence of spin-dependent interactions, we have time-reversal symmetry and therefore $T_{\mathrm{LR}}(\epsilon) = T_{\mathrm{RL}}(\epsilon)$. Second, all sidebands with $k \neq 0$ vanish, i.e., $T_{\mathrm{RL}}^{(k)}(\epsilon) = T_{\mathrm{LR}}^{(k)}(\epsilon) = \delta_{k,0} T(\epsilon)$, where

$$T(\epsilon) = \Gamma_{\mathrm{L}}(\epsilon) \Gamma_{\mathrm{R}}(\epsilon) |G_{1N}(\epsilon)|^2 \tag{97}$$

and $G(\epsilon)$ is the Green function in the absence of driving. Then the current assumes the known form (17). Moreover in a static situation, the matrix element $\langle 1| \ldots |1\rangle$ of Eq. (38) reads [51]

$$|\Gamma_{\mathrm{L}}(\epsilon) G_{11}(\epsilon) + i|^2 = 1 - T(\epsilon) \ . \tag{98}$$

This relation allows one to eliminate the backscattering terms in the second line of Eq. (50) such that the zero-frequency noise becomes (21). Obviously, if in a static situation both voltage and temperature are zero, not only the current (17) but also the noise (21) vanishes. In the presence of driving, this is no longer the case. This becomes particularly evident in the high-frequency limit studied in Section 3.4.2.

It is known that in the adiabatic limit, i.e., for small driving frequencies, the numerical solution of the Floquet equation (55) becomes infeasible because a diverging number of sidebands has to be taken into account. In more mathematical terms, Floquet theory has no proper limit as $\Omega \to 0$ [154]. The practical consequence of this is that for low driving frequencies, it is favorable to tackle the transport problem with a different strategy: if $\hbar\Omega$ is the smallest energy-scale of the Hamiltonian (1), one computes for the "frozen" Hamiltonian at each instance of time the current and the noise from the static expressions (46) and (50) being followed up by time-averaging.

3.5.2. Spatially homogeneous driving

In many experimental situations, the driving field acts as a time-dependent gate voltage, i.e., it merely shifts all on-site energies of the wire uniformly. Thus, the wire Hamiltonian is of the form

$$\mathcal{H}_{\text{wire}}(t) = \mathcal{H}_0 + f(t) \sum_n |n\rangle\langle n| \,, \tag{99}$$

where, without loss of generality, we restrict $f(t)$ to possess zero time-average. A particular case of such a homogeneous driving is realized with a system that consists of only one level [124–126]. Then trivially, the time and the position dependence of the Floquet states factorize and, therefore, the dc current can be obtained within the formalism introduced by Tien and Gordon [123]. The corresponding noise properties have been addressed by Tucker and Feldman [121,122]. Here, we establish the relation between such a treatment and the present Floquet approach.

Since the time-dependent part of the Hamiltonian is proportional to the unity operator, the solution of the Floquet equation (55) is, besides a phase factor, given by the eigenfunctions $|\alpha\rangle$ of the time-independent operator $\mathcal{H}_0 - i\Sigma$,

$$|u_\alpha(t)\rangle = e^{-iF(t)}|\alpha\rangle \,, \tag{100}$$

where $(\mathcal{H}_0 - i\Sigma)|\alpha\rangle = (\epsilon_\alpha - i\hbar\gamma_\alpha)|\alpha\rangle$ and

$$F(t) = \frac{1}{\hbar} \int_0^t \mathrm{d}t' \, f(t') \,. \tag{101}$$

The quasienergies $(\epsilon_\alpha - i\hbar\gamma_\alpha)$ coincide with the eigenvalues of the static eigenvalue problem. Note that $F(t)$ obeys the $\mathcal{T}$-periodicity of the driving field since the time-average of $f(t)$ vanishes. Thus, the phase factor in the Floquet states (100) can be written as a Fourier series,

$$e^{-iF(t)} = \sum_k a_k e^{-ik\Omega t} \tag{102}$$

and, consequently we find $|u_{\alpha,k}\rangle = a_k|\alpha\rangle$ and the adjoint states accordingly. Then, the Green function (35) becomes

$$G^{(k)}(\epsilon) = \sum_{k'} a_{k'+k} a_{k'}^* G(\epsilon - k'\hbar\Omega) \,, \tag{103}$$

where $G(\epsilon)$ denotes the Green function in the absence of the driving field. Inserting (103) into (46) and employing the sum rule $\sum_{k'} a_{k'}^* a_{k'+k} = \delta_{k,0}$, yields

$$\bar{I} = \sum_k |a_k|^2 \frac{e}{h} \int d\epsilon \, T(\epsilon - k\hbar\Omega)[f_R(\epsilon) - f_L(\epsilon)] \,, \tag{104}$$

where $T(\epsilon)$ is the transmission probability in the absence of the driving. This expression allows the interpretation, that for homogeneous driving, the Floquet channels contribute *independently* to the current $\bar{I}$. For the special case of a one-site conductor and a sinusoidal driving, this relation to the static situation has been discussed in Refs. [124,125].

Addressing the noise properties, we obtain by inserting the Green function (103) into (50) the expression

$$\bar{S} = \frac{e^2}{h} \sum_k \int d\epsilon \left\{ \left| \sum_{k'} a_{k'+k}^* a_{k'} T(\epsilon - k'\hbar\Omega) \right|^2 f_R(\epsilon) \bar{f}_R(\epsilon + k\hbar\Omega) \right.$$

$$+ \Gamma_L \Gamma_R \left| \sum_{k'} a_{k'+k}^* a_{k'} G_{1N}(\epsilon - k'\hbar\Omega) \left[\Gamma_L G_{11}^*(\epsilon - k'\hbar\Omega) - i \right] \right|^2 f_L(\epsilon) \bar{f}_R(\epsilon + k\hbar\Omega)$$

$$\left. + \text{same terms with the replacement } (L, 1) \leftrightarrow (R, N) \right\} \,. \tag{105}$$

While the term in the first line contains only the static transmission probability at energies shifted by multiples of the photon energies, the contribution in the second line cannot be brought into such a convenient form due to the sum over Fourier index k'. As a consequence, in clear contrast to the dc current, the zero-frequency noise cannot be interpreted in terms of independent Floquet channels. Only in the limit of large driving frequencies (cf. Section 3.4.2), the channels become effectively independent and we end up with an expression that depends only on the transmission probability in the absence of the driving, and the Fourier coefficients a_k.

For large voltages where $f_L = 0$ and $f_R = 1$, the sums over the Fourier coefficients in Eqs. (104) and (105) can be evaluated with the help of the sum rule $\sum_{k'} a_{k'}^* a_{k'+k} = \delta_{k,0}$. Then both the dc current and the zero-frequency noise become identical to their value in the absence of the driving. This means that for a transport voltage which is sufficiently large, a time-dependent gate voltage has no influence on the average current and the zero-frequency noise.

4. Master equation approach

An essential step in the derivation of the transmission within a weak-coupling approximation, Eq. (72), is the assumption that only terms with $\alpha = \beta$ and $k = k'$ contribute significantly to (70). As discussed after Eq. (72), this requires that the separation of any pair of resonances is larger than their widths. This condition can be fulfilled only if the quasienergy spectrum does not contain any degeneracies and if, in addition, the wire–lead coupling is very weak. Here, we refine the weak-coupling approximation scheme of Section 3.4.1 and derive a master equation approach which yields reliable results also in the presence of degeneracies and for intermediately strong wire–lead coupling [68,87].

4.1. Current formula

We start again from the asymmetric expression (41) for the time-dependent current through the left contact. After averaging over the driving period, we obtain the dc current

$$\bar{I} = \frac{2e}{h\mathscr{T}} \sum_{\ell} \int d\epsilon \int_0^{\infty} d\tau \int_0^{\mathscr{T}} dt\, \Gamma_{\ell}(\epsilon) f_{\ell}(\epsilon) \operatorname{Im} e^{i\epsilon\tau/\hbar} G_{1\ell}^*(t, \epsilon) \Gamma_L(\tau) G_{1\ell}(t - \tau, \epsilon)$$

$$+ 2e \int d\epsilon\, \Gamma_L(\epsilon) f_L(\epsilon) \operatorname{Im} G_{11}^{(0)}(\epsilon) \tag{106}$$

for which we shall derive an approximation for small wire–lead coupling.

We start with the second term which is linear in the retarded Green function $G_{11}^{(0)}(\epsilon)$. For small values of Γ, we obtain from (58) the approximation

$$\operatorname{Im} G^{(0)}(\epsilon) = 2\pi \sum_{\alpha,k} |\phi_{\alpha,k}\rangle\langle\phi_{\alpha,k}| \delta(\epsilon - \epsilon_\alpha - k\hbar\Omega) , \tag{107}$$

which allows one to perform the energy integration in Eq. (106). Then, we obtain the contribution

$$-\frac{e}{\hbar} \sum_{\alpha,k} |\langle 1|\phi_{\alpha,k}\rangle|^2 \Gamma_L(\epsilon_\alpha^0 + k\hbar\Omega) f(\epsilon_\alpha^0 + k\hbar\Omega - \mu_L) . \tag{108}$$

The first term in Eq. (106) is quadratic in the Green function and, thus, requires a more elaborate treatment since otherwise, squares of δ-functions would emerge (cf. also the discussion in Section 3.4.1). For that purpose, it is advantageous to go one step back and to use instead of the current formula (106) the current operator (40) as a starting point. The time-average of the expectation value corresponding to the first term of Eq. (106) reads

$$\frac{2e}{\hbar\mathscr{T}} \int_0^{\infty} d\tau \int_0^{\mathscr{T}} dt\, \operatorname{Re}[\Gamma_L(\tau)\langle c_1^\dagger(t)c_1(t - \tau)\rangle] . \tag{109}$$

Using the cyclic property of the trace, we can then write the correlation function appearing in the integral as $\langle c_1^\dagger(t)c_1(t - \tau)\rangle = \langle c_1^\dagger U^\dagger(t - \tau, t)c_1 U(t - \tau, t)\rangle_t$ with the expectation value $\langle \cdot \rangle_t = \operatorname{Tr}\langle \varrho(t) \cdot \rangle$ at time t. Assuming that $\Gamma_L(\epsilon)$ is a slowly varying function in the relevant energy range, the main contributions to the τ-integral in Eq. (109) stem from small values of τ. We can thus replace in the correlation function the full time-evolution operator by the corresponding zeroth-order expression, i.e., the interaction picture operator $\tilde{c}_1(t - \tau, t) = U_0^\dagger(t - \tau, t)c_1 U_0(t - \tau, t)$ with U_0 being the propagator (56) in the limit $\Gamma_{L/R} \to 0$. In order to include the coherent dynamics properly, it is convenient to introduce the "Floquet picture creation operators" $c_\alpha(t)$ which are defined by the time-dependent transformation [68,87]

$$c_\alpha(t) = \sum_n \langle\phi_\alpha(t)|n\rangle c_n . \tag{110}$$

Using the inverse transformation $c_n = \sum_\alpha \langle n|\phi_\alpha(t)\rangle c_\alpha(t)$, which follows from the completeness of the Floquet states at equal times, we obtain

$$c_n(t - \tau, t) \approx \sum_{\alpha,k} e^{-ik\Omega t} e^{i(\epsilon_\alpha^0 + k\hbar\Omega)\tau/\hbar} \langle n|\phi_{\alpha,k}\rangle c_\alpha(t) . \tag{111}$$

Inserting (111) with $n = 1$ into (109), we arrive at an expression that contains the time-dependent expectation values $P_{\alpha\beta}(t) = \langle c_\beta^\dagger(t) \, c_\alpha(t) \rangle_t$ with both operators taken at time t. The $P_{\alpha\beta}(t)$ at asymptotic times, in turn, are determined from a kinetic equation which we derive in the next subsection. Before doing so, however, we simplify Eq. (109) further by using the fact that at asymptotically long times, all $P_{\alpha\beta}(t)$ become $\mathcal{T}$-periodic functions and, thus, can be decomposed into a Fourier series $P_{\alpha\beta}(t) = \sum_k \exp(-ik\Omega t) P_{\alpha\beta,k}$. This brings Eq. (109) into the form

$$\frac{2e}{\hbar} \sum_{\alpha,\beta,k,k'} \int_0^\infty d\tau \, \mathrm{Re}[\Gamma_\mathrm{L}(\tau) e^{i(\epsilon_\alpha^0 + k\hbar\Omega)\tau/\hbar} \langle \phi_{\beta,k+k'}|1\rangle\langle 1|\phi_{\alpha,k}\rangle P_{\alpha\beta,k'}] \; . \tag{112}$$

By inserting for the lead response function $\Gamma_\mathrm{L}(\tau)$ its definition (28), we finally find for the time-averaged current through the wire the expression

$$\bar{I} = \frac{e}{\hbar} \sum_{\alpha,k} \Gamma_\mathrm{L}(\epsilon_\alpha^0 + k\hbar\Omega) \left[\sum_{\beta,k'} \mathrm{Re}\{\langle \phi_{\beta,k+k'}|1\rangle\langle 1|\phi_{\alpha,k}\rangle P_{\alpha\beta,k'}\} \right.$$

$$\left. - |\langle 1|\phi_{\alpha,k}\rangle|^2 f(\epsilon_\alpha^0 + k\hbar\Omega - \mu_\mathrm{L}) \right] \; . \tag{113}$$

Note that we have disregarded principal value terms, which correspond to an energy-renormalization due to the wire–lead coupling.

4.2. Floquet–Markov master equation

Having expressed the current in terms of the wire expectation values $P_{\alpha\beta}(t)$, we now derive for them an equation of motion valid in the regime of weak to moderately strong wire–lead coupling. We thus consider the time-derivative $\dot{P}_{\alpha\beta}(t)$, which with the help of the zeroth-order Floquet equation (67), can be written as

$$\dot{P}_{\alpha\beta}(t) = -\frac{i}{\hbar} (\epsilon_\alpha^0 - \epsilon_\beta^0) P_{\alpha\beta}(t) + \mathrm{Tr}[\dot{\rho}(t) c_\beta^\dagger(t) c_\alpha(t)] \; . \tag{114}$$

For the evaluation of the second term on the right-hand side of the last equation, we employ the standard master equation (23) presented in Section 2.5. Using twice the relation $\mathrm{Tr}\, A[B, C] = \mathrm{Tr}[A, B]C$, which directly results from the cyclic invariance of the trace, we obtain

$$\dot{P}_{\alpha\beta}(t) = -\frac{i}{\hbar} (\epsilon_\alpha^0 - \epsilon_\beta^0) P_{\alpha\beta}(t)$$

$$- \frac{1}{\hbar^2} \int_0^\infty d\tau \langle [[c_\beta^\dagger(t) c_\alpha(t), H_\mathrm{contacts}], \widetilde{H}_\mathrm{contacts}(t - \tau, t)] \rangle_t \; . \tag{115}$$

For the further evaluation of Eq. (115), we write both H_contacts and $\widetilde{H}_\mathrm{contacts}(t - \tau, t)$ in terms of $\tilde{c}_n(t - \tau, t)$ for which we insert the approximation (111). After some algebra, we arrive at a closed differential equation for $P_{\alpha\beta}(t)$. This determines the Fourier coefficients of the asymptotic solution, $P_{\alpha\beta,k}$, which obey the

inhomogeneous set of equations

$$\frac{i}{\hbar}(\epsilon_\alpha^0 - \epsilon_\beta^0 - k\hbar\Omega) P_{\alpha\beta,k}$$

$$= \frac{1}{2} \sum_{\ell=L,R} \sum_{k'} \left\{ \Gamma_\ell(\epsilon_\alpha^0 + k'\hbar\Omega)\langle\phi_{\alpha,k'}|n_\ell\rangle\langle n_\ell|\phi_{\beta,k'+k}\rangle f(\epsilon_\alpha^0 + k'\hbar\Omega - \mu_\ell) \right.$$

$$+ \Gamma_\ell(\epsilon_\beta^0 + k'\hbar\Omega)\langle\phi_{\alpha,k'-k}|n_\ell\rangle\langle n_\ell|\phi_{\beta,k'}\rangle f(\epsilon_\beta^0 + k'\hbar\Omega - \mu_\ell)$$

$$- \sum_{\alpha',k''} \Gamma_\ell(\epsilon_{\alpha'}^0 + k''\hbar\Omega)\langle\phi_{\alpha,k'+k''-k}|n_\ell\rangle\langle n_\ell|\phi_{\alpha',k''}\rangle P_{\alpha'\beta,k'}$$

$$\left. - \sum_{\beta',k''} \Gamma_\ell(\epsilon_{\beta'}^0 + k''\hbar\Omega)\langle\phi_{\beta',k''}|n_\ell\rangle\langle n_\ell|\phi_{\beta,k+k''-k'}\rangle P_{\alpha\beta',k'} \right\} \ . \tag{116}$$

Here, we have assumed that the ideal leads always stay in thermal equilibrium and, thus, are described by the expectation values (7). Moreover, principal value terms stemming from an renormalization of the wire energies due to the coupling to the leads have again been neglected.

The solution of the master equation (116) together with the current expression (113) derived earlier, permits an efficient numerical calculation of the dc current through the molecular wire even for rather large systems or for energy-dependent couplings. Furthermore, as we shall exemplify below, this approach is still applicable in the presence of degeneracies in the quasienergy spectrum.

4.3. Rotating-wave approximation

The current formula (74) valid for very weak wire–lead coupling, which was derived in Section 3.4.1, can also be obtained from the master equation approach within a rotating-wave approximation. Thereby, one assumes that the coherent oscillations of all $P_{\alpha\beta}(t)$ are much faster than their decay. Then it is useful to factorize $P_{\alpha\beta}(t)$ into a rapidly oscillating part that takes the coherent dynamics into account and a slowly decaying prefactor. For the latter, one can derive a new master equation with oscillating coefficients. Under the assumption that the coherent and the dissipative time-scales are well separated, it is possible to replace the time-dependent coefficients by their time-average. The remaining master equation is generally of a simpler form than the original one. Because we work here already with a spectral decomposition of the master equation, we give the equivalent line of argumentation for the Fourier coefficients $P_{\alpha\beta,k}$.

It is clear from the Fourier representation of the master equation (116) that if

$$\epsilon_\alpha - \epsilon_\beta + k\hbar\Omega \gg \Gamma_{L/R} \tag{117}$$

for all α, β, k, then the corresponding $P_{\alpha\beta,k}$ emerge to be small and, thus, may be neglected. Under the assumption that the wire–lead couplings are weak and that the Floquet spectrum has no degeneracies, the RWA condition (117) is well satisfied except for

$$\alpha = \beta, \quad k = 0 \ , \tag{118}$$

i.e., when the prefactor of the l.h.s. of Eq. (116) vanishes exactly. This motivates the ansatz

$$P_{\alpha\beta,k} = P_\alpha \delta_{\alpha,\beta} \delta_{k,0} \ , \tag{119}$$

which has the physical interpretation that the stationary state consists of an incoherent population of the Floquet modes. The occupation probabilities P_α are found by inserting the ansatz (119) into the master equation (116) and read

$$P_\alpha = \frac{\sum_{\ell,k} \Gamma_\ell(\epsilon_\alpha^0 + k\hbar\Omega) f(\epsilon_\alpha^0 + k\hbar\Omega - \mu_\ell)}{\sum_{\ell,k} \Gamma_\ell(\epsilon_\alpha^0 + k\hbar\Omega)} \; . \tag{120}$$

Inserting this solution into expression (113) yields in the wide-band limit the current formula (74).

4.4. Phonon damping

In order to describe the electron transport under the influence of phonon damping, commonly a boson-like heat bath is coupled to each wire site, which renders the on-site energies fluctuating with quantum noise [21–23,26–33,58,69,155–161]. This can be considered as an extension of the spin–boson model to more than two sites and the presence of leads. For the master equation (23), one then has in the first line in addition the Hamiltonian of the phonon bath, while the electron–phonon coupling enters as a further dissipative contribution to the second line. Note that this leaves the expression (113) for the current formally unchanged.

4.4.1. Hartree–Fock approximation

When evaluating the master equation, however, it turns out that in addition to the terms containing the single-electron density matrix $P_{\alpha\beta}(t)$, two-electron expectation values of the form $\langle c_\delta^\dagger c_\gamma^\dagger c_\beta c_\alpha \rangle_t$ appear. By iteration, one thus generates a hierarchy of equations up to N-electron expectation values. To obtain a description in terms of only the single-electron expectation values, one may employ the Hartree–Fock decoupling scheme defined by the approximation

$$\langle c_\delta^\dagger c_\gamma^\dagger c_\beta c_\alpha \rangle \approx \langle c_\delta^\dagger c_\alpha \rangle \langle c_\gamma^\dagger c_\beta \rangle - \langle c_\delta^\dagger c_\beta \rangle \langle c_\gamma^\dagger c_\alpha \rangle = P_{\alpha\delta} P_{\beta\gamma} - P_{\beta\delta} P_{\alpha\gamma} \; . \tag{121}$$

Clearly, such a mean-field approximation only covers certain aspects of the full many-particle problem. Nevertheless, it offers a feasible and consistent description. As a most striking consequence, the Hartree–Fock decoupling (121) leaves the master equation non-linear [69].

4.4.2. Thermal equilibrium

A potential problem of quantum master equations has been pointed out in Refs. [140,162], namely that they might not be consistent with the second law of thermodynamics—in particular, that they might not predict zero current even in the absence of both transport voltage and driving. This apparent lack of a proper equilibrium limit, however, is not inherent to master equations of the form (23) themselves, but results from an inconsistent treatment at a later stage: It is crucial to employ in the second line of Eq. (23) the interaction picture operators computed with the *exact* propagator of the uncoupled subsystems. Using any approximation indeed bears the danger of inconsistencies. Master equations which suffer from the mentioned problems, have, e.g., been derived in Ref. [163] and applied to situations with a finite transport voltage [96,97] and with time-dependent fields [157,164]. In such non-equilibrium situations, the lack of a proper equilibrium limit naturally does not give rise to obvious contradictions.

Therefore, an important consistency check for quantum master equations is an equilibrium situation, where $H_{nn'}$ is time-independent and where no external bias is present ($\mu_\ell = \mu$ for all ℓ). It can be

demonstrated [69] that the final reduced master equation in the absence of both driving and voltage has the solution $P_{\alpha\beta} = \delta_{\alpha\beta} f_\alpha$, with the population $f_\alpha = f(E_\alpha - \mu)$, determined by the Fermi distribution and the energy E_α of the eigenstates $|\phi_\alpha\rangle$ which represent the undriven limit of the Floquet states. Consequently, the current (113) vanishes in accordance with elementary principles of statistical physics.

5. Resonant current-amplification

A natural starting point for the experimental investigation of molecular conduction under the influence of laser fields is the measurement of fingerprints of resonant excitations of electrons in the current–voltage characteristics. Treating the driving as a perturbation, Keller et al. [152,165] have demonstrated that resonant electron excitations result in peaks of the current as a function of the driving frequency. Kohler et al. [70] included within a Floquet master equation approach the driving exactly and later derived an analytical solution [71] which is in good agreement with an exact numerical solution. In a related work [166], Tikhonov et al. studied this problem within a so-called independent channel approximation [167] of a Floquet transport theory. As a central result, it has been found that, in particular for long wires, such excitations enhance the current significantly. In this section, we review the analytical treatment of Ref. [71] and compare to exact numerical results.

As a working model we consider a so-called bridged molecular wire consisting of a donor and an acceptor site and $N - 2$ sites in between (cf. Fig. 3). Each of the N sites is coupled to its nearest neighbors by a hopping matrix element Δ. The dipole force (8) of the laser field renders each level oscillating in time with a position-dependent amplitude. The energies of the acceptor and the donor orbitals, $|1\rangle$ and $|N\rangle$, are assumed to be close to the chemical potentials of the attached leads, $E_1 = E_N \approx \mu_L \approx \mu_R$. The bridge levels $E_n, n = 2, \ldots, N - 1$, lie $E_B \gg \Delta, eV$ above the chemical potential.

5.1. Static conductor

Let us first discuss the static problem in the absence of the driving field, i.e., for $A = 0$. In the present case where the coupling between two neighboring sites is much weaker than the bridge energy, $\Delta \ll E_B$, one finds two types of eigenstates: one group of states is located on the bridge. It consists of $N - 2$ levels with energies in the range $[E_B - 2\Delta, E_B + 2\Delta]$. In the absence of the driving field, these bridge states
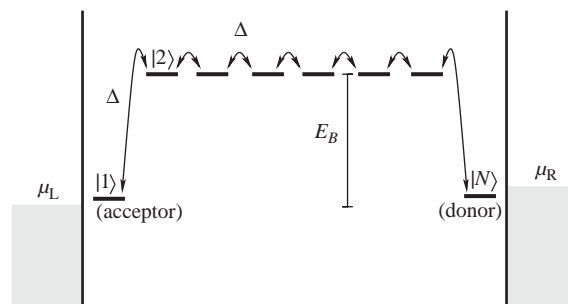

Fig. 3. Bridged molecular wire consisting of $N = 8$ sites of which the first and the last site are coupled to leads with chemical potentials μ_L and $\mu_R = \mu_L + eV$.

mediate the super-exchange between the donor and the acceptor. The two remaining states form a doublet whose states are approximately given by $(|1\rangle \pm |N\rangle)/\sqrt{2}$. Its splitting can be estimated in a perturbational approach [168–170] and is approximately given by $2\Delta(\Delta/E_B)^{N-2}$. Thus, since the electrons occupy the bridge levels only virtually, the wire can be reduced to a two-level system with the effective tunnel matrix element $\Delta_{DA} = \Delta \exp(-\kappa(N-2))$, where $\kappa = \ln(E_B/\Delta)$. If the chemical potentials of the leads are such that $\mu_L < E_A$ and $\mu_R > E_D$, i.e., for a sufficiently large voltage, the current is dominated by the total transmission and for $\Gamma \gg \Delta_{DA}$ can be evaluated to read

$$I_0 = \frac{2e|\Delta|^2}{\Gamma} e^{-2\kappa(N-2)} . \tag{122}$$

For the explicit calculation see, e.g., Ref. [94]. In particular, one finds an exponentially decaying length dependence of the current [20,24,171]. Moreover, in this limit, it is also possible to evaluate explicitly the zero-frequency noise to obtain the Fano factor $F = \bar{S}/e|\bar{I}| = 1$. This value has a direct physical interpretation: because the transmissions of electrons across a large barrier are rare and uncorrelated events, they obey Poisson statistics and, consequently, the mean number of transported electrons equals its variance. This translates to a Fano factor $F = 1$ [137].

5.2. Resonant excitations

The magnitude of the current changes significantly when a driving field with a frequency $\Omega \approx E_B/\hbar$ is switched on. Then the resonant bridge levels merge with the donor and the acceptor state to form a Floquet state. This opens a direct channel for the transport resulting in an enhancement of the electron current.

In order to estimate the magnitude of the current through the resonantly driven wire, we disregard all bridge levels besides the one that is in resonance with the donor and the acceptor. Let us assume that this resonant bridge level $|\psi_B\rangle$ extends over the whole bridge such that it occupies the sites $|2\rangle, \dots, |N-1\rangle$ with equal probability $1/\sqrt{N-2}$. Accordingly, apart from an irrelevant phasefactor, the overlap between the bridge level and the donor/acceptor reads

$$\langle 1|H_{\text{molecule}}|\psi_B\rangle = \frac{\langle 1|H_{\text{molecule}}|2\rangle}{\sqrt{N-2}} = \frac{\Delta}{\sqrt{N-2}}$$
$$= \langle \psi_B|H_{\text{molecule}}|N\rangle . \tag{123}$$

The resonance condition defines the energy of the bridge level as $\langle \psi_B|H_{\text{molecule}}|\psi_B\rangle = \hbar\Omega$ (recall that we have assumed $E_D = E_A = 0$).

We now apply an approximation scheme in the spirit of the one described in Ref. [94] and thereby derive a *static* effective Hamiltonian that describes the *time-dependent* system. We start out by a transformation with the unitary operator

$$S(t) = \exp\left\{-i \sum_{n=2}^{N-1} |n\rangle\langle n|\Omega t - i \frac{A}{\hbar\Omega} \sum_{n=1}^{N} |n\rangle\langle n| \sin(\Omega t)\right\} . \tag{124}$$

Note that $S(t)$ obeys the $\mathscr{T}$-periodicity of the original driven wire Hamiltonian. As a consequence, the transformed wire Hamiltonian

$$\widetilde{H}_{\text{molecule}}(t) = S^\dagger(t) H_{\text{molecule}}(t) S(t) - i\hbar S^\dagger(t)\dot{S}(t) \tag{125}$$

is $\mathcal{T}$-periodic as well. For $\hbar\Omega \gg \Delta$, we can separate time-scales and average $\widetilde{H}_{\text{molecule}}(t)$ over the driving period. In the subspace spanned by $|1\rangle$, $|\psi_B\rangle$, and $|N\rangle$, the time-averaged wire Hamiltonian reads

$$H_{\text{molecule,eff}} = \int_0^{\mathcal{T}} \frac{\mathrm{d}t}{\mathcal{T}} \, \widetilde{H}_{\text{molecule}}(t) = b \begin{pmatrix} 0 & 1 & 0 \\ 1 & 0 & 1 \\ 0 & 1 & 0 \end{pmatrix} \tag{126}$$

with the effective tunnel matrix element

$$b = \frac{J_1(A/\hbar\Omega)}{\sqrt{N-2}} \, \Delta \tag{127}$$

and J_1 the first-order Bessel function of the first kind.

The situation described by the Hamiltonian (126) is essentially the following: The central site $|\psi_B\rangle$ is coupled by matrix elements b to the donor and the acceptor site. Since the latter in turn couple to the external leads with a self-energy $\Gamma/2$, their density of states is

$$\rho(E) = \frac{1}{\pi} \frac{\Gamma/2}{E^2 + \Gamma^2/4} \, . \tag{128}$$

Then, the tunneling of the electrons from and to the central site is essentially given by the golden rule rate

$$w = \frac{2\pi}{\hbar} \, |b|^2 \rho(0) \, . \tag{129}$$

Like in the static case, we assume that the chemical potential of the left (right) lead lies above (below) the on-site energy of the acceptor (donor) and that therefore the donor is always occupied while the acceptor is always empty. Then, the rate of electrons tunneling from the central site to the acceptor is given by the golden rule rate (129) times the occupation probability p of the state $|\psi_B\rangle$. Accordingly, the rate of electrons from the donor to $|\psi_B\rangle$ is given by w times the probability $1 - p$ to find the central site empty. Consequently, the occupation of the resonant bridge level evolves according to

$$\dot{p} = w(1 - p) - wp \, . \tag{130}$$

Eq. (130) has the stationary solution $p = \frac{1}{2}$ and, thus, for resonant excitations, the dc contribution of the time-dependent current is given by

$$\bar{I}_{\text{res}} = ewp = e \frac{2A^2\Delta^2}{(N-2)\hbar^3\Omega^2\Gamma} \, . \tag{131}$$

Here, we have used for small arguments of the Bessel function the approximation $J_1(x) \approx x$. The dc current (131) obeys an intriguing scaling behavior as a function of the wire length: instead of the exponentially decaying length dependence (122) that has been found for the static case, in the presence of resonant driving, a scaling $\bar{I} \propto 1/N$ emerges. In particular for longer wires, this means that the external field enhances the conductance by several orders of magnitude.

5.3. Numerical results

In order to corroborate the analytical estimates presented above, we treat the transport problem for the driven wire sketched in Fig. 3 numerically by solving the corresponding Floquet equation (55) and a
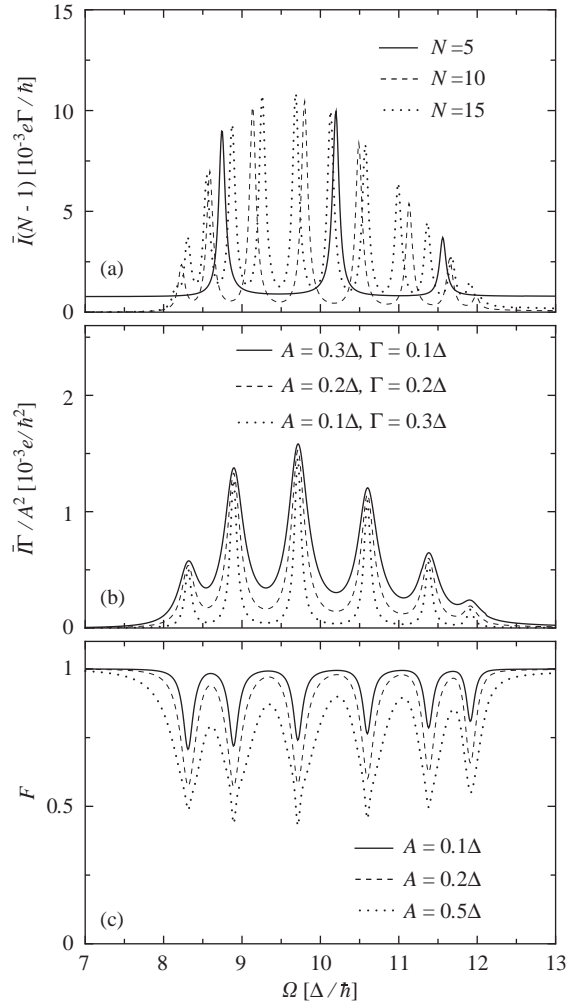
Fig. 4. (a) Average current $\bar{I}$ as a function of the driving frequency Ω for various wire lengths N. The scaled amplitude is $A = 0.1\Delta$; the applied voltage $\mu_R - \mu_L = 5\Delta/e$. The other parameters read $\Gamma = 0.1\Delta$ and $k_B T = 0$. (b) Average current for various driving amplitudes A and coupling strengths Γ for a wire of length $N = 8$. (c) Fano factor $F = \bar{S}/e\bar{I}$ for the wire length $N = 8$ and the wire–lead coupling $\Gamma = 0.1\Delta$. From Ref. [71].

subsequent evaluation of the expressions (46) and (50) for the dc current and the zero-frequency noise, respectively. For a wire with $N = 5$ sites, one finds peaks in the current when the driving frequency matches the energy difference between the donor/acceptor doublet and one of the $N - 2 = 3$ bridge levels, cf. the solid line in Fig. 4a. The applied voltage is always chosen so small that the bridge levels lie below the chemical potentials of the leads. In Fig. 4a the scale of the abscissa is chosen proportional to $(N - 1)$ such that it suggests a common envelope function. Furthermore, we find from Fig. 4b that the dc current is proportional to A^2/Γ provided that A is sufficiently small and Γ sufficiently large. Thus, the numerical

results indicate that the height of the current peaks obeys

$$\bar{I}_{\text{peak}} \propto \frac{A^2}{(N-1)\Gamma} \; , \tag{132}$$

which is essentially in accordance with our analytical estimate (131). The main discrepancy comes from the fact that the overlap between the resonant level and the donor/acceptor differs from the estimate (123) by a numerical factor of the order one. Moreover, Fig. 4c demonstrates that at the resonances, the Fano factor assumes values considerably lower than one as expected for the transport through a resonant single level [54].

6. Ratchets and non-adiabatic pumps

A widely studied phenomenon in driven transport is the so-termed ratchet effect: the conversion of ac forces without any net bias into directed motion [72–77]. The investigation of this phenomenon has been triggered by the question whether an asymmetric device can act as a Maxwell demon, i.e., whether it is possible to ultimately convert noise into work. Feynman's famous "ratchet and pawl" driven by random collisions with gas molecules, on first sight, indeed suggests that such a Maxwell demon exists. At thermal equilibrium, however, the whole nanodevice obeys the same thermal fluctuations as the surrounding gas molecules. Therefore, consistent with the second law of thermodynamics, no directed motion occurs [172] and one has to conclude that the ratchet effect can be observed only in situations far from equilibrium.

A basic model, which captures the essential physics of ratchets, is an asymmetric, periodic potential under the influence of an ac driving. In such a system, even in the absence of any net bias, directed transport has been predicted for overdamped classical Brownian motion [72,75] and also for dissipative quantum Brownian motion in the incoherent regime [78,79,173]. A related effect is found in the overdamped limit of dissipative tunneling in driven superlattices. There, the spatial symmetry is typically preserved and the directed transport is brought about by a driving field that includes higher harmonics of the driving frequency [174–176].

In the context of mesoscopic conduction, it has been found that the cyclic adiabatic change of the conductor parameters can induce a so-called pump current, where the charge pumped per cycle is determined by the area of parameter space enclosed during the cyclic evolution [43,45,177,178]. This relates the pump current to a Berry phase [44,80]. Beyond the adiabatic regime, pump effects have been investigated theoretically [47,62,81,98,179] and also been measured in coupled quantum dots [39,96,180]. Since in the non-adiabatic regime, the main contribution to the pump current comes from electrons considerably below the Fermi surface, non-adiabatic electron pumping is essentially temperature-independent [46,181].

The studies presented in this chapter were mainly motivated by two aspects: First, although infinitely extended "ideal" ratchets are convenient theoretical models, any experimental realization will have finite length, i.e., consist of a finite number of elementary units; cf. Fig. 5, below. Thus, finite size effects become relevant and it is interesting to know the number of coupled wire units that are needed to mimic the behavior of a practically infinite system. Second, prior studies of quantum ratchets focussed on incoherent tunneling [78,79]. By contrast, the present setup allows one to investigate ratchet dynamics in the coherent quantum regime which has not been explored previously.

The results of this section, have originally [68,87] been computed for finite temperatures within the master equation approach of Section 4. In the limit of zero temperature, but otherwise equal parameters,
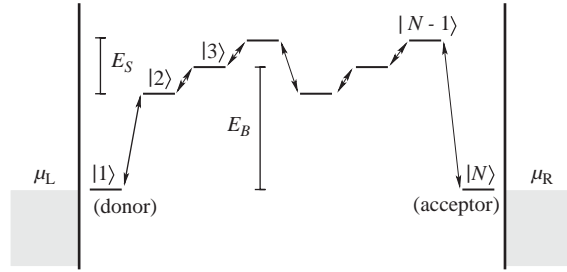
Fig. 5. Level structure of the wire ratchet with $N = 8$ sites, i.e., $N_g = 2$ asymmetric groups. The bridge levels are E_B above the donor and acceptor levels and are shifted by $\pm E_S/2$.

it has been explicitly verified in Ref. [182] that the results from such a perturbative treatment essentially agree with the corresponding exact solution obtained from Eq. (46).

6.1. Symmetry inhibition of ratchet currents

It is known from the study of deterministically rocked periodic potentials [183] and of driven classical Brownian particles [184] that the symmetry of the equations of motion may rule out any non-zero average current at asymptotic times. Thus, before starting to compute ratchet currents, let us first analyze what kind of symmetries may prevent the effect. We consider situations, where the electron distributions in both leads are identical—in particular, situations where both leads are in thermal equilibrium with a common chemical potential, $f_L(\epsilon) = f_R(\epsilon) \equiv f(\epsilon)$ for all ϵ. Then, no electromotive force acts and, consequently, in the absence of driving, all currents must vanish. An applied driving field, however, violates the equilibrium condition and can generate a finite dc current

$$I_{\text{pump}} = \frac{e}{h} \sum_k \int \mathrm{d}\epsilon \left[T_{\text{LR}}^{(k)}(\epsilon) - T_{\text{RL}}^{(k)}(\epsilon) \right] f(\epsilon) \ . \tag{133}$$

This allows the interpretation that a driving field gives rise to a dynamical electromotive force [185]. Obviously, the pump current vanishes if the condition $T_{\text{LR}}^{(k)}(\epsilon) = T_{\text{RL}}^{(k)}(\epsilon)$ is fulfilled for all k and ϵ. One might now ask whether this condition can be ensured by any symmetry relation. For the dipole driving considered here, the relevant symmetries are those studied in Appendix A.3, namely time-reversal symmetry, time-reversal parity, and generalized parity. In Section 3.3, we have already identified the symmetry-related channels which possess equal transmission probabilities.

Looking at the relations (64)–(66), it becomes clear that the generalized parity $\mathscr{S}_{\text{GP}}$ is the only symmetry that directly yields a vanishing pump current. This is so because it implies for the transmission probabilities the relation (66) and, thus, we find $I_{\text{pump}} = 0$ [68]. While time-reversal symmetry is without any consequence for the pump current, time-reversal parity has some rather subtle effect which follows from the fact that the transmission probabilities obey relation (65) and that in the weak-coupling limit of Section 3.4.1, in addition, relation (73) holds. Given these two relations, we obtain $T_{\text{LR}}^{(k)}(\epsilon) = T_{\text{RL}}^{(k)}(\epsilon)$ and, thus, the dc current vanishes. Since the weak-coupling approximation is correct to lowest order in the coupling Γ, the consequence of time-reversal parity for quantum ratchets and Brownian motors is that we no longer find the generic behavior $I_{\text{pump}} \propto \Gamma$, but rather $I_{\text{pump}} \propto \Gamma^2$.
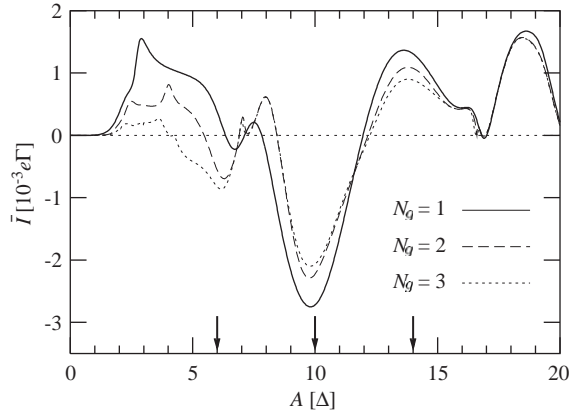
Fig. 6. Time-averaged current through a molecular wire ratchet that consists of N_g bridge units as a function of the driving strength A. The bridge parameters are $E_B = 10\Delta$, $E_S = \Delta$, the driving frequency is $\Omega = 3\Delta/\hbar$, the coupling to the leads is chosen as $\Gamma_L = \Gamma_R = 0.1\Delta/\hbar$, and the temperature is $k_B T = 0.25\Delta$. The arrows indicate the driving amplitudes used in Fig. 8. After Ref. [87].

In the following, we consider two typical cases where the generalized parity symmetry is broken and, thus, a pump current emerges, namely (i) an asymmetric structure under the influence of a harmonic dipole force, the so-called rocking ratchet, and (ii) a spatially symmetric system for which generalized parity is broken dynamically by mixing with higher harmonics.

6.2. Spatial symmetry-breaking: coherent quantum ratchets

A straightforward way to break generalized parity, is to use a conductor with an asymmetric level structure. Then, already a purely harmonic dipole driving $a(t) = A \sin(\Omega t)$ in the Hamiltonian (8) is sufficient to generate a dc current. As a tight-binding model of such a structure, we have considered a wire consisting of a donor and an acceptor site and N_g asymmetric groups in the ratchet-like configuration sketched in Fig. 5. In molecular structures, such an asymmetry can be achieved in many ways, and was explored as a source of molecular current rectification since the early work of Aviram and Ratner [3]. Later this effect has been found experimentally [7,105]. In general, an asymmetry can be created by attaching different chemical groups to the opposite sides of an otherwise symmetric molecular wire [7,105,186]. In our model, the inner wire states are arranged in N_g groups of three, i.e., $N - 2 = 3N_g$. In each group, the first (last) level is lowered (raised) by an energy $E_S/2$, forming an asymmetric saw-tooth-like structure. The energies of the donor and the acceptor orbitals are assumed to be at the level of the chemical potentials of the attached leads and since no voltage is applied, we thus have $E_1 = E_N = \mu_L = \mu_R$. The bridge levels E_n lie at E_B and $E_B \pm E_S/2$, as sketched in Fig. 5.

Fig. 6 shows the resulting stationary time-averaged current $\bar{I}$. A quantitative analysis of a tight-binding model has demonstrated that the resulting currents lie in the range of 10^{-9} A and, thus, can be measured with today's techniques [87]. In the limit of very weak driving, we find $\bar{I} \propto E_S A^2$ (Fig. 7). This behavior is expected from symmetry considerations: the asymptotic current must be independent of any initial phase of the driving field and therefore is an even function of the field amplitude A. This indicates that the ratchet effect can only be obtained from a treatment of the field beyond Kubo theory. For strong laser
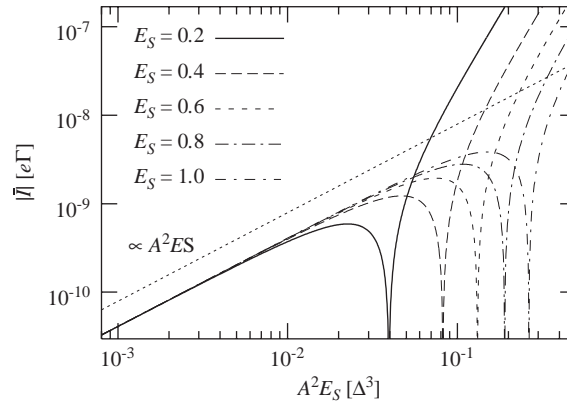
Fig. 7. Absolute value of the time-averaged current in a ratchet-like structure with $N_g = 1$ as a function of $A^2 E_S$ demonstrating the proportionality to $A^2 E_S$ for small driving amplitudes. All other parameters are as in Fig. 6. At the dips on the right-hand side, the current $\bar{I}$ changes its sign. From Ref. [68].
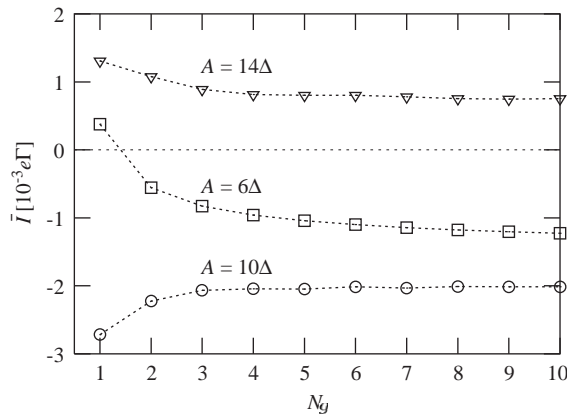

Fig. 8. Time-averaged current as a function of the number of bridge units N_g for the driving amplitudes indicated in Fig. 6. The other parameters are as in Fig. 6. The connecting lines serve as a guide to the eye. After Ref. [87].

fields, Fig. 6 also shows that $\bar{I}$ is almost independent of the wire length. If the driving is intermediately strong, $\bar{I}$ depends in a short wire sensitively on the driving amplitude A and the number of asymmetric molecular groups N_g: even the sign of the current may change with N_g, i.e., we find a current reversal as a function of the wire length. For long wires that comprise five or more wire units, the average current becomes again length-independent, as can be seen from Fig. 8. This identifies the observed current reversal as a finite size effect. As practical consequence, such relatively short wires can mimic the behavior of an (infinitely extended) quantum ratchet. Moreover, the fact that $\bar{I}$ converges to a finite value if the number of wire units is enlarged, demonstrates that the dissipation caused by the coupling to the leads is sufficient to establish the ratchet effect in the limit of long wires. In this sense, no on-wire dissipation is required. Still, if the wire–lead model (1) is extended by electron–phonon coupling, the ratchet current might be enhanced; cf. Section 6.4.
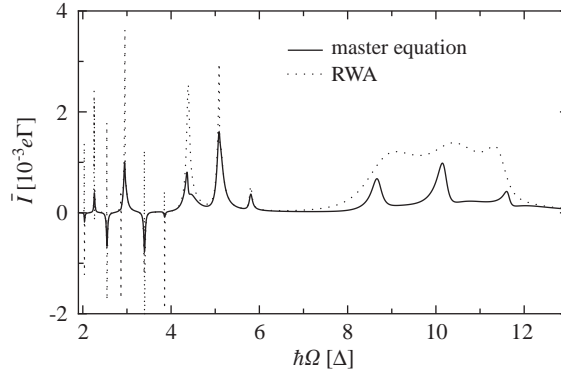
Fig. 9. Time-averaged current as a function of the driving frequency Ω for $A = \Delta$ and $N_g = 1$ (solid line). All other parameters are as in Fig. 6. The dotted line depicts the solution within the rotating-wave approximation (120). After Ref. [87].
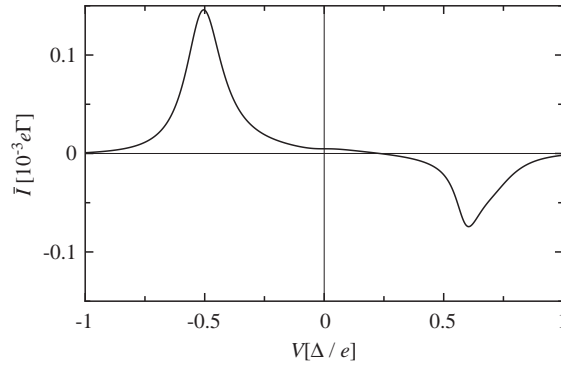

Fig. 10. Time-averaged current as a function of the applied static bias voltage V, which drops solely along the molecule. The driving amplitude is $A = \Delta$, the driving frequency $\Omega = 3\Delta/\hbar$, and $N_g = 1$. All other parameters are as in Fig. 6. After Ref. [87].

Fig. 9 depicts the average current vs. the driving frequency Ω, exhibiting resonance peaks as a striking feature. The comparison with the quasienergy spectrum reveals that each peak corresponds to a non-linear resonance between the donor/acceptor and a bridge orbital. While the broader peaks at $\hbar\Omega \approx E_B = 10\Delta$ match the 1:1 resonance (i.e., the driving frequency equals the energy difference), one can identify the sharp peaks for $\hbar\Omega \lesssim 7\Delta$ as multi-photon transitions. The appearance of these resonance peaks clearly demonstrates that the molecular bridge acts as a *coherent* quantum ratchet. Moreover, owing to the broken spatial symmetry of the wire, one expects an asymmetric current–voltage characteristic. This is indeed the case as depicted in Fig. 10.

6.3. Temporal symmetry-breaking: harmonic mixing

The symmetry analysis in Section 6.1 explains that for a symmetric bridge without a ratchet-like structure as sketched in Fig. 3, the pump current (133) vanishes if the driving is a purely harmonic dipole force. This is so because then the system is invariant under the generalized parity transformation $\mathcal{S}_{GP}$ and,
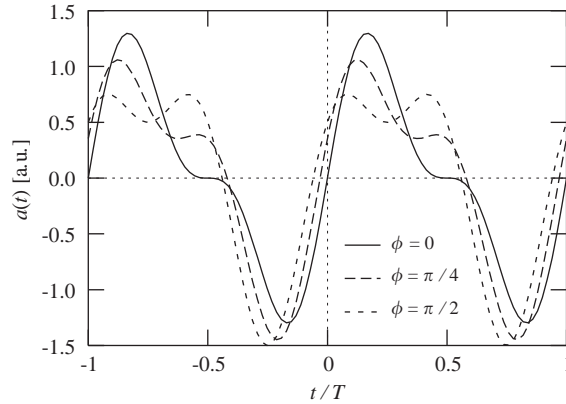
Fig. 11. Shape of the harmonic mixing field $a(t)$ in Eq. (134) for $A_1 = 2A_2$ for different phase shifts ϕ. For $\phi = 0$, the field changes its sign for $t \to -t$ which amounts to the time-reversal parity $\mathscr{S}_{\text{TP}}$.

thus, the transmission factors obey relation (66). Still, generalized parity can be broken in a dynamical way by adding a second harmonic to the driving field, i.e., a contribution with twice the fundamental frequency Ω, such that it is of the form

$$a(t) = A_1 \sin(\Omega t) + A_2 \sin(2\Omega t + \phi) , \tag{134}$$

as sketched in Fig. 11. While now shifting the time t by a half period π/Ω changes the sign of the fundamental frequency contribution, the second harmonic is left unchanged. The generalized parity is therefore no longer present and we expect to find a non-vanishing average current.

The phase shift ϕ plays here a subtle role. For $\phi = 0$ (or equivalently any multiple of π) the time-reversal parity $\mathscr{S}_{\text{TP}}$ is still present. Thus, according to the symmetry considerations in Section 6.1, the current vanishes within the weak-coupling approximation for the transmission probability, cf. Eq. (72). Since this approximation is only correct to linear order in Γ, the higher-order contributions typically remain finite and, consequently, for small coupling the pump current obeys $\bar{I} \propto \Gamma^2$. Fig. 12 confirms this prediction. Yet one observes that already a small deviation from $\phi = 0$ is sufficient to restore the usual weak coupling behavior, namely a current which is proportional to the coupling strength Γ. This effect can be employed for the detection phase lags.

Other features of the harmonic mixing current resemble the ones discussed above in the context of ratchet-like structures [68]. In particular, we again find for large driving amplitudes that the current becomes essentially independent of the wire length. Typically, the current reaches convergence for a length $N \gtrsim 10$.

6.4. Phonon damping

Including also the coupling of the wire electrons to a phonon heat bath, one can no longer employ the scattering formula (46) and for the computation of the dc current, one thus, has to resort to the master equation approach of Section 4. Here, we only mention the main findings and refer the reader to the original work, Ref. [69]: the presence of phonon damping can significantly increase the pump current. This means that for quantum ratchets, noise plays a rather constructive role. Moreover, phonon damping
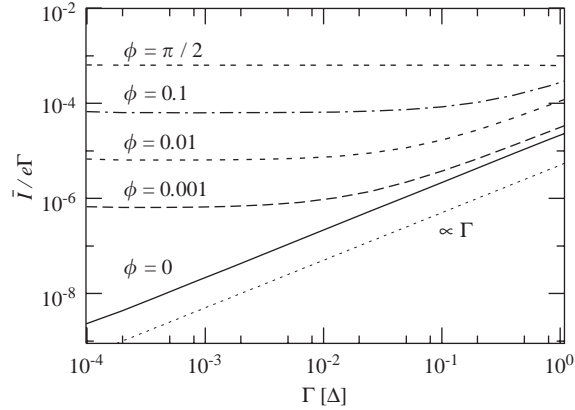
Fig. 12. Average current response to the harmonic mixing signal with amplitudes $A_1 = 2A_2 = \Delta$, as a function of the coupling strength for different phase shifts ϕ. The remaining parameters are $\Omega = 10\Delta/\hbar$, $E_B = 5\Delta$, $k_B T = 0.25\Delta$, $N = 10$. The dotted line is proportional to Γ; it represents a current which is proportional to Γ^2. From Ref. [68].

influences the dependence of the current on the phase lag by providing an additional shift towards a $\cos \phi$ behavior.

7. Control setups

A prominent example for the control of quantum dynamics is the so-called coherent destruction of tunneling, i.e., the suppression of the tunneling dynamics of a particle in a double-well potential [88] and in a two-level system [88,90]. Recently, coherent destruction of tunneling has also been predicted for the dynamics of two interacting electrons in a double quantum dot [92,187]. A closely related phenomenon is the miniband collapse in ac-driven superlattices which yields a suppression of quantum diffusion [91,151,188]. In this chapter, we address the question whether a corresponding transport effect exists: if two leads are attached to the ends of a driven tunneling system, is the suppression of tunneling visible in the conductance properties? Since time-dependent control schemes can be valuable in practice only if they operate at tolerable noise levels, the question is also whether the corresponding noise strength can be kept small or even be controlled.

7.1. Coherent destruction of tunneling

In order to introduce the reader to the essentials of coherent destruction of tunneling in isolated quantum systems, we consider a single particle in a driven two-level system described by the Hamiltonian

$$\mathscr{H}_{\text{TLS}}(t) = -\frac{\Delta}{2}\,\sigma_x + \frac{A}{2}\,\sigma_z\,\cos(\Omega t)\ . \tag{135}$$

If the energy of the quanta $\hbar\Omega$ of the driving field exceeds the energy scales of the wire, one can apply the high-frequency approximation scheme of Section 3.4.2 [90,94] and finds that the dynamics can be
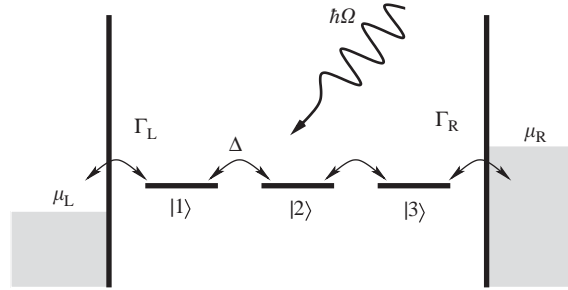
Fig. 13. Level structure of the molecular wire with $N = 3$ orbitals. The end sites are coupled to two leads with chemical potentials μ_L and $\mu_R = \mu_L - eV$.

described approximately by the static effective Hamiltonian (84) which for the present case reads

$$\mathscr{H}_{\text{TLS,eff}} = -\frac{\Delta_{\text{eff}}}{2}\,\sigma_x \ , \tag{136}$$

with the tunnel matrix element renormalized according to

$$\Delta \longrightarrow \Delta_{\text{eff}} = J_0(A/\hbar\Omega)\Delta \ . \tag{137}$$

Again, J_0 denotes the zeroth-order Bessel function of the first kind. If the ratio $A/\hbar\Omega$ equals a zero of the Bessel function J_0 (i.e., for the values 2.405…, 5.520…, 8.654…, …), the effective tunnel matrix element vanishes and the tunneling is brought to a standstill.

This reasoning is readily generalized to other tight-binding systems: If neighboring sites are coupled by a hopping matrix element Δ and the difference of their on-site energies oscillates with an amplitude A, one finds that the physics is determined by the renormalized matrix element (137), provided that $\hbar\Omega$ is the largest energy scale.

7.2. Current and noise suppressions

In order to investigate coherent destruction of tunneling in the context of transport, we consider the wire–lead setup sketched in Fig. 13 where the wire is described by the dipole Hamiltonian (8) with on-site energies $E_n = 0$. The wire is assumed to couple equally to both leads, $\Gamma_L = \Gamma_R = \Gamma$, and the numerical results are computed from the exact current formula (46).

For a driven wire described by the Hamiltonian (8), it has been found [66,67,93] that the oscillating dipole force suppresses the transport if the ratio $A/\hbar\Omega$ is close to a zero of the Bessel function J_0. Moreover, in the vicinity of such suppressions, the shot noise characterized by the Fano factor (22) assumes two characteristic minima. These suppression effects are most pronounced in the high-frequency regime, i.e., if the energy quanta $\hbar\Omega$ of the driving field exceed the energy scales of the wire. Thus, before going into a detailed discussion, we start with a qualitative description of the effect based on the static approximation for a high-frequency driving that has been derived in Section 3.4.2.

Let us consider first the limit of a voltage which is so large that in Eq. (88), $f_{R,eff} - f_{L,eff}$ can be replaced by unity. Then, the average current is determined by the effective Hamiltonian

$$\mathscr{H}_{eff} = -\Delta_{eff} \sum_{n=1}^{N-1} (|n\rangle\langle n+1| + |n+1\rangle\langle n|) + \sum_{n=1}^{N} E_n |n\rangle\langle n| , \tag{138}$$

which has been derived by inserting the time-dependent part of the Hamiltonian (8) into Eqs. (82) and (84). Then, obviously $\mathscr{H}_{eff}$ is identical to the static part of the Hamiltonian (8) but with the tunnel matrix element renormalized according to Eq. (137). Since the Bessel function J_0 assumes values between zero and one, the amplitude of the driving field allows one to switch the absolute value of the effective hopping on the wire, Δ_{eff}, between 0 and Δ. Since the transmission probability of an undriven wire is proportional to $|\Delta|^2$, the effective transmission probability $T_{eff}(\epsilon)$ acquires a factor $J_0^2(A/\hbar\Omega)$. This renormalization of the hopping then results in a current suppression [66,67,93].

For the discussion of the shot noise, we employ the Fano factor (22) as a measure. In the limit of large applied voltages, we have to distinguish two limits: (i) weak wire–lead coupling $\Gamma \ll \Delta_{eff}$ (i.e., weak with respect to the effective hopping) and (ii) strong wire–lead coupling $\Gamma \gg \Delta_{eff}$. In the first case, the tunnel contacts between the lead and the wire act as "bottlenecks" for the transport. In that sense they form barriers. Thus qualitatively, we face a double barrier situation and, consequently, expect the shot noise to exhibit a Fano factor $F \approx \frac{1}{2}$ [54]. In the second case, the links between the wire sites act as $N-1$ barriers. Correspondingly, the Fano factor assumes values $F \approx 1$ for $N=2$ (single barrier) and $F \approx \frac{1}{2}$ for $N=3$ (double barrier) [189]. At the crossover between the two limits, the conductor is (almost) "barrier free" such that the Fano factor assumes its minimum.

In order to be more quantitative, we evaluate the current and the zero-frequency noise in more detail thereby considering a finite voltage. This requires a closer look at the effective electron distribution (89); in particular, we have to quantify the concept of a "practically infinite" voltage. In a static situation, the voltage can be replaced by infinity, $f_R(\epsilon) = 1 = 1 - f_L(\epsilon)$, if all eigenenergies of the wire lie well inside the range $[\mu_L, \mu_R]$. In contrast to the Fermi functions, the effective electron distribution (89) which is decisive here, decays over a broad energy range in multiple steps of size $\hbar\Omega$. Since for our model, $T_{eff}(\epsilon)$ is peaked around $\epsilon = 0$, we replace here the effective electron distributions by their values for $\epsilon = 0$,

$$f_{\ell,eff}(0) = \sum_{k < \mu_\ell/\hbar\Omega} J_k^2 \left(\frac{A(N-1)}{2\hbar\Omega} \right) \tag{139}$$

for zero temperature. We have inserted the coefficients $a_{1,k} = J_k(A(N-1)/2\hbar\Omega)$ and $a_{N,k} = J_{-k}(A(N-1)/2\hbar\Omega)$ which have been computed directly from their definition (86); J_k denotes the kth-order Bessel functions of the first kind. The current, the noise, and the Fano factor are given by the static expressions (17) and (21) with the transmission probability and the electron distribution replaced by the corresponding effective quantities, T_{eff} and $f_{\ell,eff}$, respectively. Thus, we obtain

$$\bar{I} = \lambda \bar{I}_\infty , \tag{140}$$

$$\bar{S} = \lambda^2 \bar{S}_\infty + \frac{e}{2}(1-\lambda^2)\bar{I}_\infty , \tag{141}$$

$$F = \lambda F_\infty + \frac{1-\lambda^2}{2\lambda} , \tag{142}$$

respectively, where the subscript ∞ denotes the corresponding quantities in the infinite voltage limit,

$$\bar{I}_\infty = \frac{e}{h} \int d\epsilon \, T_{\text{eff}}(\epsilon) \ , \tag{143}$$

$$\bar{S}_\infty = \frac{e^2}{h} \int d\epsilon \, T_{\text{eff}}(\epsilon)[1 - T_{\text{eff}}(\epsilon)] \tag{144}$$

and $F_\infty = \bar{S}_\infty / e\bar{I}_\infty$. The factor

$$\lambda = f_{\text{R,eff}}(0) - f_{\text{L,eff}}(0) = \sum_{|k| \leqslant K(V)} J_k^2 \left(\frac{A(N-1)}{2\hbar\Omega} \right) \tag{145}$$

reflects the influence of a finite voltage; $K(V)$ denotes the largest integer not exceeding $e|V|/2\hbar\Omega$. Since $J_k(x) \approx 0$ for $|k| > x$ and $\sum_k J_k^2(x) \approx 1$, we find $\lambda = 1$ if $K(V) > A(N-1)/2\hbar\Omega$. This means that for small driving amplitudes $A < eV/(N-1)$, we can consider the voltage as practically infinite. With an increasing driving strength, λ decreases and, thus, the current becomes smaller by a factor λ but still exhibits suppressions. By contrast, since $F_\infty \leqslant 1$ for all situations considered here, we find from Eq. (142) that the Fano factor will increase with smaller λ.

Let us emphasize that unlike in the present case, the quenching of transmission observed in Refs. [190,191] does not result from a renormalized inter-well tunnel matrix element, but rather originates from the appearance of the Bessel function J_0 in the effective electron distribution (139). Therefore, at large voltages, the model considered in these references will not give rise to current suppressions.

7.3. Numerical results

Fig. 14a depicts the dc current and the zero-frequency noise for a wire with $N = 3$ sites and a relatively large applied voltage, $\mu_L - \mu_R = 50\Delta$. As a remarkable feature, we find that for certain values of the field amplitude A, the current drops to a value of some percent of the current in the absence of the field [66,93] with a suppression factor which is fairly independent of the wire–lead coupling Γ [69]. The small residual current corresponds to the fact that CDT is perfect only in the limit of an infinite driving frequency [90,192]. The corresponding noise strength $\bar{S}$ exhibits similar suppressions and, in addition, has some small plateaus in the vicinity of the minima. The role of the plateaus is elucidated by the *relative* noise strength characterized by the Fano factor (22) which is shown in Fig. 14b. Interestingly enough, we find that the Fano factor as a function of the driving amplitude A possesses both a sharp maximum at each current suppression and two pronounced minima nearby. For a sufficiently large voltage, the Fano factor at the maximum assumes the value $F \approx \frac{1}{2}$. Once the driving amplitude is of the order of the applied voltage, however, the Fano factor becomes much larger. The relative noise minima are distinct and provide a typical Fano factor of $F \approx 0.15$. Reducing the coupling to the leads renders these phenomena even more pronounced since then the suppressions occur in a smaller interval of the driving amplitude, cf. Fig. 14b. The overall behavior is robust in the sense that approximately the same values for the minima and the maximum are also found for larger wires, different driving frequencies, different coupling strengths, and slightly modified on-site energies, provided that $\Delta, \Gamma, E_n \ll \hbar\Omega$ and that the applied voltage is sufficiently large [67].

A comparison of these numerical results and the ones obtained in Section 7.2 analytically within a high-frequency approximation shows an excellent agreement. It quantitatively confirms both the parameter
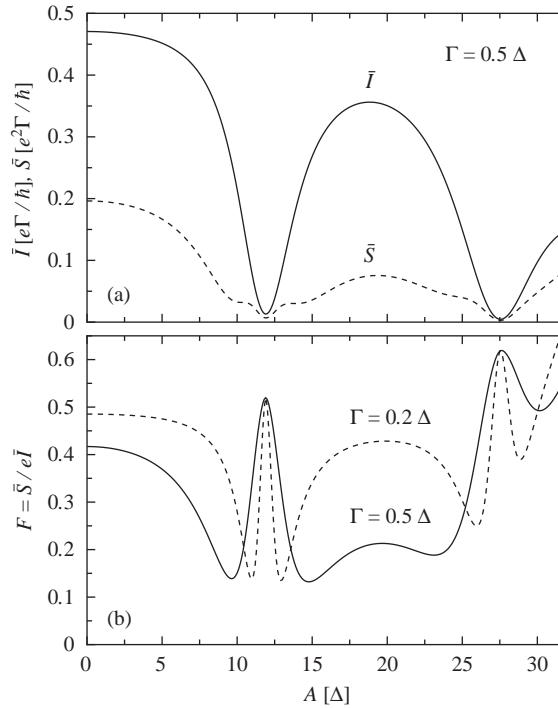
Fig. 14. Time-averaged current $\bar{I}$ and zero-frequency noise $\bar{S}$ (a) as a function of the driving amplitude A for a wire with $N = 3$ sites with on-site energies $E_n = 0$ and chemical potentials $\mu_R = -\mu_L = 25\Delta$. The other parameters read $\Omega = 5\Delta/\hbar$, $\Gamma = 0.5\Delta$, and $k_B T = 0$. Panel (b) displays the Fano F factor for these parameters (full line) and for smaller wire–lead coupling (dash–dotted line). From Ref. [66].

values for which current and noise suppressions occur and the corrections found in the large-amplitude regime $A \gtrsim eV$ [67,94].

For a much lower driving frequency of the order of the wire excitations, $\Omega = \Delta/\hbar$, the high-frequency approximation is no longer applicable. Nevertheless, the average current exhibits clear minima with a suppression factor of the order of $\frac{1}{2}$; see Fig. 15a. Compared to the high-frequency case, these minima are shifted towards smaller driving amplitudes, i.e., they occur for ratios $A/\hbar\Omega$ slightly below the zeros of the Bessel function J_0. At the minima of the current, the Fano factor still assumes a maximum with a value close to $F \approx \frac{1}{2}$ (Fig. 15b). Although the sharp minima close to the current suppressions have vanished, in-between the maxima the Fano factor assumes remarkably low values of $F \approx 0.2$.

So far, we have assumed that all on-site energies of the wire are identical. In an experimental setup, however, the applied transport voltage acts also a static dipole force which rearranges the charge distribution in the conductor and thereby causes an internal potential profile [118–120]. The self-consistent treatment of such effects is, in particular in the time-dependent case, rather ambitious and beyond the scope of this work. Thus, here we only derive the consequences of a static bias without determining its shape from microscopic considerations. We assume a position-dependent static shift of the on-site energies by an energy $-b\,x_n$, i.e., for a wire with $N = 3$ sites,

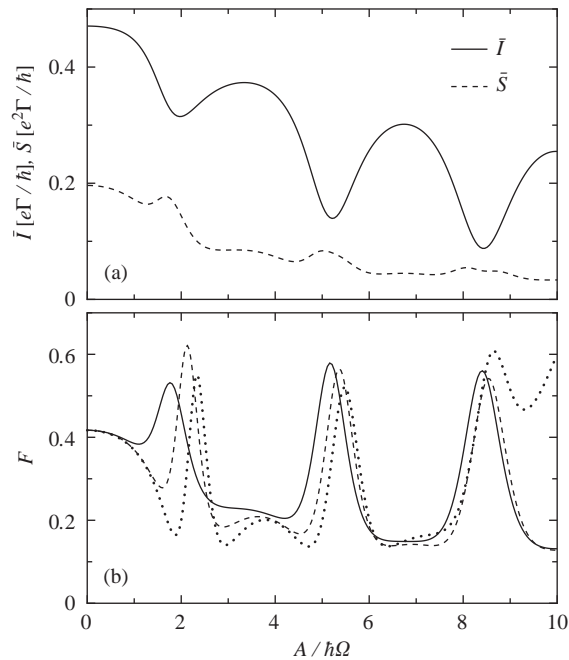$$E_1 = b, \quad E_2 = 0, \quad E_3 = -b \ . \tag{146}$$

Fig. 15. (a) Time-averaged current (solid line) and zero-frequency noise (dashed line) as a function of the driving amplitude for the driving frequency $\Omega = \Delta/\hbar$ and the transport voltage $V = 48\Delta/e$. (b) Corresponding Fano factor for the same data (solid line) and for the driving frequencies $\Omega = 1.5\Delta/\hbar$ (dashed) and $\Omega = 3\Delta/\hbar$ (dash–dotted). All other parameters are as in Fig. 14. From Ref. [67].

Fig. 16a demonstrates that the behavior of the average current is fairly stable against the bias. In particular, we still find pronounced current suppressions. Note that since $b \ll \Omega$ a high-frequency approximation is still applicable. As a main effect of the bias, we find reduced current maxima while the minima remain. By contrast, the minima of the Fano factor (Fig. 16b) become washed out: once the bias becomes of the order of the wire–lead coupling, $b \approx \Gamma$, the structure in the Fano factor vanishes and we find $F \approx \frac{1}{2}$ for all driving amplitudes $A < eV/(N-1)$ [cf. the discussion after Eq. (145)]. Interestingly, the value of the Fano factor at the current suppressions is bias-independent.

7.4. Current routers

So far, we have only considered driven transport through two-terminal devices. While the experimental realization of three and more molecular contacts is rather challenging, such systems can be described theoretically within the present formalism. As an example, we consider a planar three-terminal geometry with $N = 4$ sites as sketched in Fig. 17. We borrow from electrical engineering the designations E, C_1, and C_2. Here, an external voltage is always applied such that C_1 and C_2 have equal electro-chemical potential, i.e., $\mu_{C_1} = \mu_{C_2} \neq \mu_E$. In a perfectly symmetric molecule, where all on-site energies are equal, reflection symmetry at the horizontal axis ensures that any current which enters at E is equally distributed among $C_{1,2}$, thus $I_{C_1} = I_{C_2} = -I_E/2$.
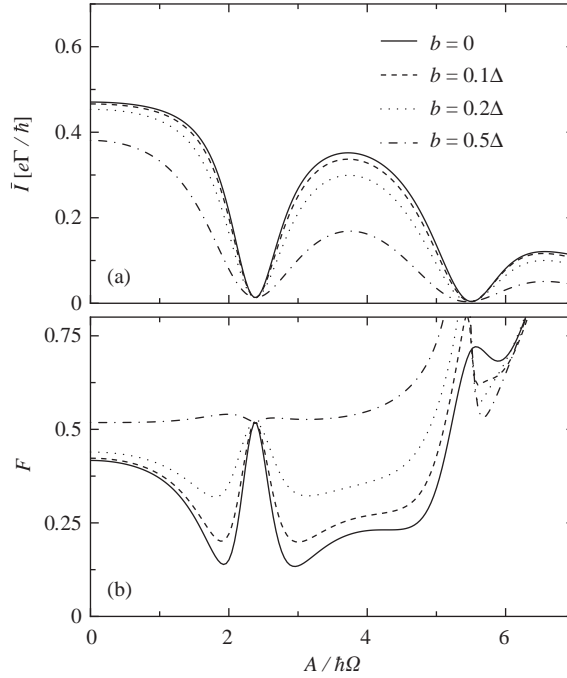
Fig. 16. Time-averaged current (a) and Fano factor (b) as a function of the driving amplitude A for a wire with $N = 3$ sites in the presence of an internal bias. The on-site energies are $E_1 = b$, $E_2 = 0$, $E_3 = -b$. All other parameters are as in Fig. 15. From Ref. [67].

The fact that this structure is essentially two-dimensional brings about a new degree of freedom, namely the polarization of the laser field. We assume it to be linear with a polarization angle ϑ as sketched in Fig. 17. The effective driving amplitudes of the orbitals that are attached to the leads acquire now a geometric factor which is only the same for both orbitals C_1 and C_2 when $\vartheta = 0$. For any other polarization angle, the mentioned symmetry is broken and the outgoing currents may be different from each other. The difference may be huge, as exemplified in Fig. 18. There, the current ratio varies from unity for $\vartheta = 0°$ up to the order of 100 for $\vartheta = 60°$. Thus, adapting the polarization angle enables one to route the current towards the one or the other drain.

For a qualitative explanation of the mechanism behind this effect, it is instructive to look at the time-averages of the overlaps $\langle |\langle n|\phi_\alpha(t)\rangle|^2 \rangle = \sum_k |\langle n|\phi_{\alpha,k}\rangle|^2$ of the Floquet states with the terminal sites $n = E, C_1, C_2$, which determine the effective tunneling rates (75) and (76) in the weak wire–lead coupling limit. Fig. 19 shows these overlaps for three different polarization angles ϑ. Let us consider, for instance, the current across contact C_1. It is plausible that only Floquet modes which have substantial overlap with both the site C_1 and also the site E contribute the current through these terminals. For a polarization angle $\vartheta = -60°$, we can infer from Fig. 19 that the Floquet states with indices $\alpha = 1, 3$ and 4 fulfill this condition and, consequently, a current flows from lead E into lead C_1. By contrast, for $\vartheta = 0°$ and $\vartheta = 60°$ such current carrying states do not exist and the respective current vanishes.
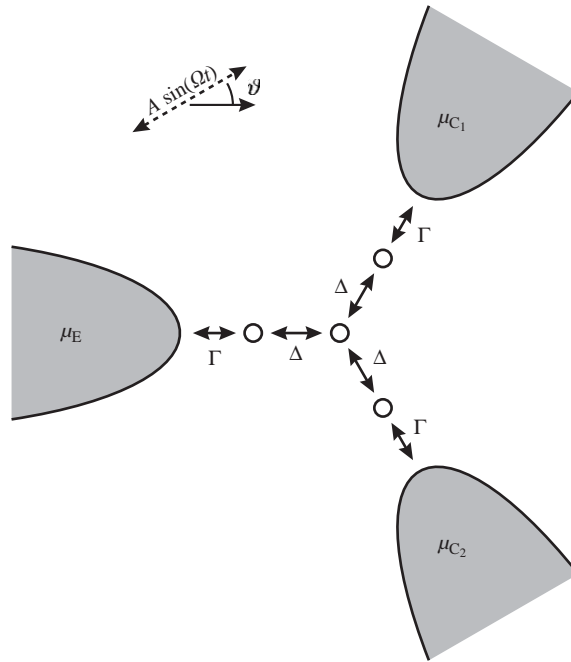
Fig. 17. Schematic top view of a setup where a molecule connected to three leads allows one to control the current flowing between the different leads (electro-chemical potentials μ_E, μ_{C_1}, and μ_{C_2}). The laser field is linearly polarized and propagates perpendicular to the drawing; the polarization angle ϑ is indicated by the dashed arrow.
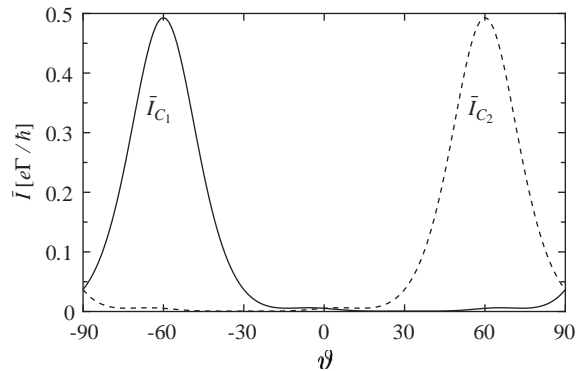

Fig. 18. Average currents (calculated within the master equation formalism) through contacts C_1 (solid) and C_2 (dashed) as a function of the polarization angle ϑ for the three-terminal device depicted in the Fig. 17. The chemical potentials are $\mu_E = -\mu_{C_1} = -\mu_{C_2} = 50\Delta$; the on-site energies $E_n = 0$. The driving field is specified by the strength $A = 25\Delta$ and the angular frequency $\Omega = 10\Delta/\hbar$; the effective coupling is $\Gamma = 0.1\Delta$ and the temperature $k_B T = 0.25\Delta$. From Ref. [93].

7.5. Phonon damping

A further question to be addressed is the robustness of the current suppressions against dissipation. In the corresponding tunneling problem, the driving alters both the coherent and the dissipative time scale
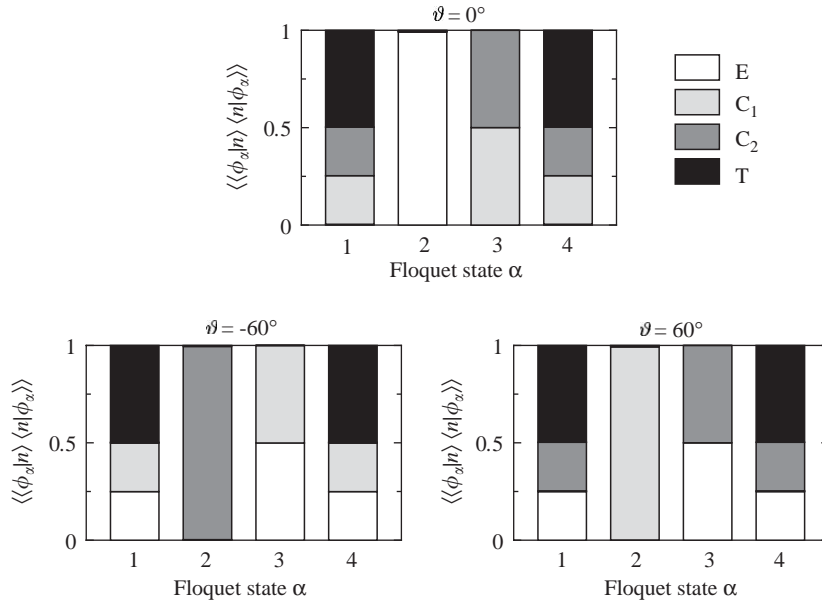
Fig. 19. Time-average $\langle\langle\phi_\alpha(t)|n\rangle\langle n|\phi_\alpha(t)\rangle\rangle$ of the overlaps $|\langle n|\phi_\alpha(t)\rangle|^2$ of the sites $n = $ E, C_1, C_2, and T (central site) to a Floquet state $|\phi_\alpha(t)\rangle$ for three different polarization angles ϑ. All parameters are as in Fig. 18. Adapted from Ref. [182].

by the same factor [193]. Thus, one might speculate that a vibrational coupling leaves the effect of the driving on the current qualitatively unchanged. This, however, is not the case: With increasing dissipation strength, the characteristic current suppressions become washed out until they finally disappear when the damping strength becomes of the order of the tunnel coupling Δ [69]. This detracting influence underlines the importance of quantum coherence for the observation of those current suppressions. Moreover, for the model employed in Ref. [69], we do not find the analogue of the effect of a stabilization of coherent destruction of tunneling within a certain temperature range [194–196] or, likewise, with increasing external noise [197], as it has been reported for driven, dissipative symmetric bistable systems.

8. Conclusion and outlook

In the present survey, we have reviewed the role of external driving for various transport quantities in nanosystems. In particular, we have focussed on the possibilities to selectively control, manipulate and optimize transport through such systems. In this context, we have studied various aspects of the electron transport through time-dependent tight-binding systems. For the theoretical description, two formalisms have been employed which both take advantage of the Floquet theorem: a Floquet scattering approach provides an exact solution of the time-averaged electrical current beyond the linear response limit and, moreover, yields an expression for the corresponding noise power. Interestingly, unlike in the undriven case, the noise depends also on the phases of the transmission amplitudes. As a drawback, this scattering approach is limited to the case of purely coherent transport in the absence of electron–electron interactions. As soon as other degrees of freedom like, e.g., a phonon bath, come into play, it is advantageous to resort to other formalisms like a Floquet master equation approach which, however, is limited to a weak wire–lead coupling.

We have investigated several driven transport phenomena such as resonant current amplification (Section 5), electron pumping (Section 6), and coherent current control (Section 7). Of foremost interest in view of ongoing experiments is the enhancement of molecular conduction by resonant excitations. We have derived an analytical expression for the current enhancement factor and, moreover, have found that the relative current noise is reduced approximately by a factor of one-half.

Both molecular wires and quantum dot arrays can act as coherent quantum ratchets and thereby operate in a regime where the quantum ratchet dynamics has not been studied previously. Of particular practical relevance is the fact that already relatively short wires or arrays behave like infinite systems. For the investigation of such driven nanodevices, symmetries play a crucial role: The driven nanosystem may exhibit a dynamical symmetry which includes a time transformation. Breaking this dynamical symmetry, for instance by using a non-harmonic driving force, can be exploited for the generation of a pump current. Moreover, the symmetry analysis revealed that a ratchet or pump can only be observed in the absence of the so-called generalized parity.

Coherent destruction of tunneling has a corresponding transport effect which exhibits an even richer variety of phenomena. For driving parameters, where the tunneling in isolated unbiased systems is suppressed, the dc current drops to a small residual value. This effect is found to be stable against a static bias. Moreover, the investigation of the corresponding noise level characterized by the Fano factor, has revealed that the current suppressions as a function of the driving amplitude are accompanied by a noise maximum and two remarkably low minima. This allows one to selectively control both the current and its noise by ac fields. Of crucial interest for potential applications are the noise properties of non-adiabatic pumps. For resonant excitations, these can be treated analytically within an approximation scheme in the spirit of the one applied in Ref. [94].

An experimental realization of the phenomena discussed in this paper is obviously not a simple problem. The requirement for asymmetric molecular structures is easily realized as discussed above, however difficulties associated with the many possible effects of junction illumination have to be surmounted [198]. Firstly, there is the issue of bringing the light into the junction. This is a difficult problem in a break-junction setup but possible in an scanning probe microscope configuration. Secondly, in addition to the modulation of electronic states on the molecular bridge as discussed in this work, other processes involving the excitation of the metal surface may also affect electron transport. A complete theory of illuminated molecular junctions should consider such possible effects. Moreover, the junction response to an oscillating electromagnetic field may involve displacement currents associated with the junction capacity. Finally, junction heating may constitute a severe problem when strong electromagnetic fields are applied. On the other hand, the light-induced rectification discussed in this paper is generic in the sense that it does not require a particular molecular electronic structure as long as an asymmetry is present.

An alternative experimental realization of the presented results is possible in semiconductor heterostructures, where, instead of a molecule, coherently coupled quantum dots [38] form the central system. A suitable radiation source that matches the frequency scales in this case must operate in the microwave spectral range. Compared to molecular wires, these systems by now are well-established. This is evident from the fact that in microwave-driven coupled quantum dots, electron pumping has already been observed [39].

The authors share the belief that this survey on driven quantum transport on the nanoscale provides the reader with a good starting point for future own research: many other intriguing phenomena await becoming unraveled.

Notation

n	wire site index, $n = 1, \ldots, N$
ℓ	= L, R, lead index
n_ℓ	wire site attached to lead ℓ: $n_{\mathrm{L}} = 1$, $n_{\mathrm{R}} = N$
α, β	Floquet state indices
k	side-band/Fourier index
$\epsilon_\alpha + \mathrm{i}\hbar\gamma_\alpha$	complex quasienergy
Ω	driving (angular) frequency
$\mathscr{T}$	$= 2\pi/\Omega$, driving period
$k_{\mathrm{B}}T$	Boltzmann constant times temperature
$\Gamma_\ell(\epsilon)$	spectral density of lead ℓ
Σ	imaginary part of self-energy
$|n\rangle$	wire site, $n = 1, \ldots, N$
$|u_\alpha(t)\rangle$	$= \sum_k \exp(-\mathrm{i}k\Omega t)|u_{\alpha,k}\rangle$, Floquet state for finite self-energy
$|u_{\alpha,k}\rangle$	kth Fourier coefficient of Floquet state $|u_\alpha(t)\rangle$
$|\phi_\alpha(t)\rangle$	Floquet state for self-energy $\Sigma = 0$
$E_\alpha, |\alpha\rangle$	eigenenergy and eigenstate of a static Hamiltonian
$P_{\alpha\beta}(t)$	$= \langle c_\beta^\dagger c_\alpha \rangle$, single particle density matrix in Floquet basis
$f(x)$	$= [\exp(x/k_{\mathrm{B}}T) + 1]^{-1}$, Fermi function

Acknowledgements

Appendix A. A primer to Floquet theory

In this review, we deal with time-periodically driven quantum systems whose dynamics is governed by the Schrödinger-like equation of motion

$$\mathrm{i}\hbar \frac{\mathrm{d}}{\mathrm{d}t}|\psi(t)\rangle = (H(t) - \mathrm{i}\Sigma)|\psi(t)\rangle \tag{A.1}$$

with the $\mathscr{T}$-periodic Hamiltonian $H(t) = H(t + \mathscr{T})$. The hermitian self-energy term Σ results from an elimination of environmental degrees of freedom and renders the time-evolution non-unitary.

The explicit time dependence in the Hamiltonian rules out the standard separation ansatz $|\psi(t)\rangle = \exp(-\mathrm{i}Et/\hbar)|\varphi\rangle$, where E is the (complex) eigenenergy of a state $|\varphi\rangle$, for the solution of Eq. (A.1). Yet, the time-periodicity of the Hamiltonian allows one to apply Floquet theory, a powerful tool, which we briefly review in this appendix.

A.1. Floquet theorem for non-unitary time-evolution

Floquet theory is based on the Floquet theorem which states that for a time-periodic Hamiltonian, $H(t) = H(t + \mathscr{T})$, there exists a complete set $\{|\psi_\alpha(t)\rangle\}$ of solutions of Eq. (A.1) which is of the form

$$|\psi_\alpha(t)\rangle = \mathrm{e}^{-(\mathrm{i}\epsilon_\alpha/\hbar + \gamma_\alpha)t}|u_\alpha(t)\rangle, \quad |u_\alpha(t)\rangle = |u_\alpha(t + \mathscr{T})\rangle \ . \tag{A.2}$$

The time-periodic functions $|u_\alpha(t)\rangle$ are called Floquet modes or Floquet states; the quantities ϵ_α are referred to as quasienergies with corresponding width γ_α and can be measured spectroscopically [199]. By inserting the ansatz (A.2) into Eq. (A.1), one easily verifies that the Floquet states fulfill the eigenvalue equation

$$\left(H(t) - \mathrm{i}\Sigma - \mathrm{i}\hbar\frac{\mathrm{d}}{\mathrm{d}t}\right)|u_\alpha(t)\rangle = (\epsilon_\alpha - \mathrm{i}\hbar\gamma_\alpha)|u_\alpha(t)\rangle \ . \tag{A.3}$$

Different methods can be used to prove the Floquet theorem. Here, we present a constructive argument. Upon diagonalization of the one-period propagator $U(\mathscr{T}, 0)$, where $U(t, t')$ is the time-evolution operator corresponding to the dynamical equation (A.1), we obtain

$$U(\mathscr{T}, 0)|u_\alpha(0)\rangle = \mathrm{e}^{-(\mathrm{i}\epsilon_\alpha/\hbar + \gamma_\alpha)\mathscr{T}}|u_\alpha(0)\rangle \ . \tag{A.4}$$

Here, we have written the complex eigenvalue as exponential for some ϵ_α and γ_α. Next, we use the eigenstates $|u_\alpha(0)\rangle$ as initial states for the time-evolution according to Eq. (A.1), yielding the solutions $|\psi_\alpha(t)\rangle = U(t, 0)|u_\alpha(0)\rangle$ of Eq. (A.1). This allows us to define the Floquet modes $|u_\alpha(t)\rangle = \exp[(\mathrm{i}\epsilon_\alpha/\hbar + \gamma_\alpha)t]|\psi_\alpha(t)\rangle$, which are indeed $\mathscr{T}$-periodic functions:

$$\begin{aligned}|u_\alpha(t + \mathscr{T})\rangle &= \mathrm{e}^{(\mathrm{i}\epsilon_\alpha/\hbar + \gamma_\alpha)(t+\mathscr{T})}U(t + \mathscr{T}, 0)|u_\alpha(0)\rangle \\ &= \mathrm{e}^{(\mathrm{i}\epsilon_\alpha/\hbar + \gamma_\alpha)(t+\mathscr{T})}U(t, 0)U(\mathscr{T}, 0)|u_\alpha(0)\rangle \\ &= \mathrm{e}^{(\mathrm{i}\epsilon_\alpha/\hbar + \gamma_\alpha)t}|\psi_\alpha(t)\rangle = |u_\alpha(t)\rangle \ . \end{aligned} \tag{A.5}$$

In the second line, we have used that owing to the time-periodicity of the Hamiltonian, the relation $U(t + \mathscr{T}, \mathscr{T}) = U(t, 0)$ holds true for arbitrary time t. Finally, the completeness of the set of solutions $\{|\psi_\alpha(t)\rangle\}$ follows, if we assume the completeness of the eigenstates of $U(\mathscr{T}, 0)$.

Since the one-period propagator $U(\mathscr{T}, 0)$ is in general non-unitary, its eigenstates $|u_\alpha(0)\rangle$ are not mutually orthogonal. We therefore also have to consider the left eigenstates of $U(\mathscr{T}, 0)$, i.e., the solutions of the adjoint equation

$$\left(H(t) + \mathrm{i}\Sigma - \mathrm{i}\hbar\frac{\mathrm{d}}{\mathrm{d}t}\right)|u_\alpha^+(t)\rangle = (\epsilon_\alpha + \mathrm{i}\hbar\gamma_\alpha)|u_\alpha^+(t)\rangle \ . \tag{A.6}$$

Here, we have used the fact that the eigenvalues of the adjoint equation are the complex conjugates of the eigenvalues of the original eigenvalue equation (A.3). This follows from the secular equations corresponding to the eigenvalue problems (A.3) and (A.6) by using the relation $\det O = \det O^{\mathrm{T}}$, which

holds for an arbitrary operator O. Assuming completeness of the eigenstates of $U(\mathscr{T}, 0)$, the Floquet modes and its adjoint modes may be chosen to form a bi-orthonormal basis at equal times t,

$$\langle u_\alpha^+(t) | u_\beta(t) \rangle = \delta_{\alpha\beta} \quad \text{and} \quad \sum_\alpha | u_\alpha^+(t) \rangle \langle u_\alpha(t) | = 1 \ . \tag{A.7}$$

The time-evolution operator $U(t, t')$ can be expressed explicitly in terms of the Floquet modes and quasienergies to read

$$U(t, t') = \sum_\alpha \mathrm{e}^{-\mathrm{i}(\epsilon_\alpha/\hbar + \gamma_\alpha)(t - t')} | u_\alpha(t) \rangle \langle u_\alpha^+(t') | \ . \tag{A.8}$$

This relation is readily checked by noting that due to Eq. (A.2) the right-hand side solves the differential equation (A.1). The initial condition $U(t, t) = 1$ is ensured by the completeness (A.7) of the Floquet modes.

It is worthwhile to remark that the conceptual importance of Floquet theory lies in the fact that it allows one to separate the long-time dynamics, governed by the eigenvalues $\epsilon_\alpha - \mathrm{i}\hbar\gamma_\alpha$, from the dynamics within one driving period, determined by the Floquet modes $|u_\alpha(t)\rangle$ [cf. Eq. (A.2)]. Note also that the quasienergies and the Floquet states in Eq. (A.2) are not defined uniquely. In fact, the replacement

$$\epsilon_\alpha \to \epsilon_\alpha + k_\alpha \hbar\Omega, \quad |u_\alpha(t)\rangle \to \mathrm{e}^{\mathrm{i}k_\alpha \Omega t} |u_\alpha(t)\rangle \ , \tag{A.9}$$

where $\Omega = 2\pi/\mathscr{T}$ is the angular frequency of the driving and $\{k_\alpha\}$ is an arbitrary sequence of integers, yields a new set of quasienergies and Floquet states corresponding to the same solutions $\{|\psi_\alpha(t)\rangle\}$ of Eq. (A.1). In other words, the quasienergies and Floquet modes come in classes, out of which one is allowed to select a single representative, usually with quasienergy in a single "Brillouin zone" $E - \hbar\Omega/2 \leqslant \epsilon_\alpha < E + \hbar\Omega/2$, where E is an arbitrary but fixed energy.

A.2. Extended Hilbert space formalism

According to the basic postulates of quantum mechanics, the state of a system is described by a vector $|\psi\rangle$ in a Hilbert space $\mathbb{R}$ with the inner product $\langle \psi' | \psi \rangle$. Without loss of the generality, we assume that there exists a countable and complete set $\{|n\rangle\}$ of orthonormal states, i.e.,

$$\langle n | n' \rangle = \delta_{nn'}, \quad \sum_n |n\rangle\langle n| = 1 \ . \tag{A.10}$$

The Hilbert space $\mathbb{T}$ of all $\mathscr{T}$-periodic, complex-valued functions possesses the inner product

$$(u, v) = \frac{1}{\mathscr{T}} \int_0^\mathscr{T} \mathrm{d}t \, u^*(t) v(t) \tag{A.11}$$

and the functions $\exp(\mathrm{i}k\Omega t)$ with $k = 0, \pm 1, \pm 2, \dots$ form the corresponding complete and orthonormal set. The decomposition of an arbitrary $\mathscr{T}$-periodic, complex-valued function into this basis yields the standard Fourier series.

As first noted by Sambe [144], the time-periodicity of the Floquet modes suggests to consider them as a vector of the composite Hilbert space $\mathbb{R} \otimes \mathbb{T}$. Its elements, for which we adopt the notation $|u\rangle\!\rangle$ [144], are the $\mathscr{T}$-periodic state vectors $|u(t)\rangle = |u(t + \mathscr{T})\rangle$. Introducing the inner product in this space in the canonical way via

$$\langle\!\langle u'|u\rangle\!\rangle = \frac{1}{\mathscr{T}} \int_0^{\mathscr{T}} \mathrm{d}t \, \langle u'(t)|u(t)\rangle \;, \tag{A.12}$$

an orthogonal basis of $\mathbb{R} \otimes \mathbb{T}$ is given by the set of states $\{|u_n^k\rangle\!\rangle\}$ defined by

$$|u_n^k(t)\rangle = \mathrm{e}^{\mathrm{i}k\Omega t}|n\rangle \;. \tag{A.13}$$

The arbitrary integer k is sometimes called the sideband index. The decomposition of a state $|u_\alpha(t)\rangle$ into this basis is equivalent to the Fourier representation

$$|u_\alpha(t)\rangle = \sum_k \mathrm{e}^{-\mathrm{i}k\Omega t} |u_{\alpha,k}\rangle \;,$$

$$|u_{\alpha,k}\rangle = \frac{1}{\mathscr{T}} \int_0^{\mathscr{T}} \mathrm{d}t \, \mathrm{e}^{\mathrm{i}k\Omega t} |u_\alpha(t)\rangle \;. \tag{A.14}$$

Employing the extended Hilbert space formalism, one should keep two points in mind. First, the solution $|\psi(t)\rangle$ of the equation of motion (A.1) is generally not $\mathscr{T}$-periodic in time and, thus, not an element of the composite Hilbert space. The decomposition of $|\psi(t)\rangle$ into elements of $\mathbb{R} \otimes \mathbb{T}$ requires time-dependent phase factors whose period is not a multiple of $2\pi/\Omega$. Second, the states $|u_{\alpha,k}\rangle$ are not orthogonal, because the Floquet modes are only mutually orthogonal at equal times [cf. Eq. (A.7)].

By the introduction of a Hilbert space structure for the time dependence, we have formally traced back the computation of Floquet states to the computation of eigenstates of a time-independent Hamiltonian with an additional degree of freedom. In particular, in the composite Hilbert space the Floquet equation (A.3) maps to the time-independent eigenvalue problem

$$(\mathscr{H}(t) - \mathrm{i}\Sigma)|u_\alpha\rangle\!\rangle = \epsilon_\alpha|u_\alpha\rangle\!\rangle \tag{A.15}$$

with the so-called Floquet Hamiltonian

$$\mathscr{H}(t) = H(t) - \mathrm{i}\hbar \, \frac{\mathrm{d}}{\mathrm{d}t} \;. \tag{A.16}$$

A wealth of methods for the solution of this eigenvalue problem can be found in the literature [145,200]. One such method is given by the direct numerical diagonalization of the operator on the left-hand side of Eq. (A.15). For a harmonic driving, the eigenvalue problem (A.15) is band-diagonal, i.e., only matrix elements with $k' = k, k \pm 1$ are non-vanishing. Therefore, eigenvalues and eigenvectors can be computed by a matrix-continued fraction scheme [200,201].

In cases where many Fourier coefficients (in the present context frequently called "sidebands") must be taken into account for the decomposition (A.14), direct diagonalization is often not very efficient and one has to apply more elaborated schemes. For example, in the case of a large driving amplitude, one can treat the static part of the Hamiltonian as a perturbation [90,144,151]. The Floquet states of the oscillating part of the Hamiltonian then form an adapted basis set for a subsequently more efficient numerical diagonalization.

A completely different strategy to obtain the Floquet states is to propagate the Schrödinger equation for a complete set of initial conditions over one driving period to yield the one-period propagator. Its eigenvalues represent the Floquet states at time $t = 0$, i.e., $|u_\alpha(0)\rangle$. Fourier transformation of their time-evolution results in the desired sidebands. Yet another, very efficient propagation scheme is the so-called (t, t')-formalism [202].

A.3. Parity of a system under dipole driving

Although we focus in this work on tight-binding systems, it is more convenient to study symmetries as a function of a continuous position and to regard the discrete models as a limiting case. Moreover, we consider in this section the Hamiltonian of the entire system including the leads. Consequently, we do not have to include any self-energy contribution.

A static Hamiltonian $H_0(x)$ is called invariant under the parity transformation $\mathscr{P} : x \to -x$ if it is an even function of x. Then, its eigenfunctions φ_α can be divided into two classes: even and odd ones, according to the sign in $\varphi_\alpha(x) = \pm\varphi_\alpha(-x)$. Adding a periodically time-dependent dipole force $xa(t)$ to such a Hamiltonian evidently breaks parity symmetry since $\mathscr{P}$ changes the sign of the interaction with the radiation. In a Floquet description, however, we deal with states that are functions of both position and time—we work in the extended space $\mathbb{R} \otimes \mathbb{T}$. Instead of the stationary Schrödinger equation, we address the eigenvalue problem

$$\mathscr{H}(x, t)\phi(x, t) = \epsilon\phi(x, t) \tag{A.17}$$

with the Floquet Hamiltonian for zero self-energy given by

$$\mathscr{H}(t) = H_0(x) + xa(t) - i\hbar \frac{\partial}{\partial t} , \tag{A.18}$$

where we assume a symmetric static part, $H_0(x) = H_0(-x)$. Our aim is now to generalize the notion of parity to the extended space $\mathbb{R} \otimes \mathbb{T}$ such that the overall transformation leaves the Floquet equation (A.17) invariant. This can be achieved if the shape of the driving $a(t)$ is such that an additional time transformation "repairs" the acquired minus sign. We consider two types of transformation: generalized parity and time-reversal parity. Both occur for purely harmonic driving, $a(t) = \cos(\Omega t)$. In the following we derive their consequences for the Fourier coefficients

$$\phi_k(x) = \frac{1}{\mathscr{T}} \int_0^{\mathscr{T}} dt \, e^{ik\Omega t}\phi(x, t) \tag{A.19}$$

of a Floquet states $\phi(x, t)$.

A.3.1. Time-reversal symmetry

Before discussing parity symmetry, let us comment on time-reversal symmetry which is not relevant for the spectral properties but still has some computational importance. It is known that the energy eigenfunctions of an non-driven Hamiltonian, which obeys time-reversal symmetry, can be chosen real [149]. Time-reversal symmetry is typically broken by a magnetic field (recall that a magnetic field is described by an axial vector and, thus, changes its sign under time-reversion) or by an explicit

time-dependence of the Hamiltonian. However, for a cosine driving, time-reversal symmetry

$$\mathscr{S}_{\mathrm{T}} : t \to -t \ , \tag{A.20}$$

is retained and the Floquet Hamiltonian (A.18) obeys $\mathscr{H}(t) = [\mathscr{H}(-t)]^*$. With the same line of reasoning as in the case of time-reversal symmetry, but with the additional replacement $x \to -x$, we obtain that one can choose the Floquet states such that they obey $\phi(x, t) = \phi^*(x, -t)$. Then, the Fourier coefficients (A.19) are real

$$\phi_k(x) = \phi_k^*(x) \ , \tag{A.21}$$

which helps to reduce numerical effort.

A.3.2. Time-reversal parity

A further symmetry is found if a is an odd function of time, $a(t) = -a(-t)$, e.g., for $a(t) = \sin(\Omega t)$. Then, time inversion transforms the Floquet Hamiltonian (A.18) into its complex conjugate such that the corresponding symmetry is given by the anti-linear transformation

$$\mathscr{S}_{\mathrm{TP}} : (\phi, x, t) \to (\phi^*, -x, -t) \ . \tag{A.22}$$

This transformation represents a generalization of the parity $\mathscr{P}$; we will refer to it as *time-reversal parity* since in the literature the term generalized parity is mostly used in the context of the transformation (A.24).

Again we are interested in the Fourier decomposition (A.19) and obtain

$$\phi_k(x) = \phi_k^*(-x) \ . \tag{A.23}$$

The time-reversal discussed here can be generalized by an additional time-shift to read $t \to t_0 - t$. Then, we find by the same line of argumentation that $\phi_k(x)$ and $\phi_k^*(-x)$ differ at most by a phase factor. However, for convenience one may choose already from the start the origin of the time axis such that $t_0 = 0$.

A.3.3. Generalized parity

It has been noted [88,89,150] that a Floquet Hamiltonian of the form (A.18) with $a(t) = \sin(\Omega t)$ may possess degenerate quasienergies due to its symmetry under the so-called generalized parity transformation

$$\mathscr{S}_{\mathrm{GP}} : (x, t) \to (-x, t + \pi/\Omega) \ , \tag{A.24}$$

which consists of spatial parity plus a time shift by half a driving period. This symmetry is present in the Floquet Hamiltonian (A.18), if the driving field obeys $a(t) = -a(t + \pi/\Omega)$, since then $\mathscr{S}_{\mathrm{GP}}$ leaves the Floquet equation invariant. Owing to $\mathscr{S}_{\mathrm{GP}}^2 = 1$, we find that the corresponding Floquet states are either even or odd, $\mathscr{S}_{\mathrm{GP}}\phi(x, t) = \phi(-x, t + \pi/\Omega) = \pm\phi(x, t)$. Consequently, the Fourier coefficients (A.19) obey the relation

$$\phi_k(x) = \pm(-1)^k \phi_k(-x) \ . \tag{A.25}$$

References

[1] R.P. Feynman, There's plenty of room at the bottom, Eng. Sci. 23 (1960) 22 lecture given at the APS meeting 1959.
[2] G. Binnig, H. Rohrer, Scanning tunneling microscopy, Physica B & C 127 (1984) 37.
[3] A. Aviram, M.A. Ratner, Molecular rectifiers, Chem. Phys. Lett. 29 (1974) 277.
[4] B. Mann, H. Kuhn, Tunneling through fatty acid salt monolayers, J. Appl. Phys. 42 (1971) 4398.
[5] M.A. Reed, C. Zhou, C.J. Muller, T.P. Burgin, J.M. Tour, Conductance of a molecular junction, Science 278 (1997) 252.
[6] X.D. Cui, A. Primak, X. Zarate, J. Tomfohr, O.F. Sankey, A.L. Moore, T.A. Moore, D. Gust, G. Harris, S.M. Lindsay, Reproducible measurement of single-molecule conductivity, Science 294 (2001) 571.
[7] J. Reichert, R. Ochs, D. Beckmann, H.B. Weber, M. Mayor, H. von Löhneysen, Driving current through single organic molecules, Phys. Rev. Lett. 88 (2002) 176804.
[8] A. Nitzan, M.A. Ratner, Electron transport in molecular wire junctions, Science 300 (2003) 1384.
[9] J.R. Heath, M.A. Ratner, Molecular electronics, Phys. Today 56 (5) (2003) 43.
[10] P. Hänggi, M. Ratner, S. Yaliraki, Processes in molecular wires, Chem. Phys. 281 (2002) 111.
[11] V. Balzani, M. Venturi, A. Credi, Molecular Devices and Machines: A Journey into the Nanoworld, Wiley-VCH, Weinheim, 2003.
[12] K. Goser, P. Glösekötter, J. Dienstuhl, Nanoelectronics and Nanosystems: From Transistors to Molecular and Quantum Devices, Springer, Berlin, Heidelberg, 2004.
[13] G. Cunibert, G. Fagas, K. Richter (Eds.), Molecular Electronics, Springer, Berlin, 2005.
[14] M. Di Ventra, S.T. Pantelides, N.D. Lang, First-principles calculation of transport properties of a molecular device, Phys. Rev. Lett. 84 (2000) 979.
[15] M. Di Ventra, N.D. Lang, Transport in nanoscale conductors from first principles, Phys. Rev. B 65 (2002) 045402.
[16] Y. Xue, S. Datta, M.A. Ratner, First-principles based matrix Green's function approach to molecular electronic devices: general formalism, Chem. Phys. 281 (2002) 151.
[17] P. Damle, A.W. Ghosh, S. Datta, First-principles analysis of molecular conduction using quantum chemistry software, Chem. Phys. 281 (2002) 171.
[18] J. Heurich, J.C. Cuevas, W. Wenzel, G. Schön, Electrical transport through single-molecule junctions: from molecular orbitals to conduction channels, Phys. Rev. Lett. 88 (2002) 256803.
[19] F. Evers, F. Weigend, M. Koentopp, Conductance of molecular wires and transport calculations based on density-functional theory, Phys. Rev. B 69 (2004) 235411.
[20] V. Mujica, M. Kemp, M.A. Ratner, Electron conduction in molecular wires, I: a scattering formalism, J. Chem. Phys. 101 (1994) 6849.
[21] D. Segal, A. Nitzan, W.B. Davis, M.R. Wasielewski, M.A. Ratner, Electron transfer rates in bridged molecular systems, 2: a steady-state analysis of coherent tunneling and thermal transitions, J. Phys. Chem. B 104 (2000) 3817.
[22] D. Boese, H. Schoeller, Influence of nanomechanical properties on single-electron tunneling: a vibrating single-electron transistor, Europhys. Lett. 54 (2001) 668.
[23] E.G. Petrov, P. Hänggi, Nonlinear electron current through a short molecular wire, Phys. Rev. Lett. 86 (2001) 2862.
[24] A. Nitzan, Electron transmission through molecules and molecular interfaces, Annu. Rev. Phys. Chem. 52 (2001) 681.
[25] M.H. Hettler, W. Wenzel, M.R. Wegewijs, H. Schoeller, Current collapse in tunneling transport through benzene, Phys. Rev. Lett. 90 (2003) 076805.
[26] M. Olson, Y. Mao, T. Windus, M. Kemp, M. Ratner, N. Leon, V. Mujica, A conformational study of the influence of vibrations on conduction in molecular wires, J. Phys. Chem. B 102 (1998) 941.
[27] Z.G. Yu, D.L. Smith, A. Saxena, A.R. Bishop, Green's function approach for a dynamical study of transport in metal/organic/metal structures, Phys. Rev. B 59 (1999) 16001.
[28] E.G. Emberly, G. Kirczenow, Landauer theory, inelastic scattering, and electron transport in molecular wires, Phys. Rev. B 61 (2000) 5740.
[29] Mikrajuddin, K. Okuyama, F.G. Shi, Mechanical effect on the electronic properties of molecular wires, Phys. Rev. B 61 (2000) 8224.
[30] L.E.F. Foa Torres, H.M. Pastawski, S.S. Makler, Tuning a resonance in Fock space: optimization of phonon emission in a resonant-tunneling device, Phys. Rev. B 64 (2001) 193304.
[31] H. Ness, S.A. Shevlin, A.J. Fisher, Coherent electron–phonon coupling and polaronlike transport in molecular wires, Phys. Rev. B 63 (2001) 125422.

[32] E.G. Petrov, V. May, P. Hänggi, Controlling electron transfer processes through short molecular wires, Chem. Phys. 281 (2002) 211.

[33] V. May, Electron transfer through a molecular wire: consideration of electron–vibrational coupling within the Liouville space pathway technique, Phys. Rev. B 66 (2002) 245411.

[34] E.G. Petrov, V. May, P. Hänggi, Spin–boson description of electron transmission through a molecular wire, Chem. Phys. 296 (2004) 251.

[35] G. Fagas, G. Cuniberti, K. Richter, Electron transport in nanotube-molecular wire hybrids, Phys. Rev. B 63 (2001) 045416.

[36] G. Cuniberti, G. Fagas, K. Richter, Fingerprints of mesoscopic leads in the conductance of a molecular wire, Chem. Phys 281 (2002) 465.

[37] R. Gutierrez, G. Fagas, G. Cuniberti, F. Grossmann, R. Schmidt, K. Richter, Theory of an all-carbon molecular switch, Phys. Rev. B 65 (2002) 113410.

[38] R.H. Blick, R.J. Haug, J. Weis, D. Pfannkuche, K. von Klitzing, K. Eberl, Single-electron tunneling through a double quantum dot: the artificial molecule, Phys. Rev. B 53 (1996) 7899.

[39] W.G. van der Wiel, S. De Franceschi, J.M. Elzerman, T. Fujisawa, S. Tarucha, L.P. Kouwenhoven, Electron transport through double quantum dots, Rev. Mod. Phys. 75 (2003) 1.

[40] T. Fujisawa, S. Tarucha, Photon assisted tunnelling in single and coupled quantum dot systems, Superlattice Microstruct. 21 (1997) 247.

[41] T.H. Oosterkamp, T. Fujisawa, W.G. van der Wiel, K. Ishibashi, R.V. Hijman, S. Tarucha, L.P. Kouwenhoven, Microwave spectroscopy of a quantum-dot molecule, Nature 395 (1998) 873.

[42] G. Platero, R. Aguado, Photon-assisted transport in semiconductor nanostructures, Phys. Rep. 395 (2004) 1.

[43] D.J. Thouless, Quantization of particle transport, Phys. Rev. B 27 (1983) 6083.

[44] B.L. Altshuler, L.I. Glazman, Pumping electrons, Science 283 (1999) 1864.

[45] M. Switkes, C.M. Marcus, K. Campman, A.C. Gossard, An adiabatic quantum electron pump, Science 283 (1999) 1905.

[46] M. Wagner, F. Sols, Subsea electron transport: pumping deep within the Fermi sea, Phys. Rev. Lett. 83 (1999) 4377.

[47] Y. Levinson, O. Entin-Wohlman, P. Wölfle, Acoustoelectric current and pumping in a ballistic quantum point contact, Phys. Rev. Lett. 85 (2000) 634.

[48] R. Landauer, Spatial variation of currents and fields due to localized scatterers in metallic conduction, IBM J. Res. Dev. 1 (1957) 223.

[49] M. Büttiker, Four-terminal phase-coherent conductance, Phys. Rev. Lett. 57 (1986) 1761.

[50] Y. Imry, Introduction to Mesoscopic Physics, Mesoscopic Physics and Nanotechnology, vol. 1, Oxford University Press, New York, 1997.

[51] S. Datta, Electronic Transport in Mesoscopic Systems, Cambridge University Press, Cambridge, 1995.

[52] R. Landauer, Conductance from transmission: common sense points, Phys. Scripta. T 42 (1992) 110.

[53] Y. Imry, R. Landauer, Conductance viewed as transmission, Rev. Mod. Phys. 71 (1999) S306.

[54] Ya.M. Blanter, M. Büttiker, Shot noise in mesoscopic conductors, Phys. Rep. 336 (2000) 1.

[55] M. Henseler, T. Dittrich, K. Richter, Signatures of chaos and tunneling in AC-driven quantum scattering, Europhys. Lett. 49 (2000) 289.

[56] M. Henseler, T. Dittrich, K. Richter, Classical and quantum periodically driven scattering in one dimension, Phys. Rev. E 64 (2001) 046218.

[57] W. Li, L.E. Reichl, Floquet scattering through a time-periodic potential, Phys. Rev. B 60 (1999) 15732.

[58] F. Sols, Scattering, dissipation, and transport in mesoscopic systems, Ann. Phys. (NY) 214 (1992) 386.

[59] S. Datta, M.P. Anantram, Steady-state transport in mesoscopic systems illuminated by alternating fields, Phys. Rev. B 45 (1992) 13761.

[60] M. Wagner, Probing Pauli blocking factors in quantum pumps with broken time-reversal symmetry, Phys. Rev. Lett. 85 (2000) 174.

[61] A.-P. Jauho, N.S. Wingreen, Y. Meir, Time-dependent transport in interacting and noninteracting resonant-tunneling systems, Phys. Rev. B 50 (1994) 5528.

[62] C.A. Stafford, N.S. Wingreen, Resonant photon-assisted tunneling through a double quantum dot: an electron pump from spatial Rabi oscillations, Phys. Rev. Lett. 76 (1996) 1916.

[63] A. Prêtre, H. Thomas, M. Büttiker, Dynamic admittance of mesoscopic conductors: discrete-potential model, Phys. Rev. B 54 (1996) 8130.

[64] M.H. Pedersen, M. Büttiker, Scattering theory of photon-assisted electron transport, Phys. Rev. B 58 (1998) 12993.

[65] G.B. Lesovik, L.S. Levitov, Noise in an ac biased junction: nonstationary Aharonov–Bohm effect, Phys. Rev. Lett. 72 (1994) 538.
[66] S. Camalet, J. Lehmann, S. Kohler, P. Hänggi, Current noise in ac-driven nanoscale conductors, Phys. Rev. Lett. 90 (2003) 210602.
[67] S. Camalet, S. Kohler, P. Hänggi, Shot-noise control in ac-driven nanoscale conductors, Phys. Rev. B 70 (2004) 155326.
[68] J. Lehmann, S. Kohler, P. Hänggi, A. Nitzan, Rectification of laser-induced electronic transport through molecules, J. Chem. Phys. 118 (2003) 3283.
[69] J. Lehmann, S. Kohler, V. May, P. Hänggi, Vibrational effects in laser-driven molecular wires, J. Chem. Phys. 121 (2004) 2278.
[70] S. Kohler, J. Lehmann, S. Camalet, P. Hänggi, Resonant laser excitation of molecular wires, Israel J. Chem. 42 (2002) 135.
[71] S. Kohler, J. Lehmann, M. Strass, P. Hänggi, Molecular wires in electromagnetic fields, Adv. Solid State Phys. 44 (2004) 157.
[72] P. Hänggi, R. Bartussek, Brownian rectifiers: how to convert Brownian motion into directed transport, in: J. Parisi, S.C. Müller, W.W. Zimmermann (Eds.), Nonlinear Physics of Complex Systems—Current Status and Future Trends, Lecture Notes in Physics, vol. 476, Springer, Berlin, 1996, pp. 294–308.
[73] R.D. Astumian, Thermodynamics and kinetics of a Brownian motor, Science 276 (1997) 917.
[74] F. Jülicher, A. Adjari, J. Prost, Modeling molecular motors, Rev. Mod. Phys. 69 (1997) 1269.
[75] P. Reimann, Brownian motors: noisy transport far from equilibrium, Phys. Rep. 361 (2002) 57.
[76] P. Reimann, P. Hänggi, Introduction to the physics of Brownian motors, Appl. Phys. A 75 (2002) 169.
[77] R.D. Astumian, P. Hänggi, Brownian motors, Phys. Today 55 (11) (2002) 33.
[78] P. Reimann, M. Grifoni, P. Hänggi, Quantum ratchets, Phys. Rev. Lett. 79 (1997) 10.
[79] M. Grifoni, M.S. Ferrreira, J. Peguiron, J.B. Majer, Quantum ratchets with few bands below the barrier, Phys. Rev. Lett. 89 (2002) 146801.
[80] P.W. Brouwer, Scattering approach to parametric pumping, Phys. Rev. B 58 (1998) 10135.
[81] B. Wang, J. Wang, H. Guo, Parametric pumping at finite frequency, Phys. Rev. B 65 (2002) 073306.
[82] H. Linke, T.E. Humphrey, A. Löfgren, A.O. Shuskov, R. Newbury, R.P. Taylor, P. Omling, Experimental tunneling ratchets, Science 286 (1999) 2314.
[83] H. Linke, T.E. Humphrey, P.E. Lindelof, A. Löfgren, R. Newbury, P. Omling, A.O. Sushkov, R.P. Taylor, H. Xu, Quantum ratchets and quantum heat pumps, Appl. Phys. A 75 (2002) 237.
[84] J.B. Majer, J. Peguiron, M. Grifoni, M. Tusveld, J.E. Mooij, Quantum ratchet effect for vortices, Phys. Rev. Lett. 90 (2003) 056802.
[85] S. de Haan, A. Lorke, J.P. Kotthaus, W. Wegscheider, M. Bichler, Rectification in mesoscopic systems with broken symmetry: quasiclassical ballistic versus classical transport, Phys. Rev. Lett. 92 (2004) 056806.
[86] S. Yasutomi, T. Morita, Y. Imanishi, S. Kimura, A molecular photodiode system that can switch photocurrent direction, Science 304 (2004) 1944.
[87] J. Lehmann, S. Kohler, P. Hänggi, A. Nitzan, Molecular wires acting as coherent quantum ratchets, Phys. Rev. Lett. 88 (2002) 228305.
[88] F. Grossmann, T. Dittrich, P. Jung, P. Hänggi, Coherent destruction of tunneling, Phys. Rev. Lett. 67 (1991) 516.
[89] F. Großmann, P. Jung, T. Dittrich, P. Hänggi, Tunneling in a periodically driven bistable system, Z. Phys. B 84 (1991) 315.
[90] F. Großmann, P. Hänggi, Localization in a driven two-level dynamics, Europhys. Lett. 18 (1992) 571.
[91] M. Holthaus, Collapse of minibands in far-infrared irradiated superlattices, Phys. Rev. Lett. 69 (1992) 351.
[92] C.E. Creffield, G. Platero, ac-driven localization in a two-electron quantum dot molecule, Phys. Rev. B 65 (2002) 113304.
[93] J. Lehmann, S. Camalet, S. Kohler, P. Hänggi, Laser controlled molecular switches and transistors, Chem. Phys. Lett. 368 (2003) 282.
[94] S. Kohler, S. Camalet, M. Strass, J. Lehmann, G.-L. Ingold, P. Hänggi, Charge transport through a molecule driven by a high-frequency field, Chem. Phys. 296 (2004) 243.
[95] A.H. Dayem, R.J. Martin, Quantum interaction of microwave radiation with tunneling between superconductors, Phys. Rev. Lett. 8 (1962) 246.
[96] W.G. van der Wiel, T. Fujisawa, T.H. Oosterkamp, L.P. Kouwenhoven, Microwave spectroscopy of a double quantum dot in the low- and high-power regime, Physica B 272 (1999) 31.

[97] T.H. Stoof, Yu.V. Nazarov, Time-dependent resonant tunneling via two discrete states, Phys. Rev. B 53 (1996) 1050.

[98] Ph. Brune, C. Bruder, H. Schoeller, Photon-assisted transport through ultrasmall quantum dots: influence of intradot transitions, Phys. Rev. B 56 (1997) 4730.

[99] L. Bányai, D.B. Tran Thoai, E. Reitsamer, H. Haug, D. Steinbach, M.U. Wehner, M. Wegener, T. Marschner, W. Stolz, Exciton-LO-phonon quantum kinetics: evidence of memory effects in bulk GaAs, Phys. Rev. Lett. 75 (1995) 2188.

[100] C. Fürst, A. Leitenstorfer, A. Laubereau, R. Zimmermann, Quantum kinetic electron–phonon interaction in GaAs: energy nonconserving scattering events and memory effects, Phys. Rev. Lett. 78 (1997) 3733.

[101] P. Král, A.P. Jauho, Resonant tunneling in a pulsed phonon field, Phys. Rev. B 59 (1999) 7656.

[102] A. Zrenner, E. Beham, S. Stufler, F. Findeis, M. Bichler, G. Abstreiter, Coherent properties of a two-level system based on a quantum-dot photodiode, Nature 418 (2002) 612.

[103] I.I. Rabi, Space quantization in a gyrating magnetic field, Phys. Rev. 51 (1937) 652.

[104] C. Kergueris, J.-P. Bourgoin, S. Palacin, D. Esteve, C. Urbina, M. Magoga, C. Joachim, Electron transport through a metal–molecule–metal junction, Phys. Rev. B 59 (1999) 12505.

[105] H.B. Weber, J. Reichert, F. Weigend, R. Ochs, D. Beckmann, M. Mayor, R. Ahlrichs, H. von Löhneysen, Electronic transport through single conjugated molecules, Chem. Phys. 281 (2002) 113.

[106] S. Datta, W. Tian, S. Hong, R. Reifenberger, J.I. Henderson, C.P. Kubiak, Current–voltage characteristics of self-assembled monolayers by scanning tunneling microscopy, Phys. Rev. Lett. 79 (1997) 2530.

[107] F. Jäckel, M.D. Watson, K. Müllen, J.P. Rabe, Prototypical single-molecule chemical-field-effect transistor with nanometer-sized gates, Phys. Rev. Lett. 92 (2004) 188303.

[108] J. Würfel, H.B. Weber, private communication.

[109] R. Bavli, H. Metiu, Properties of an electron in a quantum double well driven by a strong laser: localization, low-frequency, and even-harmonic generation, Phys. Rev. A 47 (1993) 3299.

[110] D.M. Newns, Self-consistent model of hydrogen chemisorption, Phys. Rev. 178 (1969) 1123.

[111] V. Mujica, M. Kemp, A. Roitberg, M.A. Ratner, Current–voltage characteristics of molecular wires: eigenvalue staircase, Coulomb blockade, and rectification, J. Chem. Phys. 104 (1996) 7296.

[112] L.E. Hall, J.R. Reimers, N.S. Hush, K. Silverbrook, Formalism, analytical model, and a priori Green's-function-based calculations of the current–voltage characteristics of molecular wires, J. Chem. Phys. 112 (2000) 1510.

[113] F. Demming, J. Jersch, K. Dickmann, P.I. Geshev, Calculation of the field enhancement on laser-illuminated scanning probe tips by the boundary element method, Appl. Phys. B 66 (1998) 593.

[114] A. Otto, Theory of first layer and single molecule surface enhanced Raman scattering (SERS), Phys. Stat. Sol. (a) 188 (2001) 1455.

[115] M. Fleischmann, P.J. Hendra, A.J. McQuillan, Raman spectra of pyridine adsorbed at a silver electrode, Chem. Phys. Lett. 26 (1974) 163.

[116] D.L. Jeanmaire, R.P. Van Duyne, Surface Raman spectroelectrochemistry part I. Heterocyclic, aromatic, and aliphatic amines adsorbed on the anodized silver electrode, J. Electroanal. Chem. 84 (1977) 1.

[117] B. Pellegrini, Extension of the electrokinematics theorem to the electromagnetic-field and quantum-mechanics, Il Nuovo Cimento 15 (1993) 855.

[118] A. Nitzan, M. Galperin, G.-L. Ingold, H. Grabert, On the electrostatic potential profile in biased molecular wires, J. Chem. Phys. 117 (2002) 10837.

[119] S. Pleutin, H. Grabert, G.-L. Ingold, A. Nitzan, The electrostatic potential profile along a biased molecular wire: a model quantum-mechanical calculation, J. Chem. Phys. 118 (2003) 3756.

[120] G.C. Liang, A.W. Ghosh, M. Paulsson, S. Datta, Electrostatic potential profiles of molecular conductors, Phys. Rev. B 69 (2004) 115302.

[121] J.R. Tucker, Quantum limited detection in tunnel junction mixers, IEEE J. Quantum Electron. QE-15 (1979) 1234.

[122] J.R. Tucker, M.J. Feldman, Quantum detection at millimeter wavelength, Rev. Mod. Phys. 57 (1985) 1055.

[123] P.K. Tien, J.P. Gordon, Multiphoton process observed in the interaction of microwave fields with the tunneling between superconductor films, Phys. Rev. 129 (1963) 647.

[124] N.S. Wingreen, Rectification by resonant tunneling diodes, Appl. Phys. Lett. 56 (1990) 253.

[125] V. Kislov, A. Kamenev, High-frequency properties of resonant tunneling devices, Appl. Phys. Lett. 59 (1991) 1500.

[126] R. Aguado, J. Iñarrea, G. Platero, Coherent resonant tunneling in ac fields, Phys. Rev. B 53 (1996) 10030.

[127] E.N. Economou, C.M. Soukoulis, Static conductance and scaling theory of localization in one dimension, Phys. Rev. Lett. 46 (1981) 618.

[128] D.C. Langreth, E. Abrahams, Derivation of the Landauer conductance formula, Phys. Rev. B 24 (1981) 2978.

[129] A.D. Stone, A. Szafer, What is measured when you measure a resistance?—the Landauer formula revisited, IBM J. Res. Dev. 32 (1988) 384.

[130] H.-L. Engquist, P.W. Anderson, Definition and measurement of the electrical and thermal resistances, Phys. Rev. B 24 (1981) 1151.

[131] D.S. Fisher, P.A. Lee, Relation between conductivity and transmission matrix, Phys. Rev. B 23 (1981) 6851.

[132] F. Sols, Gauge-invariant formulation of electron linear transport, Phys. Rev. Lett. 67 (1991) 2874.

[133] C. Caroli, R. Combescot, P. Noziere, D. Saint-James, Direct calculation of the tunneling current, J. Phys. C 4 (1971) 916.

[134] Y. Meir, N.S. Wingreen, Landauer formula for the current through an interacting electron region, Phys. Rev. Lett. 68 (1992) 2512.

[135] N.S. Wingreen, A.-P. Jauho, Y. Meir, Time-dependent transport through a mesoscopic structure, Phys. Rev. B 48 (1993) 8487.

[136] A. Wacker, A.-P. Jauho, Quantum transport: the link between standard approaches in superlattices, Phys. Rev. Lett. 80 (1998) 369.

[137] U. Fano, Ionization yield of radiations, II: the fluctuations of the number of ions, Phys. Rev. 72 (1947) 26.

[138] S. Nakajima, On quantum theory of transport phenomena, Prog. Theor. Phys. 20 (1958) 948.

[139] R. Zwanzig, Ensemble methods in the theory of irreversibility, J. Chem. Phys. 33 (1960) 1338.

[140] T. Novotný, Investigation of apparent violation of the second law of thermodynamics in quantum transport studies, Europhys. Lett. 59 (2002) 648.

[141] V. May, O. Kühn, Charge and Energy Transfer Dynamics in Molecular Systems, second ed., Wiley-VCH, Weinheim, 2003.

[142] P. Hänggi, H. Thomas, Stochastic processes: time evolution, symmetries and linear response, Phys. Rep. 88 (1982) 206.

[143] C. Bruder, H. Schoeller, Charging effects in ultrasmall quantum dots in the presence of time-varying fields, Phys. Rev. Lett. 72 (1994) 1076.

[144] H. Sambe, Steady states and quasienergies of a quantum-mechanical system in an oscillating field, Phys. Rev. A 7 (1973) 2203.

[145] M. Grifoni, P. Hänggi, Driven quantum tunneling, Phys. Rep. 304 (1998) 229.

[146] A. Buchleitner, D. Delande, J. Zakrzewski, Non-dispersive wave packets in periodically driven quantum systems, Phys. Rep. 368 (2002) 409.

[147] J.H. Shirley, Solution of the Schrödinger equation with a Hamiltonian periodic in time, Phys. Rev. 138 (1965) B979.

[148] P. Jung, P. Hänggi, Resonantly driven Brownian motion: basic concepts and exact results, Phys. Rev. A 41 (1990) 2977.

[149] J.J. Sakurai, Modern Quantum Mechanics, second ed., Addison-Wesley, Reading, MA, 1995.

[150] A. Peres, Dynamical quasidegeneracies and quantum tunneling, Phys. Rev. Lett. 67 (1991) 158.

[151] M. Holthaus, The quantum theory of an ideal superlattice responding to far-infrared laser radiation, Z. Phys. B 89 (1992) 251.

[152] A. Keller, O. Atabek, M. Ratner, V. Mujica, Laser-assisted conductance of molecular wires, J. Phys. B 35 (2002) 4981.

[153] T. Brandes, Truncation method for Green's functions in time-dependent fields, Phys. Rev. B 56 (1997) 1213.

[154] D.W. Hone, R. Ketzmerick, W. Kohn, Time-dependent Floquet theory and absence of an adiabatic limit, Phys. Rev. A 56 (1997) 4045.

[155] T. Holstein, Studies of polaron motion, I: molecular-crystal model, Ann. Phys. (NY) 8 (1959) 325.

[156] H.M. Pastawski, Classical and quantum transport from generalized Landauer–Büttiker equations, II: time-dependent resonant tunneling, Phys. Rev. B 46 (1992) 4053.

[157] T. Brandes, B. Kramer, Spontaneous emission of phonons by coupled quantum dots, Phys. Rev. Lett. 83 (1999) 3021.

[158] J. Lehmann, G.-L. Ingold, P. Hänggi, Incoherent charge transport through molecular wires: interplay of Coulomb interaction and wire population, Chem. Phys. 281 (2002) 199.

[159] D. Segal, A. Nitzan, Conduction in molecular junctions: inelastic effects, Chem. Phys. 281 (2002) 235.

[160] R. Aguado, T. Brandes, Shot noise spectrum of open dissipative quantum two-level systems, Phys. Rev. Lett. 92 (2004) 206601.

[161] T. Brandes, R. Aguado, G. Platero, Charge transport through open driven two-level systems with dissipation, Phys. Rev. B 69 (2004) 205326.

[162] P. Talkner, The failure of the quantum regression hypothesis, Ann. Phys. (NY) 167 (1986) 390.

[163] Yu.V. Nazarov, Quantum interference, tunnel junctions and resonant tunneling interferometer, Physica B 189 (1993) 57.

[164] B.L. Hazelzet, M.R. Wegewijs, T.H. Stoof, Yu.V. Nazarov, Coherent and incoherent pumping of electrons in double quantum dots, Phys. Rev. B 63 (2001) 165313.
[165] I. Urdaneta, A. Keller, O. Atabek, V. Mujica, Laser-assisted conductance of molecular wires: two-photon contributions, Int. J. Quantum Chem. 99 (2004) 460.
[166] A. Tikhonov, R.D. Coalson, Y. Dahnovsky, Calculating electron current in a tight-binding model of a field-driven molecular wire: application to xylyl-dithiol, J. Chem. Phys. 117 (2002) 567.
[167] A. Tikhonov, R.D. Coalson, Y. Dahnovsky, Calculating electron current in a tight-binding model of a field-driven molecular wire: Floquet theory approach, J. Chem. Phys. 116 (2002) 10909.
[168] H.M. McConnell, Intramolecular charge transfer in aromatic free radicals, J. Chem. Phys. 35 (1961) 508.
[169] M.A. Ratner, Bridge-assisted electron transfer: effective electronic coupling, J. Phys. Chem. 94 (1990) 4877.
[170] P.R. Levstein, H.M. Pastawski, J.L. D'Amato, Tuning the through-bond interaction in a two-centre problem, J. Phys.: Condens. Matter 2 (1990) 1781.
[171] V. Mujica, M. Kemp, M.A. Ratner, Electron conduction in molecular wires, II: application to scanning tunneling microscopy, J. Chem. Phys. 101 (1994) 6856.
[172] R.P. Feynman, R.B. Leighton, M. Sands, The Feynman Lectures on Physics, vol. 1, Addison-Wesley, Reading, MA, 1963.
[173] J.L. García-Palacios, D. Zueco, The Caldeira–Leggett quantum master equation in Wigner phase space: continued-fraction solution and application to Brownian motion in periodic potentials, J. Phys. A: Math. Gen. 37 (2004) 10735.
[174] I. Goychuk, M. Grifoni, P. Hänggi, Nonadiabatic quantum Brownian rectifiers, Phys. Rev. Lett. 81 (1998) 649 erratum: ibid. 81 (1998) 2837.
[175] I. Goychuk, P. Hänggi, Quantum rectifiers from harmonic mixing, Europhys. Lett. 43 (1998) 503.
[176] I. Goychuk, P. Hänggi, Minimal quantum Brownian rectifiers, J. Phys. Chem. B 105 (2001) 6642.
[177] L.P. Kouwenhoven, A.T. Johnson, N.C. van der Vaart, C.J.P.M. Harmans, Quantized current in a quantum-dot turnstile using oscillating tunnel barriers, Phys. Rev. Lett. 67 (1991) 1626.
[178] S.W. Kim, Floquet scattering in parametric electron pumps, Phys. Rev. B 66 (2002) 235304.
[179] M. Moskalets, M. Büttiker, Floquet scattering theory of quantum pumps, Phys. Rev. B 66 (2002) 205320.
[180] L. DiCarlo, C.M. Marcus, J.S. Harris Jr., Photocurrent, rectification, and magnetic field symmetry of induced current through quantum dots, Phys. Rev. Lett. 91 (2003) 246804.
[181] M. Wagner, F. Sols, Pipeline model for the Fermi-sea electron pump, Ann. Phys. (Leipzig) 9 (2000) 776.
[182] S. Kohler, J. Lehmann, P. Hänggi, Controlling currents through molecular wires, Superlattice Microstruct. 34 (2004) 419.
[183] S. Flach, O. Yevtushenko, Y. Zolotaryuk, Directed current due to broken time–space symmetry, Phys. Rev. Lett. 84 (2000) 2358.
[184] P. Reimann, Supersymmetric ratchets, Phys. Rev. Lett. 86 (2001) 4992.
[185] M. Rey, F. Sols, Electromotive force and internal resistance of an electron pump, Phys. Rev. B 70 (2004) 125315.
[186] J. Chen, M.A. Reed, A.M. Rawlett, J.M. Tour, Large on–off ratios and negative differential resistance in a molecular electronic device, Science 286 (1999) 1550.
[187] C.E. Creffield, G. Platero, Dynamical control of correlated states in a square quantum dot, Phys. Rev. B 66 (2002) 235303.
[188] M. Holthaus, D. Hone, Quantum-wells and superlattices in strong time-dependent fields, Phys. Rev. B 47 (1993) 6499.
[189] M.J.M. de Jong, C.W.J. Beenakker, Semiclassical theory of shot-noise suppression, Phys. Rev. B 51 (1995) 16867.
[190] M. Wagner, Quenching of resonant transmission through an oscillating quantum well, Phys. Rev. B 49 (1994) 16544.
[191] M. Wagner, Photon-assisted transmission through an oscillating quantum well: a transfer-matrix approach to coherent destruction of tunneling, Phys. Rev. A 51 (1995) 798.
[192] C.E. Creffield, Phase dependence of localization in the driven two-level model, Europhys. Lett. 66 (2004) 631.
[193] K.M. Fonseca-Romero, S. Kohler, P. Hänggi, Coherence control for qubits, Chem. Phys. 296 (2004) 307.
[194] T. Dittrich, B. Oelschlägel, P. Hänggi, Driven tunneling with dissipation, Europhys. Lett. 22 (1993) 5.
[195] T. Dittrich, F. Grossmann, P. Jung, B. Oelschlägel, P. Hänggi, Localization and tunneling in periodically driven bistable systems, Physica A 194 (1993) 173.
[196] D.E. Makarov, N. Makri, Stochastic resonance and nonlinear response in double-quantum-well structures, Phys. Rev. E 52 (1995) R2257.
[197] F. Grossmann, T. Dittrich, P. Jung, P. Hänggi, Coherent transport in a periodically driven bistable system, J. Stat. Phys. 70 (1993) 229.
[198] V. Gerstner, A. Knoll, W. Pfeiffer, A. Thon, G. Gerber, Femtosecond laser assisted scanning tunneling microscopy, J. Appl. Phys. 88 (2000) 4851.

[199] K. Johnsen, A.-P. Jauho, Quasienergy spectroscopy of excitons, Phys. Rev. Lett. 83 (1999) 1207.
[200] P. Hänggi, Driven quantum systems, in: T. Dittrich, P. Hänggi, G.-L. Ingold, B. Kramer, G. Schön, W. Zwerger, Quantum Transport and Dissipation, Wiley-VCH, Weinheim, 1998, pp. 249–286 (Chapter 5).
[201] H. Risken, The Fokker–Planck Equation, second ed., Springer Series in Synergetics, vol. 18, Springer, Berlin, 1989.
[202] U. Peskin, N. Moiseyev, The solution of the time-dependent Schrödinger equation by the (t, t') method: theory, computational algorithm and applications, J. Chem. Phys. 99 (1993) 4590.